

---

Theses and Dissertations

---

Spring 2013

## The kinetics and physical properties of epoxides, acrylates, and hybrid epoxy-acrylate photopolymerization systems

Brian F. Dillman  
*University of Iowa*

Follow this and additional works at: <https://ir.uiowa.edu/etd>

 Part of the [Chemical Engineering Commons](#)

Copyright 2013 Brian Frank Dillman

This dissertation is available at Iowa Research Online: <https://ir.uiowa.edu/etd/2476>


---

### Recommended Citation

Dillman, Brian F.. "The kinetics and physical properties of epoxides, acrylates, and hybrid epoxy-acrylate photopolymerization systems." PhD (Doctor of Philosophy) thesis, University of Iowa, 2013.  
<https://doi.org/10.17077/etd.protydqk>

---

Follow this and additional works at: <https://ir.uiowa.edu/etd>

 Part of the [Chemical Engineering Commons](#)

THE KINETICS AND PHYSICAL PROPERTIES OF EPOXIDES, ACRYLATES,  
AND HYBRID EPOXY-ACRYLATE PHOTOPOLYMERIZATION SYSTEMS

by  
Brian F. Dillman

An Abstract

Of a thesis submitted in partial fulfillment  
of the requirements for the Doctor of  
Philosophy degree in Chemical and Biochemical Engineering  
in the Graduate College of  
The University of Iowa

May 2013

Thesis Supervisor: Associate Professor Julie L.P. Jessop

## ABSTRACT

Photopolymerization, which uses light rather than heat to initiate polymerization, is a facile technique used to fabricate adhesives, protective coatings, thin films, photo-resists, dental restoratives, and other materials. Epoxide monomers, which are polymerized via cationic photoinitiation, have received less attention in fundamental research in comparison to free radical polymerized acrylate monomers. The characterization of propagation mechanisms, network structures, and physical properties is yet lacking.

This project focused on the reactivity and physical properties of 3,4-epoxycyclohexylmethyl-3,4-epoxycyclohexane carboxylate (EEC), and the kinetic and physical effects of chain transfer agents (CTAs) in EEC based formulations were characterized. This characterization was carried out using real-time Raman spectroscopy, real-time infrared spectroscopy, dynamic mechanical analysis, simple gel fraction measurements, and atomic force microscopy. The effects of water, organic alcohols, processing conditions (e.g., UV light intensity, humidity, post-illumination curing temperature), and photoinitiation systems were investigated.

In general, increasing the concentration of CTAs in a crosslinking epoxide resin increases the rate of polymerization and the overall epoxide conversion level. High CTA levels also correspond to lower glass transition temperatures ( $T_g$ ) and lower crosslink densities. A post-illumination annealing was critical in obtaining stable physical properties for high  $T_g$  epoxide materials. In addition, humidity (water being the most universal contaminant type of CTA) was found to impact the surface properties of an epoxide polymer negatively by reducing the surface hardness.

Hybrid acrylate-epoxide systems are much more complex and unpredictable in curing behavior. The use of hydroxy acrylates in hybrid systems allows for grafting between the epoxide and the acrylate domains, via the AM mechanism. Another intricacy

of hybrid systems is the initiation system. In order to maximize the conversion of both the epoxide and the acrylate moieties, the free-radical photoinitiator must not hinder the polymerization of the epoxide monomer. Some very efficient free-radical photoinitiators limit the epoxide polymerization by absorbing the majority of the deep-UV incident photons.

Finally, a renewable acrylate oligomer was synthesized to provide a green alternative to petroleum-based oligomers currently used. The oligomer was freely miscible and readily photopolymerized with a wide range of commercial monomers. The  $T_g$  relationship between the commercial monomers and the parent resin followed the Fox equation.

The results of this research provide strategies for controlling epoxide kinetics and physical properties in neat and hybrid systems. This information is useful for tailoring resin formulations to specific end-use applications, especially in films, coatings, and adhesives.

Abstract Approval: \_\_\_\_\_

Thesis Supervisor

\_\_\_\_\_  
Title and Department

\_\_\_\_\_  
Date

THE KINETICS AND PHYSICAL PROPERTIES OF EPOXIDES, ACRYLATES,  
AND HYBRID EPOXY-ACRYLATE PHOTOPOLYMERIZATION SYSTEMS

by  
Brian F. Dillman

A thesis submitted in partial fulfillment  
of the requirements for the Doctor of  
Philosophy degree in Chemical and Biochemical Engineering  
in the Graduate College of  
The University of Iowa

May 2013

Thesis Supervisor: Associate Professor Julie L.P. Jessop

Graduate College  
The University of Iowa  
Iowa City, Iowa

CERTIFICATE OF APPROVAL

---

PH.D. THESIS

---

This is to certify that the Ph.D. thesis of

Brian F. Dillman

has been approved by the Examining Committee  
for the thesis requirement for the Doctor of Philosophy  
degree in Chemical and Biochemical Engineering at the May 2013 graduation.

Thesis Committee: \_\_\_\_\_  
Julie L.P. Jessop, Thesis Supervisor

\_\_\_\_\_  
C. Allan Guymon

\_\_\_\_\_  
David G. Rethwisch

\_\_\_\_\_  
Gary A. Aurand

\_\_\_\_\_  
Ned B. Bowden

To my wonderful wife and happy children.

## ACKNOWLEDGMENTS

First and foremost this work was made possible by my patient wife Kellie. Without her support I would not have pursued education to the length that I have. She and I have struggled together during our time in Iowa while I have collected, reduced, and compiled the research that makes up this thesis.

Others who have helped me along way include my research advisor Dr. Julie L.P. Jessop who was always supportive of new ideas and approaches to research problems; my committee members Dr. Guymon, Dr. Rethwisch, Dr. Aurand and Dr. Bowden; undergraduate researchers Kenneth Mineart, Na Yeon Kang, Samantha Weber, Vincent Gutsell, Chengxuan Guo, Elliott Glenn, and Sean Conway; fellow graduate students Clinton Cook, Anna Volkert, Kristan Worthington, Bradley Forney, Brad Tuft, Hajime Kitano, Ho Seop Eom, Leroy Magwood, Jon Scholte, Sage Schissel and others; Chris Coretsopoulos who is always up for conversation; the IUCRC advisors and students; and the University as a whole. Many other people, too many to enumerate, have surely contributed to my success and I acknowledge and thank them.

Lastly I would like to thank my immediate and extended family who have supported and loved me a throughout my life regardless of my choices. I have been blessed to be born into a wonderful caring family that has encouraged and enabled me to pursue all of my ambitions.

It is my hope that my graduate work as well as my continued professional and personal conduct will empower and inspire others to achieve more than they thought possible, as I have.

--Brian F. Dillman



## ABSTRACT

Photopolymerization, which uses light rather than heat to initiate polymerization, is a facile technique used to fabricate adhesives, protective coatings, thin films, photo-resists, dental restoratives, and other materials. Epoxide monomers, which are polymerized via cationic photoinitiation, have received less attention in fundamental research in comparison to free radical polymerized acrylate monomers. The characterization of propagation mechanisms, network structures, and physical properties is yet lacking.

This project focused on the reactivity and physical properties of 3,4-epoxycyclohexylmethyl-3,4-epoxycyclohexane carboxylate (EEC), and the kinetic and physical effects of chain transfer agents (CTAs) in EEC based formulations were characterized. This characterization was carried out using real-time Raman spectroscopy, real-time infrared spectroscopy, dynamic mechanical analysis, simple gel fraction measurements, and atomic force microscopy. The effects of water, organic alcohols, processing conditions (e.g., UV light intensity, humidity, post-illumination curing temperature), and photoinitiation systems were investigated.

In general, increasing the concentration of CTAs in a crosslinking epoxide resin increases the rate of polymerization and the overall epoxide conversion level. High CTA levels also correspond to lower glass transition temperatures ( $T_g$ ) and lower crosslink densities. A post-illumination annealing was critical in obtaining stable physical properties for high  $T_g$  epoxide materials. In addition, humidity (water being the most universal contaminant type of CTA) was found to impact the surface properties of an epoxide polymer negatively by reducing the surface hardness.

Hybrid acrylate-epoxide systems are much more complex and unpredictable in curing behavior. The use of hydroxy acrylates in hybrid systems allows for grafting between the epoxide and the acrylate domains, via the AM mechanism. Another intricacy

of hybrid systems is the initiation system. In order to maximize the conversion of both the epoxide and the acrylate moieties, the free-radical photoinitiator must not hinder the polymerization of the epoxide monomer. Some very efficient free-radical photoinitiators limit the epoxide polymerization by absorbing the majority of the deep-UV incident photons.

Finally, a renewable acrylate oligomer was synthesized to provide a green alternative to petroleum-based oligomers currently used. The oligomer was freely miscible and readily photopolymerized with a wide range of commercial monomers. The  $T_g$  relationship between the commercial monomers and the parent resin followed the Fox equation.

The results of this research provide strategies for controlling epoxide kinetics and physical properties in neat and hybrid systems. This information is useful for tailoring resin formulations to specific end-use applications, especially in films, coatings, and adhesives.

## TABLE OF CONTENTS

LIST OF TABLES .....	ix
LIST OF FIGURES .....	x
<b>CHAPTER</b>	
1. INTRODUCTION AND BACKGROUND .....	1
1.1 Photopolymerization.....	1
1.1.1 Free Radical Systems .....	1
1.1.2 Cationic Systems .....	7
1.1.3 Hybrid Systems .....	10
1.2 Analytical Methods.....	13
1.2.1 Raman and Infrared Spectroscopy.....	13
1.2.2 Dynamic Mechanical Analysis.....	16
Notes .....	29
2. OBJECTIVES.....	36
3. EPOXIDE KINETICS IN WATER CONTAINING FORMULATIONS .....	39
3.1 Introduction.....	39
3.2 Experimental.....	40
3.2.1 Materials .....	40
3.2.2 Methods .....	41
3.2.2.1 RT-MIR spectroscopy .....	41
3.2.2.2 RT-NIR spectroscopy.....	41
3.3 Results and Discussion .....	42
3.4 Conclusions.....	43
Notes .....	51
4. CHAIN TRANSFER AGENTS IN CATIONIC PHOTOPOLYMERIZATION OF A BIS-CYCLOALIPHATIC EPOXIDE MONOMER: KINETIC AND PHYSICAL PROPERTY EFFECTS.....	53
4.1 Introduction.....	53
4.2 Experimental.....	55
4.2.1 Materials .....	55
4.2.2 Formulations.....	55
4.2.3 Methods .....	56
4.2.3.1 Kinetics.....	56
4.2.3.2 Physical/Mechanical properties.....	57
4.3 Results and discussion .....	58
4.3.1 Reactivity of neat EEC .....	58
4.3.2 General CTA effects.....	58
4.3.3 CTA size: mono-ols.....	60
4.3.4 CTA size: diols.....	61
4.3.5 Variation in nucleophilicity: sterics.....	63

4.3.6	Variation in nucleophilicity: electronics .....	64
4.4	Conclusions.....	66
	Notes .....	80
5.	<b>THE INFLUENCE OF HUMIDITY ON SURFACE MODULUS OF PHOTO-CURED EPOXY COATINGS.....</b>	<b>83</b>
5.1	Introduction.....	83
5.2	Experimental.....	83
5.2.1	Materials .....	83
5.2.2	Methods .....	84
5.3	Results and Discussion .....	85
5.4	Conclusions.....	86
	Notes .....	92
6.	<b>POST ILLUMINATION PROPERTY DEVELOPMENT IN EPOXIDE PHOTOPOLYMERS.....</b>	<b>93</b>
6.1	Introduction.....	93
6.2	Experimental.....	94
6.2.1	Materials .....	94
6.2.2	Methods .....	95
6.2.2.1	Mechanical Analysis .....	95
6.3	Results and Discussion .....	95
6.3.1	Mechanical Analysis .....	95
6.4	Conclusions.....	97
	Notes .....	101
7.	<b>EPOXIDE-ACRYLATE HYBRID PHOTOPOLYMERS: FORMATION OF GRAFTED POLYMER NETWORKS.....</b>	<b>104</b>
7.1	Introduction.....	104
7.2	Experimental.....	106
7.2.1	Materials .....	106
7.2.1.1	RAFT agent .....	107
7.2.1.2	RAFT polymers.....	107
7.2.1.3	Linear Epoxide Polymers .....	107
7.2.1.4	Cross-linked Epoxide Polymers .....	107
7.2.2	Methods .....	109
7.2.2.1	Gel Permeation Chromatography.....	109
7.2.2.2	Dynamic Mechanical Analysis.....	110
7.3	Results and Discussion .....	110
7.3.1	Demonstration of Grafting via GPC.....	110
7.3.2	Physical/Mechanical Properties.....	111
7.4	Conclusions.....	113
	Notes .....	120
8.	<b>DUAL PHOTO-INITIATION SYSTEMS IN EPOXIDE MONOMERS AND HYBRID EPOXIDE-ACRYLATE SYSTEMS.....</b>	<b>122</b>
8.1	Introduction.....	122
8.2	Experimental.....	123
8.2.1	Materials .....	123
8.2.1.1	Formulations.....	124
8.2.2	Methods .....	125

8.2.2.1 Kinetic Analysis .....	125
8.2.2.2 UV-Vis .....	125
8.3 Results and Discussion .....	126
8.3.1 Kinetic Analysis .....	126
8.3.1.1 Neat Epoxide Monomers.....	126
8.3.1.2 Hybrid Acrylate-Epoxy Systems.....	126
8.3.2 UV-Vis .....	127
8.4 Conclusions.....	128
Notes .....	136
9. SOLVENTLESS SYNTHESIS AND FREE-RADICAL PHOTOPOLYMERIZATION OF A CASTOR OIL-BASED ACRYLATE OLIGOMER.....	139
9.1 Introduction.....	139
9.2 Experimental.....	140
9.2.1 Materials .....	140
9.2.2 Synthesis of ACO .....	141
9.2.3 Formulations.....	142
9.2.4 Photopolymerization kinetics .....	142
9.2.5 Dynamic mechanical analysis .....	143
9.3 Results and Discussion .....	144
9.3.1 Synthesis of ACO .....	144
9.3.2 Photo-induced polymerization and co-polymerizations.....	145
9.3.3 Polymer properties.....	146
9.4 Conclusions.....	148
Notes .....	160
10. CONCLUSIONS AND RECOMMENDATIONS .....	163
10.1 Conclusions.....	163
10.2 Recommendations.....	167
Notes .....	172
REFERENCES .....	174

## LIST OF TABLES

Table 9.1: Monomer structures and physical properties of polymers formed from neat resins and blended formulations.....	159
---	-----

## LIST OF FIGURES

Figure 1.1: Photogeneration of initiating radicals by a Type I photoinitiating system, Irgacure 651. The two major initiating species produced are the benzoyl radical and the methyl radical. ....	18
Figure 1.2: Photogeneration of initiating radicals by a Type II photoinitiating system composed of ITX and MDEA. ITX is promoted to an excited state by photon absorption. While in the excited state ITX abstracts a proton from a carbon alpha to the nitrogen of MDEA, producing a carbon-centered radical that initiates polymerization. ....	19
Figure 1.3: Radical photoinitiators and co-initiators. A Type I (cleavage) initiators: i) 2,2-Dimethoxy-2-phenylacetophenone, Irgacure 651; ii) 2-Hydroxy-2-methyl-1-phenyl-propan-1-one, Darocur 1173; iii) Bis(2,4,6-trimethylbenzoyl)-phenylphosphineoxide, Irgacure 819. B Type II (H abstraction) initiators: iv) Benzophenone, BP; v) 4-Isopropyl-9-thioxanthone, ITX; vi) Camphorquinone CQ. C Co-initiators: (H-donor): vii) Triethylamine, TEA; viii) N-methyldiethanolamine, MDEA; ix) N,N,4-trimethylaniline, TMA. ....	20
Figure 1.4: Simplified radical chain propagation of 2-hydroxyethyl acrylate (HEMA) .....	21
Figure 1.5: Radical mediated thiol-ene coupling reactions. An initiator fragment abstracts a proton from a thiol, producing a thiyl radical. Thiyl radical is inserted to the carbon-carbon double bond, making a carbon-centered radical. Chain transfer regenerates the thiyl radical and completes the thiol-ene coupling. ....	22
Figure 1.6: Possible modes of oxygen inhibition. The first mode is triplet-state deactivation followed by initiator fragment and monomer/polymer termination by peroxy radical formation. Oxygen inhibition is limited in the presence of proton donors, DH, like amines and thiols, which react with peroxy radicals to form propagating species. ....	23
Figure 1.7: Cationic photoinitiator components. A Cations i) Triarylsulfonium, TAS; ii) diaryliodonium, DAI. B Anions: iii) hexafluoroarsenate, AsF <sub>6</sub> <sup>-</sup> ; iv) hexafluoroantimonate, SbF <sub>6</sub> <sup>-</sup> ; v) hexafluorophosphate, PF <sub>6</sub> <sup>-</sup> ; vi) triflate; vii) tetrakis(pentafluorophenyl)borate. ....	24
Figure 1.8: Photo-acid generation by direct photolysis of DAI. HMTX <sub>n</sub> is a very strong Bronsted acid produced from reactions between various photolysis products of DAI. ....	25
Figure 1.9: Cationic chain propagation of VCM by the ACE mechanism: Monomer protonation and formation of a secondary oxonium ion, followed by formation of tertiary oxonium ion. ....	26
Figure 1.10: Cationic propagation of VCM by the AM mechanism with water as the CTA. Monomer protonation, formation of secondary oxonium ion	

and reaction with CTA to produce organic hydroxyls and regenerate acid.....	27
Figure 1.11: Energy-level diagram illustrating the different types of light scattering modes.....	28
Figure 3.1: Molecular structure of epoxide monomer EEC.....	44
Figure 3.2: Characteristic MIR spectral bands of epoxide monomer EEC before and after photopolymerization. Reactive epoxide band is located at $760\text{ cm}^{-1}$ , and the band for ether linkages formed by polymerization are located at $1080\text{ cm}^{-1}$ .....	45
Figure 3.3: Characteristic NIR spectral bands of water and alkyl hydroxyl groups changing during the cationic ring-opening photopolymerization of EEC. The peak frequency of water is located at $5226\text{ cm}^{-1}$ and of the alkyl hydroxyl groups at $4778\text{ cm}^{-1}$ .....	46
Figure 3.4: Epoxide conversion profiles obtained from RT-MIR spectra for the cationic ring-opening photopolymerization of EEC formulations containing varying concentrations of water. Arrows indicate increased induction time and conversion with increasing water concentration.....	47
Figure 3.5: Water consumption profiles obtained from RT-NIR spectra for the cationic ring-opening photopolymerization of EEC formulations containing varying concentrations of water. The arrow indicates increased induction time with increased water concentration.....	48
Figure 3.6: Overlaid NIR and MIR experiments during the the cationic ring-opening photopolymerization of EEC formulation containing 1.43 mol H <sub>2</sub> O/L. Water consumption and hydroxyl production obtained from RT-NIR experiments, and epoxide conversion obtained from RT-MIR experiments.....	49
Figure 3.7: Long term study of the cationic ring-opening photopolymerization of EEC formulation containing 1.43 mol H <sub>2</sub> O/L: illumination started at $t = 0$ and stopped at $t = 10$ min. Water consumption and hydroxyl production obtained from RT-NIR experiments, and epoxide conversion obtained from RT-MIR experiments.....	50
Figure 4.1: Synthesis of EEC carried out via aldehyde coupling(Tischenko reaction) followed by oxidation/epoxidation.....	68
Figure 4.2: Chemical structures of (A) the di-epoxide monomer(EEC) and (B) the cationic photoinitiator (PC2506) used in this study.....	69
Figure 4.3: Chemical structures of CTAs used in this study. From top to bottom: (A) Mono-ols: methanol, ethanol, n-propanol, n-butanol, n-hexanol, n-octanol, n-decanol, and n-dodecanol; (B) diols: 1,2-propanediol, 1,2-ethanediol, 1,4-butanediol, polyTHF 250, polyTHF 650, polyTHF 1000, and polyTHF 2000; (C) primary, secondary, and tertiary CTAs: n-propanol, s-propanol, n-butanol, s-butanol, t-butanol; (D) acidic CTAs and aliphatic analogs: phenol, cyclohexanol, 2,2,2-trifluoroethanol, and 2,2,2-trichloroethanol.....	70



Figure 4.4: Epoxide conversion profiles. Formulations varied in increments of 0.1 OH equivalents from neat EEC (dashed line) to 0.5 OH equivalents from n-octanol (A) and 1.0 OH equivalents from 1,2-propanediol (B).....	71
Figure 4.5: DMA traces showing the tan d (left) and the storage modulus (right) for EEC formulations containing n-octanol (A and B) or 1,2-propanediol (C and D) as CTA. Polymer specimens were annealed before measurements.....	72
Figure 4.6: Gel fraction data for polymers prepared from EEC:octanol (open triangles) and EEC:1,2-propanediol (filled circles) formulations.....	73
Figure 4.7: A comparison of a propagating cationic active center reacting with two types of CTAs (Case 1: a mono-ol, Case 2: a diol). ....	74
Figure 4.8: Glass transition temperature (filled circles) and rubbery modulus (open circles) of polymers prepared from EEC:- mono-ols formulations as a function of the carbon chain length of aliphatic alcohols used as CTAs. All formulations contained 0.3 OH equiv CTA and were photocured and annealed before analysis. Carbon chain length $\frac{1}{4}$ 0 for neat EEC.....	75
Figure 4.9: Final conversions (A) and maximum rates of epoxide consumption (B) observed in EEC formulated with diols. Each CTA was formulated to 0.1 (black bar), 0.2 (light gray bar), and 0.3 (dark gray bar) OH equivalents. The horizontal line represents the conversion and maximum rate observed in neat EEC.....	76
Figure 4.10: Glass transition temperature (filled circles) and rubbery storage modulus (open circles) of polymers prepared from EEC:diol formulations as a function of the molecular weight of the diols used as CTAs. All formulations contained 0.3 OH equiv CTA and were photocured and annealed before analysis. MW $\frac{1}{4}$ 0 for neat EEC. ....	77
Figure 4.11: Conversion profiles for EEC:(n, s, or t) butanol formulations. The OH concentration was equal to the oxirane concentration in all cases.....	78
Figure 4.12: Final conversions (A) and maximum rates of epoxide consumption (B) observed in EEC formulated with acidic CTAs and their aliphatic analogs. Each CTA was formulated to 0.1 (black bar), 0.2 (light gray bar), and 0.3 (dark gray bar) OH equivalents. The horizontal line represents the conversion and maximum rate observed in neat EEC. ....	79
Figure 5.1: Epoxy silicone monomer, PC-1000 (top); chain transfer agent, n-decanol (middle); and photoinitiator PC-2506 (bottom) .....	88
Figure 5.2: Storage modulus (A) and tan delta (B) profiles of a photocured and annealed silicone epoxy formulation .....	89
Figure 5.3: Cross sections of the polymer specimens after indentation procedure were acquired. Dry-cured materials are represented in A and humid-cured materials are represented in B. Indentations were obtained by applying 12.5, 10.0, and 8.5 $\mu$ N from left to right. ....	90

Figure 5.4: Force curves obtained during the indentation procedure via AFM. Solid traces represent the penetration step and the dashed lines represent the retraction step.....	91
Figure 6.1: Molecular structure of epoxide monomer EEC.....	98
Figure 6.2: Storage modulus and $\tan \delta$ profiles obtained from EEC formulations with dodecanol (A,B), and n-butanol (C,D) as CTAs. Solid lines represent data collected from specimens that were photocured and the dashed lines were obtained from specimens that were photocured and annealed above the glass transition temperature.....	99
Figure 6.3: Storage modulus and $\tan \delta$ profiles obtained from EEC formulations with 1,4-butanediol (A,B), and t-butanol (C,D) as CTAs. Solid lines represent data collected from specimens that were photocured and the dotted lines were obtained from specimens that were photocured and annealed above the glass transition temperature.....	100
Figure 7.1: Network structures formed from hybrid polymerizations: (A) full-IPN, Polymers 1 and 2 are cross-linked; (B) semi-IPN, Polymer 1 is cross-linked, Polymer 2 is linear; (C) full-GPN, Polymers 1 and 2 are cross-linked and grafting occurs; (D) semi-GPN, Polymer 1 is cross-linked, Polymer 2 is grafted to Polymer 1; (E) GP, Polymer 1 is linear, Polymer 2 is grafted to Polymer 1.....	114
Figure 7.2: Molecular structure of the polyether formed via ACE propagation of cyclohexene oxide.....	115
Figure 7.3: Molecular structure of the polyacrylates formed via RAFT polymerization. The butyl acrylate homopolymer (poly(BA)) is left and the random copolymer of butyl acrylate and 4-hydroxybutyl acrylate (poly(BA-ran-HBA)) right.....	116
Figure 7.4: GPC traces of linear polyacrylates, linear polyethers, polymer blends, and grafted polymers. The polymer blends were formed by polymerizing cyclohexene oxide in the presence of poly(BA) or poly(BA-ran-HBA), not by simply mixing the polymer products. Depictions of polymers on the left include solid lines for polyacrylates, and solid lines broken by unfilled circles for polyethers. ....	117
Figure 7.5: DMA traces showing the storage modulus (left) and the $\tan \delta$ (right) for formulations of neat diepoxide monomer (solid line) and diepoxide with poly(BA) (squares) or poly(BA-ran-HBA) (circles). Polyacrylates were 30 wt% of the epoxide monomer mass. Polymer specimens were annealed before measurements.. ....	118
Figure 7.6: DMA traces showing the storage modulus (left) and the $\tan \delta$ (right) for formulations of diepoxide monomer and polyTHF 250. PolyTHF 250 mass was equal to 0 wt% (solid line), 7 wt% (squares), 15 wt% (circles), and 30 wt% (triangles) of the epoxide monomer mass. Polymer specimens were annealed before measurements. ....	119
Figure 8.1: A generalized reaction sequence for the production of cationic active centers via the radical promoted cationic polymerization mechanism. ....	130

Figure 8.2: Monomer structures: (A) EEC, (B) BGE, (C) VCM, (D) HEA, (E) EGMEA. ....	131
Figure 8.3: Photoinitiator structures: (A) PC-2506, (B) Irgacure 651, (C) Irgacure 819, (D) Lucirin TPO.....	132
Figure 8.4: Final epoxide conversions of (A) EEC, and (B) BGE and epoxide conversion profiles (C) VCM systems.....	133
Figure 8.5: Conversion profiles for hybrid acrylate-epoxide systems varying in free-radical initiator: (A) PC-2506 only, (B) PC-2506:Irgacure 651, (C) PC-2506:Irgacure 819, (D) PC-2506:Lucirin TPO. Closed circles indicate acrylate conversion; open triangles indicate epoxide conversion. ....	134
Figure 8.6: Molar absorptivities as a function of wavelength for the initiators used: PC-2506 ( <i>open circles</i> ), Lucirin TPO ( <i>filled triangles</i> ), Irgacure 819 ( <i>filled squares</i> ), Irgacure 651 ( <i>filled diamonds</i> ). ....	135
Figure 9.1: Chemical structure of ricinoleic acid in triglyceride form. ....	150
Figure 9.2: Isocyanate and alcohol functional groups readily couple with the hydrogen-bonded complex as the intermediate.isocyanate-coupling reaction.....	151
Figure 9.3: Castor oil reacts with AOI monomer in the presence of a tertiary amine catalyst to form acrylated castor oil (ACO), represented by an ideal triglyceride composed of three ricinoleic acid residues.....	152
Figure 9.4: FT-IR spectra of neat AOI monomer (A), neat castor oil (B), and the product of AOI-castor oil coupling (C). Spectrum A shows the strong absorbance of the NCO band centered around $2270\text{ cm}^{-1}$ , as well as the carbonyl peak centered around $1710\text{ cm}^{-1}$ and the acrylate peaks at $1640\text{ cm}^{-1}$ and $810\text{ cm}^{-1}$ . Spectrum B shows the broad OH band centered around $3300\text{ cm}^{-1}$ and the carbonyl centered at $1710\text{ cm}^{-1}$ . Spectrum C indicates quantitative consumption of the NCO functional group as there is no peak at $2270\text{ cm}^{-1}$ . In addition to the NCO consumption, the acrylate functional group is retained according to the absorbances at $1640\text{ cm}^{-1}$ and $810\text{ cm}^{-1}$ . Dashed lines highlight the peaks at 2270, 1640, and $810\text{ cm}^{-1}$ .....	153
Figure 9.5: The isocyanate conversion by coupling with castor oil monitored by FT-IR spectroscopy. The isocyanate band centered at $2270\text{ cm}^{-1}$ was used for analysis.....	154
Figure 9.6: $^1\text{H}$ NMR spectra of neat AOI monomer (A), neat castor oil (B), and the product of AOI-castor oil coupling (C). Spectrum A shows peaks characteristic of the olefinic protons of the acrylate double bond and the methylene protons on carbons adjacent to the ester and isocyanate functional groups. Spectrum B is more complex due to the variety of protons present. The bands diagnostic of the reaction are the hydroxyl proton (2.74 ppm) and the proton of the carbon alpha to the hydroxyl group (3.56 ppm). Spectrum C shows the consumption of the O-H band and the appearance of the N-H band (4.96 ppm), as well as the shift of	

the alpha-hydroxy proton (3.56 ppm) to an alpha-carbamate proton (4.69 ppm).....	155
Figure 9.7: Acrylate conversions obtained by RT-IR spectroscopy: Neat ACO and co-polymerizations with mono-acrylate monomers (A) and multi-acrylate monomers (B). Room-temperature photopolymerizations with 1wt% free-radical photoinitiator and 50 mW/cm <sup>2</sup> effective irradiance. ....	156
Figure 9.8: Dynamic mechanical analysis of photopolymerized films with a nominal thickness of 300 μm: tan δ profiles of polymerized ACO and copolymers of mono-acrylate monomers (A) and multi-acrylate monomers (B), as well as storage modulus as a function of temperature for polymerized ACO and copolymers of mono-acrylate monomers (C) and multi-acrylate monomers (D).....	157
Figure 9.9: A comparison of the Fox correlation-derived T <sub>g</sub> and the measured copolymer T <sub>g</sub> taken as the temperature corresponding to the tan δ maximum. The line represents perfect correlation between measured and predicted T <sub>g</sub> 's.....	158
Figure 10.1: An experimental matrix designed to compare dark cure and shadow cure in epoxide systems that vary in T <sub>g</sub> without promoted the AM mechanism ( <i>left column</i> ) to epoxide systems that vary in T <sub>g</sub> but do have CTAs which strongly promote the AM mechanism ( <i>right column</i> ). ....	171

## CHAPTER 1

### INTRODUCTION AND BACKGROUND

#### 1.1 Photopolymerization

Photopolymerization, which uses light rather than heat to initiate polymerization, is a facile technique used to fabricate adhesives, protective coatings, thin films, photoresists, dental restoratives, and other materials.<sup>1-5</sup> One attractive feature of photopolymerization is the high level of spatial and temporal control afforded by it. The photo-radical, photo-acid and photo-base generators used in photopolymerization are dormant until photons of sufficient energy promote the absorbing species to an excited electronic state. The excited molecule then decays into reactive species or transfers energy by radiative or non-radiative mechanisms. Therefore, the pot life of photopolymerizable formulations is very long and allows for handling or processing of the polymerizable resins in ways that other coating systems, such as epoxy gel coats, do not.<sup>6-9</sup> Additionally, the reactivity of monomers used in photopolymerization is very high at room temperature and results in extraordinary manufacturing line speeds without the need of thermal treatment to ensure tack-free surfaces and high levels of monomer conversion.<sup>10-12</sup> The monomers and resins used in photopolymerization most often have an average functionality greater than two. As a result, cross-linked polymers that are thermally stable and chemically resistant, two characteristics required by many photopolymerization applications, are produced.<sup>1,2</sup>

##### 1.1.1 Free-Radical Systems

The most common polymerization mechanism used in photopolymerization is free-radical chain polymerization. Free-radical photopolymerizations are generally very fast (cure achieved < 10 seconds) and reach very high conversions (conversion > 70-90% depending on the system).<sup>4,13</sup> There are a variety of effective photoinitiating systems for

free-radical photopolymerization, as well as many types of monomers that are polymerizable via free radical mechanisms.<sup>6,14-17</sup> Some of the important monomer classes include: acrylates, methacrylates, acrylamides, methacrylamides, vinyl esters, and thiol-ene systems, where “ene” refers to a non-specific carbon-carbon double bond.<sup>4,5</sup> One major difficulty with free-radical polymerizations is the potent inhibitory effect of atmospheric oxygen, which severely hinders the photopolymerization of thin films in normal atmospheric conditions.<sup>18</sup> Many researchers have worked to resolve the non-trivial problem oxygen inhibition poses, and these efforts are discussed in more detail below.

The initiation reactions are collectively the rate limiting step in chain polymerizations and normally require external heating for the initiator to decay to free-radical active centers and initiate polymerization. The design of organic molecules that are thermally stable, yet yield radicals through photolytic processes with high photochemical yields, enables photopolymerization at low temperatures.<sup>19</sup> These polymerizations are generally initiated by one of two types of free-radical photoinitiators. Type I photoinitiators, also referred to as cleavage initiators, absorb a photon of appropriate energy, which promotes the molecule to an excited state. The excited molecule then releases the energy by luminescence or non-radiative energy transfer or undergoes homolytic cleavage, resulting in reactive radical species that initiate polymerization. An example of photodecomposition of a common Type I photoinitiator, 2,2-dimethoxyphenyl acetophenone (DMPA), is shown in Figure 1.1.<sup>1,2,5</sup>

Type II photoinitiators undergo proton abstraction and/or electron transfer to generate active radicals. Similar to Type I photoinitiators, the Type II photoinitiator molecule absorbs a photon of appropriate energy, which promotes it to an excited state. From the excited state, the molecule can lose its energy through luminescence, non-radiative energy transfer, or reaction with a proton-donating species, or co-initiator, such as a tertiary amine. The radical produced alpha to the nitrogen on the tertiary amine can

initiate polymerization. The absorbing species is referred to as the photoinitiator in photoinitiating system as it is the species responsible for photosensitivity. An example of Type II photoinitiation with 4-isopropyl-9-thioxanthone (ITX) as the photoinitiator and N-methyldiethanolamine as the co-initiator/proton donor is shown in Figure 1.2.<sup>1,2,15,17,20</sup>

While both Type I and Type II photoinitiating systems result in low temperature photopolymerizations, there are important distinctions to be made between these systems. Type I photoinitiation is a monomolecular process involving the photolysis of the absorbing species. The cleavage-type initiators have high photochemical efficiencies and absorb short-wavelength UV to visible light, depending on the particular molecule; many of the common effective initiators absorb at wavelengths less than 380 nm. Type II photoinitiation is a bimolecular process, which makes it inherently slower than Type I, and the photoinitiators often absorb mid-UV to visible light. For high-speed production processes using mercury arc lamps, which produce intense UV light, Type I initiators are favored for the high photo efficiency and resultant high rates of cure. In applications that cannot use high-intensity UV lamps and must maintain low curing temperatures, such as dental restorative materials, the Type II systems are favored for the red-shifted absorbance and the lower polymerization rates that provide a lower temperature rise during curing. It is the curing conditions, established by the application, which will determine the type of photoinitiation system to be used.<sup>1,2</sup> Examples of type I and type II photoinitiators are shown in Figure 1.3.

In radical chain polymerization a radical, from an initiator fragment, adds across the double bond of a monomer resulting in a carbon-centered free radical on the monomer. This free radical is now the active center that reacts similarly with another monomer. An example of the chain polymerization of 2-hydroxyethyl methacrylate (HEMA) is shown in Figure 1.4. The propagation reactions occur in concert with termination reactions: free-radical coupling or disproportionation. When the termination reactions occur faster than the propagation reactions or the monomer is depleted,

polymerization rates decrease, and the polymerization is stopped. Using the quasi-steady state approximation, which states that radical production equals consumption or the rate of radical termination equals the rate of initiation, the rate of polymerization for free-radical chain kinetics can be expressed as shown in Eq. 1.1 below:

$$R_p = k_p [M] \left( \frac{R_i}{2k_t} \right)^{1/2} \quad 1.1$$

Where  $R_p$  is the rate of polymerization,  $k_p$  is the propagation rate coefficient,  $k_t$  is the termination rate coefficient,  $[M]$  is the monomer concentration, and  $R_i$  is the rate of initiation. The rate of initiation for photopolymerization is defined in Eq. 1.2 below:

$$R_i = 2\Phi I_a \quad 1.2$$

Where  $I_a$  is the absorbed light intensity, which is proportional to the initiator concentration and the incident light intensity, and  $\Phi$  is number of propagating chains produced per photon absorbed often called the quantum yield for initiation and the factor 2 means for this particular initiating system two free-radicals are produced from one initiator molecule. For a initiator generating only one active free radical 2 would be replaced by 1. Substitution of Eq. 1.2 into 1.1 gives Eq. 1.3 below:

$$R_p = k_p [M] \left( \frac{\Phi I_a}{k_t} \right)^{1/2} \quad 1.3$$

Where  $I_a$  is the absorbed light intensity, which is proportional to the initiator concentration and the incident light intensity, and  $\Phi$  is quantum yield for initiation. This equation shows that the rate of polymerization is proportional to the square root of light intensity and/or the initiator concentration.<sup>4,13</sup>

The wide selection of available monomers produces materials that vary dramatically in physical and mechanical properties. Acrylates and methacrylates, in particular, are easily modified, enabling property tailoring through judicious monomer selection. These rapidly polymerizing species produce very broad glass transitions when



polymerized in bulk by UV light, as opposed to those resulting from traditional solution polymerization. This characteristic results from microgels that form early in photopolymerization due to slight spatial variances in light intensity, creating spatial variances in polymerization rates.<sup>21,22</sup> The distribution of polymerization rates produces a material that has a distribution in moduli, which accounts for the distinctively broad glass transitions associated with multi-(meth)acrylates.

Another important group of radically polymerizable monomers is the family of thiol-enes.<sup>23</sup> Thiols bear a proton that is labile to abstraction by some radical species, such as an initiator fragment, which results in a thiyl radical. This radical can react with a carbon-carbon double bond (i.e., the propagation reaction), producing a carbon-centered radical. This carbon-centered radical then can abstract a proton from thiol functional groups (i.e., the chain transfer reaction) to complete the catalytic cycle that is depicted in Figure 1.5.<sup>24,25</sup> This mechanism is a radical-mediated step polymerization and differs from the radical chain polymerizations discussed earlier in that each thiol couples with one “ene” and homopolymerization of the “ene” species is negligible or significantly suppressed. This coupling effectively changes the functionality of the “ene” species to one rather than a functionality of two, as is needed in the radical chain mechanism. The kinetics of thiol-ene photopolymerization is also different from that of acrylate photopolymerization: the rate of thiol-ene photopolymerization is based on step-growth kinetics, which suggests stoichiometric dependence, and is proportional to initiator concentration and light intensity. In addition to differing from chain photopolymerized materials kinetically, the thiol-ene materials possess unique mechanical properties, including much lower and narrower glass transitions.<sup>26,27</sup>

A major problem for free-radical polymerization is inhibition by molecular oxygen.<sup>18,28</sup> The photopolymerization of thin films suffers considerably from oxygen inhibition due to the extremely high surface area to volume ratio, which means molecular oxygen can penetrate a large percentage of the resin and hinder, or in very thin films halt,

polymerization. Simulations and experiment have shown that the top 15-20 microns of a polymerizable resin will not react to form polymers even if very high photoinitiator concentrations are used.<sup>28,29</sup> Molecular oxygen inhibits radical polymerization in two ways. First, it quenches the initiator. Ground-state molecular oxygen is a triplet state, meaning it can transfer energy from the excited triplet-state initiator molecules and return them to the ground state rather than producing active centers. The second and more considerable way by which oxygen inhibits polymerization is due to the diradical nature of oxygen. Thus, oxygen can rapidly convert free-radical species, whether initiator fragments or free radicals on a propagating chain, to peroxy radicals that do not react with (meth)acrylate monomers.<sup>18</sup> Oxygen inhibition reactions are shown in Figure 1.6.

Some techniques have been developed to overcome oxygen inhibition. One method involves displacing the oxygen with an inert gas such as nitrogen or carbon dioxide.<sup>30</sup> While displacement is effective, it is very expensive. In another method, sacrificial barriers like waxes are applied on top of the resin and removed post-polymerization. Not all resins or applications lend themselves to this barrier treatment, and resulting film surface properties are not desirable or well controlled. The third way oxygen has been circumvented is by using high initiating light intensities and/or high initiator concentrations in order to maximize the polymerization rate in the presence of oxygen.<sup>31</sup> The use of chemical additives that effectively scavenge oxygen is yet another way to overcome oxygen inhibition. These include amines and thiols. This method often results in unreacted chemicals that have plasticizing effects and can later leach from the polymer, causing toxicity issues. In the case of thiol-ene systems, this method is not a problem since multifunctional thiols are often used. The resulting thiol conversions are often very high, which means the remaining thiol-bearing species are covalently bonded to the polymer matrix and the thiols are rendered intractable. Since thiol-ene chemistry is not inhibited by oxygen, it is an attractive alternative to chain photopolymerization of (meth)acrylates.<sup>23</sup>

Free radical polymerizable monomer systems are in abundance and variety. Many free radical systems have been studied and well characterized. It is the use of reaction kinetics, property development, and formulation capabilities that new materials can be developed by suitable monomer combinations or novel oligomer synthesis by thiol-ene reactions.<sup>27,32</sup>

### 1.1.2 Cationic Systems

The cationic ring-opening polymerization (CROP) of cyclic ethers, particularly epoxides, is another important reaction in photopolymerization. In some cases, cationic photopolymerizations of select monomers can meet or exceed the polymerization rates of (meth)acrylate species.<sup>33,34</sup> However, in general, cationic photopolymerizations are slower than free-radical photopolymerizations.<sup>2,5</sup> In contrast to free-radical reactions, the CROP mechanism is unaffected by molecular oxygen. Epoxide formulations containing a photo-acid generator (PAG) are readily polymerized at room temperature in air.<sup>8</sup> Although oxygen does not affect CROP, water, another ubiquitous chemical species, has a significant impact. Water and other hydroxyl-containing species are chain transfer agents that alter both the rate of polymerization and the crosslink density or number-average degree of polymerization.<sup>35,35,36</sup> Control of humidity is difficult in a production environment, which makes use of moisture-sensitive systems problematic in that the properties of the polymers are not necessarily readily reproducible due to variances in the humidity levels in production facilities.

Photoinitiation of CROPs is done using PAGs, which produce highly acidic species with Hammett acidity values or very low/negative pKa values. Diaryliodonium (DAI) and triarylsulfonium (TAS) salts were developed in the 1970s and are highly efficient photoinitiators for CROP-type reactions.<sup>7,8</sup> These salts consist of either the DAI or TAS cation and a non-nucleophilic anion, such as hexafluorophosphate, hexafluoroantimonate, hexafluoroarsenate, triflate, tetrafluoroborate, or

tetrakis(pentafluorophenyl)borate. The onium salts are not soluble in water, but are soluble in polar organic solvents such as propylene carbonate. To further aid the dissolution of onium salts into a variety of resins, the cations are modified with hydrophobic R-groups or the salts are available in concentrated solutions of propylene carbonate. These initiators are shown as components in Figure 1.7.

The cation determines the photochemistry of the initiator, most importantly the wavelengths at which initiator is effective, and the efficiency of acid production. The anion governs the acidity of the photogenerated acid and acts as the counterion to the propagating cationic active center.<sup>8</sup> The anion has the largest impact on the rates of polymerization in dark curing (i.e., curing after the initiating UV source has been shuttered), shadow curing (i.e., curing in un-illuminated regions), and particularly curing at high conversions where mobility issues become significant.<sup>37,38</sup> The high acidity of the photo-generated acids and non-nucleophilic nature of the anions affords the cationic active centers very long lifetimes such that photoinitiated CROP reactions are considered living. Photoinitiation occurs by promotion of the initiator molecule to an excited state by photon absorption. From the excited state, the molecule sheds energy by luminescence, non-radiative energy transfer or decay into a variety of free radicals and cationic species. Further reactions with solvent molecules and the species resulting from photochemical decay of the initiator produce the photo generated acid. Although this process involves radical species, the photolysis of DAI and TAS initiators has been shown to be unaffected by molecular oxygen and is shown in Figure 1.8.<sup>7,39</sup>

The CROP reactions can occur in a variety of cyclic ether compounds including cycloaliphatic epoxides (in particular, those based on cyclohexane rings), glycidyl ethers, epoxidized alpha olefins, epoxidized triglycerides, and oxetanes. While there are other cationic polymerizable materials such as styrene and vinyl ethers, the focus of this research is limited to cyclic ethers of the oxirane variety. Similar to acrylate monomers, there are a variety of epoxide monomers available that allow for wide ranges of polymer

properties to be achieved. In general, the monofunctional glycidyl ethers produce rubbery materials, and the higher functionality monomers produce materials with higher crosslink densities. However, the most reactive cyclic ether monomers, cycloaliphatic epoxides, produce very brittle polymers.<sup>40</sup>

CROPs propagate by two mechanisms: the Active Chain End (ACE) and the Activated Monomer (AM) mechanisms. Both ACE and AM mechanisms begin by protonation of the oxygen on the oxirane ring by a photo-generated acid. This protonation produces a secondary oxonium ion, and the monomer that has been protonated is considered activated. The protonation draws electron density away from carbons alpha to the oxygen due to the third bond made with the oxygen and hydrogen. A partial positive charge on carbons in the oxirane ring results thereby promoting nucleophilic attack. The two mechanisms differ in the second step. In the ACE mechanism, the secondary oxonium ion is attacked by a neutral monomer; while in the AM mechanism, the secondary oxonium ion is attacked by a weak nucleophile such as water or alcohol. The ACE mechanism produces a tertiary oxonium, and the AM mechanism yields a hydroxyl group and a proton. The ACE mechanism continues to propagate with neutral monomers reacting with tertiary oxonium ions. For particular monomers the tertiary oxonium ions have lower activation energies and therefore a different rate constant than those associated with the reaction between a neutral monomer and a secondary oxonium ion. In some cases, the energy barrier for secondary oxonium ion attack is similar or indiscernible from that of tertiary oxonium ion attack.<sup>41,42</sup> In the AM mechanism, a hydroxyl species and an acidic proton are regenerated with each reaction. The AM mechanism is a chain transfer reaction: the active center is transferred between many different growing chains rather than isolated to one propagating polymer chain.<sup>43</sup> The chain transfer reactions have different kinetics and result in different polymer properties relative the epoxide polymers synthesized solely by the ACE mechanism. In particular, for monomers which produce linear polymers, the average molecular weight is reduced;

for multifunctional monomers that produce crosslinked networks, the crosslink density is reduced.<sup>44,45</sup> Schematic representations of the ACE and AM mechanisms are shown in Figures 1.9 and 1.10, respectively.

In photopolymerization of thin films, the AM mechanism is important to consider as it is promoted by the presence of water, which is present as vapor and is highly variable in concentration. Variance in water content leads to uncertainty in photopolymerization kinetics and polymer properties, in particular at and near the surface. The surface and near surface of the film are most affected by water vapor, for similar reasons as oxygen in free-radical systems, because water can diffuse into the surface and near surface regions from the time the resin is applied to a substrate and during photopolymerization.<sup>35,41</sup>

Formulation of a cationic system containing cycloaliphatic monomers and chain transfer agents could improve kinetics and film properties.<sup>46,47</sup> While some researchers have produced select reports on some epoxide monomers and the kinetic effects of humidity and/or alcohols, there is a need for a more comprehensive understanding of the types of alcohols that may be used in photopolymerization of epoxides. In addition, the effects on polymer physical properties need to be studied and understood.

### 1.1.3 Hybrid Systems

A method that has been pursued to reduce the deleterious effects of atmospheric factors is the combination of radical and ionic formulations in what is called a hybrid system.<sup>29,48-50</sup> While ionic reactions are not affected by oxygen, the radical systems are not affected by water. Hybrid systems provide photopolymerizable formulations that can be cured in ambient atmospheric conditions. Since hybrid systems are composed of monomers that polymerize by separate, independent reactions, different degrees of phase separation occur. Two linear systems combine to produce a polymer blend (PB), a linear with a cross-linking system makes a semi-interpenetrating network (semi-IPN), and two

cross-linkable monomers make a fully interpenetrating network (full-IPN).<sup>51</sup> PBs often result in macro-scale phase separation; semi-IPNs and full-IPNs range from micro- to nano-scale phase separation and either broad or multiple thermal transitions.<sup>52</sup> Hybrid systems are therefore rich in materials engineering opportunities beyond air-curable resins. Many combinations of ionic and radical photopolymerizable resins are possible. Those that have been studied include hybrid epoxide/(meth)acrylate monomers<sup>29,48,53,54</sup>, epoxy/(meth)acrylate monomer mixtures,<sup>55</sup> vinyl ether/methacrylate<sup>49</sup>, thiol/epoxy/methacrylate ternary systems<sup>56</sup>, and thiol-ene/isocyanate ternary systems<sup>26,57,58</sup>. Many of these reports have been limited to kinetic information, while others showed formulation-dependent physical and mechanical properties. In general, systems under the hybrid paradigm suffer less oxygen inhibition and are not significantly influenced by moisture levels.

Photoinitiation in hybrid systems is unique in that it requires two types of active centers to be formed, free radicals and cations or anions. The DAI and TAS photoinitiators used in cationic photopolymerizations produce both active cations and active radicals.<sup>7,8,39</sup> The radicals produced are not capable of initiating radical polymerization of all types of monomers, but a few select systems have used only DAI or TAS and achieved significant acrylate monomer conversions.<sup>53,54</sup> To ensure efficient free-radical polymerization in cationic-free radical hybrid photopolymerizations, a free-radical photoinitiator must be added to the formulation in addition to DAI or TAS.<sup>55</sup> This dual photoinitiator system complicates the initiation process.<sup>59</sup> With two photosensitive species present, beneficial or detrimental effects can occur. DAI or TAS, which typically absorb only in the deep-UV region, can be photo-sensitized<sup>60,61</sup> (*i.e.*, promoted to an excited state by non-radiative energy transfer by another photosensitive species, the secondary radical generator), thereby broadening the wavelengths that effectively initiate cationic polymerization. DAI, not TAS, is a strong oxidant, which has been demonstrated to oxidize radicals of appropriate reduction potentials to carbon, phosphorous or even

germanium-centered cationic species that effectively initiate CROP reactions.<sup>62-66</sup>

Conversely, the second initiator may have poor photo-sensitizing efficiencies and/or not produce oxidizable radicals that allow for radical-promoted cationic polymerization. In the latter case, cationic polymerization would be significantly hindered by the addition of a secondary radical generator since it would simply serve as a UV filter competing for initiating photons. Photoinitiation in cationic/free-radical hybrid photopolymerizations is complex and requires experimentation to develop effective and robust initiating systems.

The anionic thiol/isocyanate coupling and radical thiol-ene hybrid photopolymerization studied by Shin *et al.* have demonstrated a synergistic photoinitiation system that has potential to be generalized to many other anionic/free-radical formulations.<sup>58</sup> Tri-butyl amine was shown to catalyze the thiol-isocyanate coupling reaction and was prepared as a photo-latent base with tetraphenyl borate, as discussed in the anionic section. The photoinitiator suffered from poor photoefficiency unless coupled with ITX, which served as a photosensitizer and red shifted the initiator such that photobase generation was achieved upon 365 nm light illumination. Once the amine was released, it could act as a base catalyst for the anionic reaction and a co-initiator for the free-radical thiol-ene reaction. This relatively simple system was able to initiate the two reactions simultaneously.

In addition to lower sensitivity to atmospheric factors, hybrid systems allow for property tuning in very simple ways. Magwood showed modulation of glass transition temperature ( $T_g$ ) over more than 100°C in several epoxy/acrylate systems, and Hoyle *et al.* has shown similar tuning capabilities in thiol-ene/acrylate and thiol-ene/isocyanate systems by simply adjusting the mole ratios of the high and low  $T_g$  components.<sup>26,57,58,67</sup> Thus, hybrid systems present the formulator with a robust set of tools to meet a variety of polymeric material specifications.



## 1.2 Analytical methods

### 1.2.1 Raman and Infrared Spectroscopy

Polymerization occurs by repeated chemical reactions during which chemical bonds of one type are broken and another type are formed. For example, in vinyl polymerizations, the carbon-carbon double bond is broken, and a new carbon-carbon single bond is formed. The analytical method appropriate for detecting changes in chemical bonds is vibrational spectroscopy. In a vibrational spectrum, different chemical bonds can be resolved, and the amount/concentration of a particular chemical bond can be measured over the course of a reaction by monitoring the intensity of the band associated with the bond of interest. Assuming constant sample geometry and optical properties, the decrease in band signal, usually peak area or peak height, means a decrease in concentration of that particular chemical species. This information can be used to calculate conversion of monomer to polymer, in the basest case, by obtaining pre- and post-illumination spectra or in real-time, depending on the temporal resolution of the instrument relative to the speed of the reaction of interest. The two types of spectroscopy commonly used in photopolymerization research are Raman and infrared (IR) spectroscopy. These two spectroscopic techniques are both vibrational spectroscopic techniques; they probe the same type of information, but arrive at vibrational spectra by two distinctly different mechanisms.

Raman spectroscopy is one type of vibrational spectroscopy based on the Raman effect, which involves inelastic scattering of photons.<sup>68,69</sup> In the Raman effect, a photon incident to the sample interacts with a particular chemical bond by polarizing it and promoting it to a virtual excited state. As the bond relaxes to some vibrational level in the ground state, a second photon is released or scattered. If the vibrational level is the same as the original level, the frequency of the scattered photon matches the frequency of the incident photon and is termed Rayleigh scattering. If the scattered photon's frequency is

less than the incident photon's frequency, Raman scattering occurs and is termed the Stokes shift. The other form of Raman scattering is the anti-Stokes shift, which occurs when the scattered photon has a frequency larger than the incident photon's. These different types of scattering are shown in Figure 1.11. Stokes and anti-Stokes shifts give the same vibrational information. Stokes-shifted scattering is more probable due to the greater population of molecules in the ground state vs. excited state and therefore often gives higher intensities. The difference between the shifted photon frequency and the incident photon frequency is equal to the frequency of vibration of the chemical bond associated with the scattering event. Therefore, a vibrational spectrum of a particular compound is simply a collection of scattered light as a function of frequency relative to the incident frequency.<sup>70</sup>

The intensity of scattering and therefore the Raman spectral intensity is dependent on several variables. One factor in the scattering intensity is the polarizability of the scattering species.<sup>70</sup> Polarizability dependence is apparent in the vibrational spectra of thiols. For example, in the IR absorbance spectrum, the band associated with S-H bonds in thiols is very weak, while in the Raman spectrum it is very strong and well resolved. This difference is due to the high polarizability of thiols. A second factor affecting the intensity of the Raman spectrum is the intensity of the incident light source. This dependence is intuitive in that the scattering events have a certain probability to occur and if the number of photons that induce the Raman scattering is increased, the probability of the scattering to occur increases proportionately. Additionally, the frequency of the incident light source increases the scattered light intensity as the incident light source frequency increases. Therefore, for high intensity spectra, it would follow that high intensity UV lasers would be the best choice for incident light sources. If the sample has no fluorescent species present, UV lasers would produce the highest scattering intensity, but in the case of photopolymerizable resins, the photoinitiators added to the systems are very likely to fluoresce. Since fluorescence is much more

probable than Raman scattering, the fluorescence spectrum overwhelms the Raman spectrum, and no useful vibrational data are obtained. The use of near-IR lasers limits this problem, since the long wavelength photons do not have sufficient energy to promote the fluorescent species to an excited state, and has allowed for polymer samples to be analyzed by Raman spectroscopy.<sup>71,72</sup>

IR spectroscopy gives the same type of spectral information, but by a different simple mechanism: absorbance. The range of vibrational frequencies of chemical bonds coincides with frequencies in the mid- and near-IR region of the electromagnetic spectrum. A broad-band IR source is introduced to the sample; the frequencies that match the vibrational frequencies of the bonds/functional groups of the sample are absorbed by the sample. An IR spectrometer simply compares the intensity, as a function of frequency, of the light source that reaches the detector after passing through the sample to the intensity of the light source that did not pass through the sample to produce a spectrum.<sup>73</sup>

Several variables dictate the absorbance of a particular absorbing species in a sample. All absorbance spectroscopic techniques are based on the Beer-Lambert law:

$$A = \epsilon bc \quad 1.4$$

Where  $A$  is the absorbance,  $\epsilon$  is the molar absorptivity or extinction coefficient,  $b$  is the path length, and  $c$  is the concentration of the species of interest. The molar absorptivity is an intensive property, while the path length is an extensive property that can be changed to modulate the absorbance value. In the mid-IR region of the electromagnetic spectrum, organic functional groups have very high molar absorptivities that limit the path length to 10-20  $\mu\text{m}$ . This limit is to ensure absorbance responses have linear Beer-Lambert law behavior. In the near-IR region, organic functional groups have much lower molar absorptivities, which allow for much longer path lengths, about 1 mm. One advantage of

the near-IR region is that the band associated with aliphatic hydroxyl groups and the bands for water are well resolved, unlike in the mid-IR.<sup>74</sup>

Raman and IR spectroscopy are complementary analytical techniques. As mentioned earlier, Raman scattering is most intense with highly polarizable bonds. Non-polar bonds are often highly polarizable. Conversely, IR absorption requires a dipole moment. It is generally, but not exclusively true that, bonds with high IR molar absorptivities often show very poor Raman signal intensities and species that are highly polarizable give intense Raman signals but very weak IR absorption. Therefore, it is advantageous to have both techniques available in order to study a variety of polymerization reactions, using a variety of monomer types, thereby allowing the researcher to use the technique giving the best signal, assuming other experimental considerations are equal.<sup>73</sup> For real time kinetic experiments the characteristic signals from IR absorbance or Raman scattering spectra are used to generate conversion profiles. The peak height or area for a particular sample can give the relative abundance of unreacted monomer species remaining, which is used to calculate,  $x$ :

$$x = 1 - \frac{S_t}{S_0} \quad 1.5$$

Where  $S_t$  is the functional group signal at time  $t$  and  $S_0$  is the functional group signal at the beginning of the kinetic experiment ( $t = 0$ ). This is a powerful technique for probing polymerization kinetics.

### 1.2.2 Dynamic Mechanical Analysis

Once a polymer is formed, the utility of the material is determined by its mechanical performance. A dynamic mechanical analyzer (DMA) is an invaluable tool in determining the physical and mechanical properties of a polymer. Polymers differ from other materials in that they have complex mechanical behavior known as viscoelasticity. A sample of geometry compatible with the test type (tensile, shear, compression, *etc.*) is

subjected to a sinusoidal strain at a set frequency or range of frequency sweeps, and the resulting stress is measured, which allows for computation of the complex modulus. The complex modulus is composed of a storage and loss modulus. The storage modulus is related to the energy stored in the polymer, representing the elastic portion; while the loss modulus is related to the energy lost as dissipated heat, representing the viscous portion. The ratio of the loss modulus to the storage modulus is called the  $\tan \delta$ , phase angle, loss tangent, or loss factor. The relationships of mechanical properties are shown in the following equations:

$$\sigma = \sigma_o \sin(\omega t + \delta) \quad 1.6$$

$$\varepsilon = \varepsilon_o \sin(\omega t) \quad 1.7$$

$$E' = \frac{\sigma_o}{\varepsilon_o} \cos(\delta) \quad 1.8$$

$$E'' = \frac{\varepsilon_o}{\sigma_o} \sin(\delta) \quad 1.9$$

$$\tan \delta = \frac{E''}{E'} \quad 1.10$$

Where  $\varepsilon$  is strain,  $\sigma$  is stress,  $E'$  is the storage modulus,  $E''$  is the loss modulus,  $\omega$  is the frequency, and  $\delta$  is the phase angle. The  $\tan \delta$  recorded as a function of temperature gives the onset of primary and secondary transition temperatures, breadth of transition temperatures, and the temperature range within which the polymer can effectively absorb mechanical energy. Energy absorption usually occurs in the form of vibration damping by heat dissipation. In addition to transition temperatures and damping functions, DMA can be used to generate stress-strain curves at various temperatures and strain rates to accurately describe the behavior of the material under stress.<sup>75</sup>

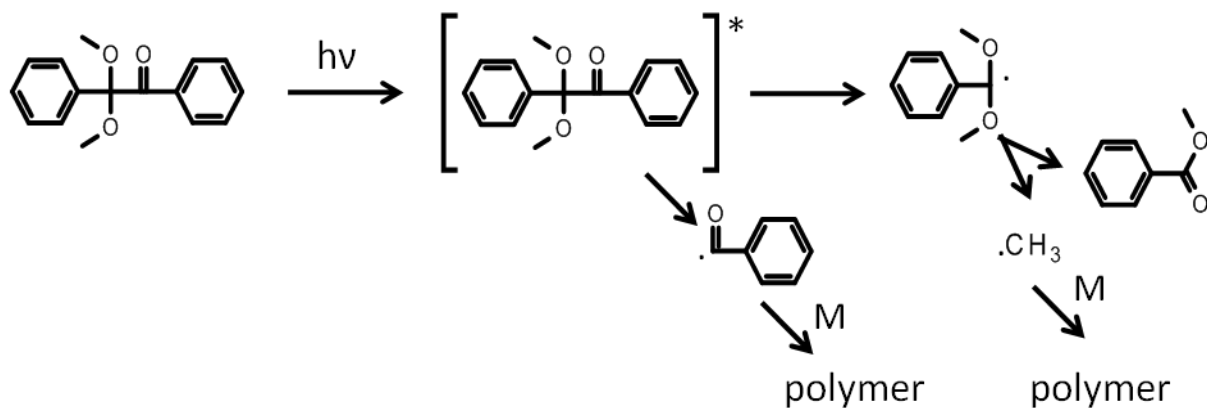


Figure 1.1: Photogeneration of initiating radicals by a Type I photoinitiating system, Irgacure 651. The two major initiating species produced are the benzoyl radical and the methyl radical.

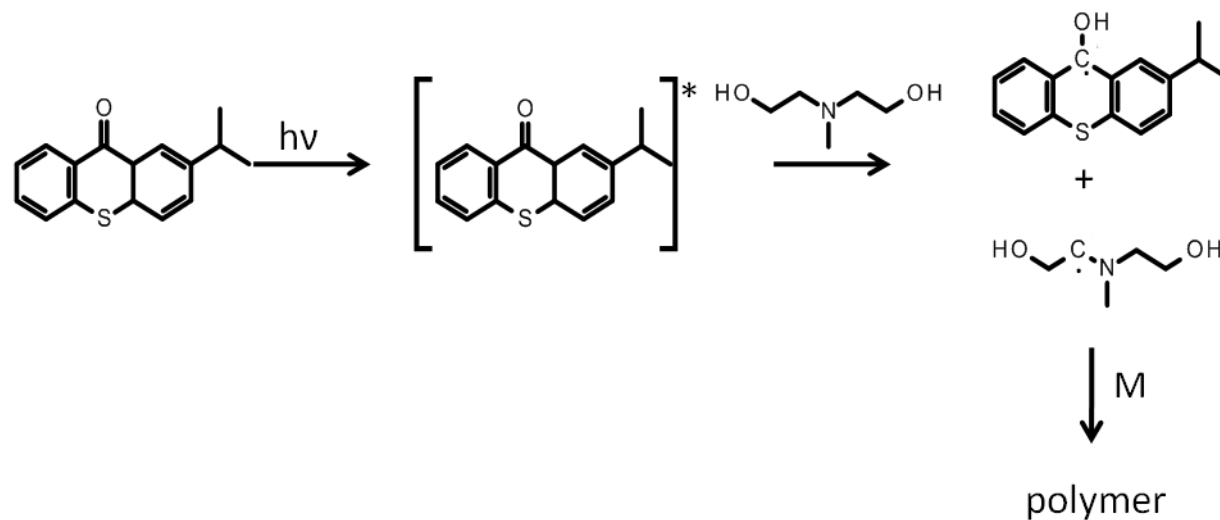


Figure 1.2: Photogeneration of initiating radicals by a Type II photoinitiating system composed of ITX and MDEA. ITX is promoted to an excited state by photon absorption. While in the excited state ITX abstracts a proton from a carbon alpha to the nitrogen of MDEA, producing a carbon-centered radical that initiates polymerization.

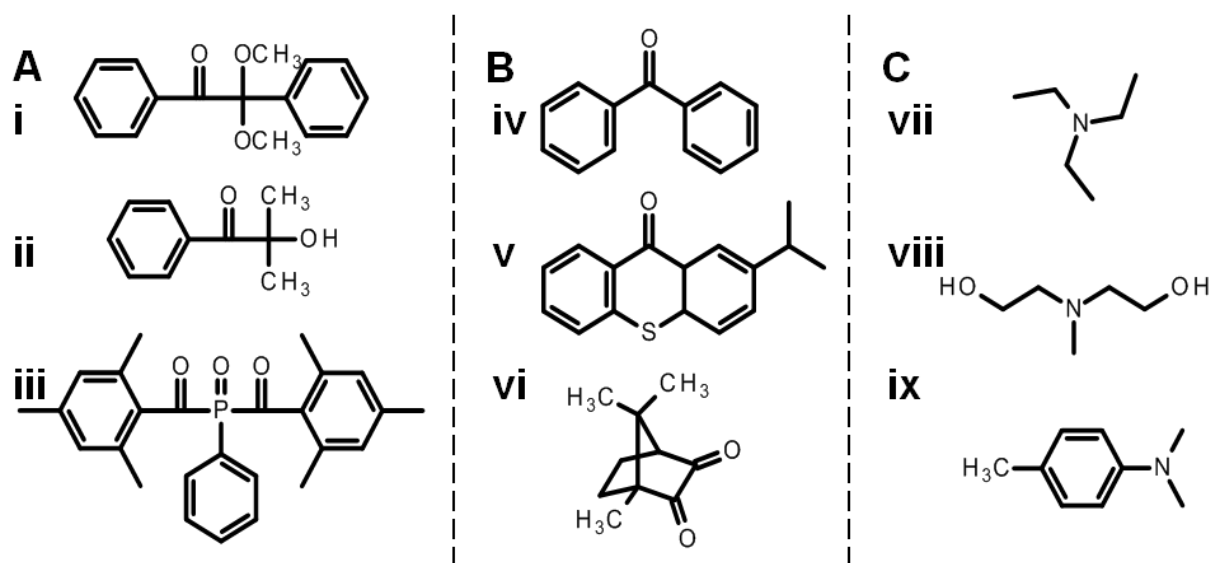


Figure 1.3: Radical photoinitiators and co-initiators. A Type I (cleavage) initiators: i) 2,2-Dimethoxy-2-phenylacetophenone, Irgacure 651; ii) 2-Hydroxy-2-methyl-1-phenyl-propan-1-one, Darocur 1173; iii) Bis(2,4,6-trimethylbenzoyl)-phenylphosphineoxide, Irgacure 819. B Type II (H abstraction) initiators: iv) Benzophenone, BP; v) 4-Isopropyl-9-thioxanthene, ITX; vi) Camphorquinone CQ. C Co-initiators: (H-donor): vii) Triethylamine, TEA; viii) N-methyldiethanolamine, MDEA; ix) N,N,4-trimethylaniline, TMA.



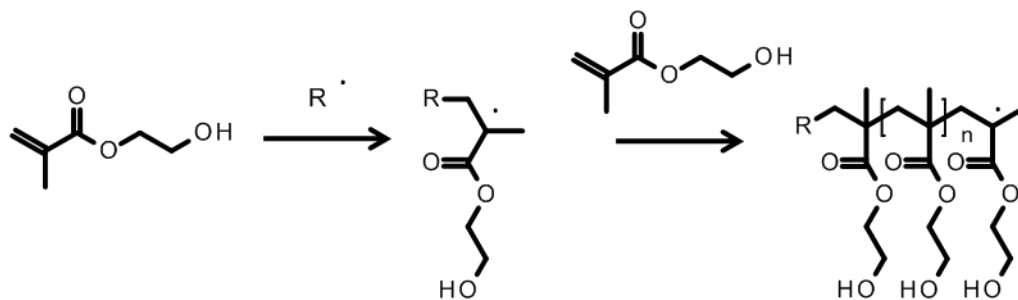


Figure 1.4: Simplified radical chain propagation of 2-hydroxyethyl acrylate (HEMA)

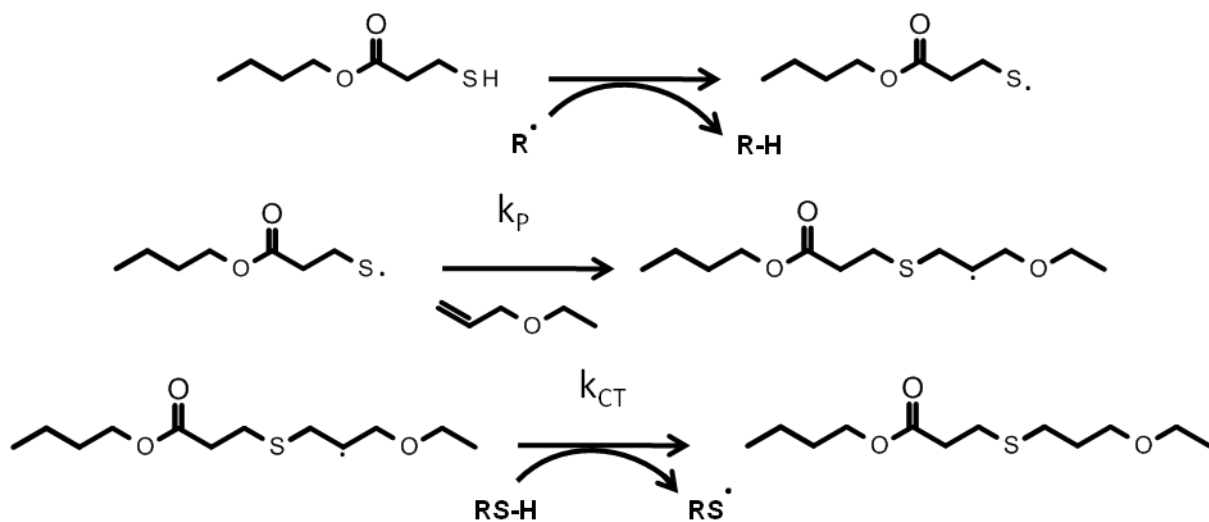


Figure 1.5: Radical mediated thiol-ene coupling reactions. An initiator fragment abstracts a proton from a thiol, producing a thiyl radical. Thiyl radical is inserted to the carbon-carbon double bond, making a carbon-centered radical. Chain transfer regenerates the thiyl radical and completes the thiol-ene coupling.

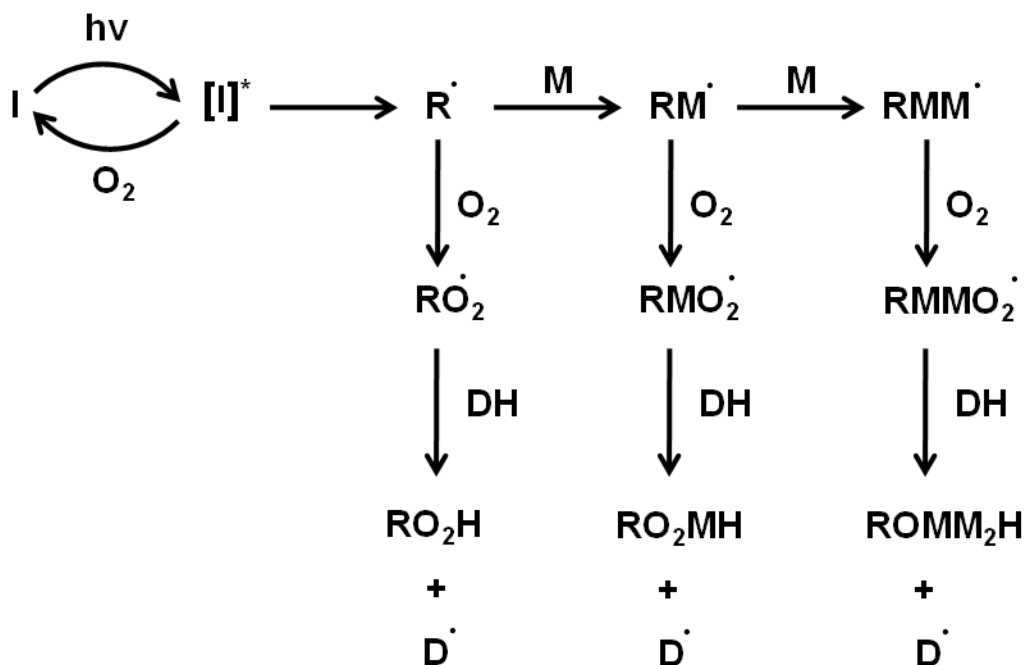


Figure 1.6: Possible modes of oxygen inhibition. The first mode is triplet-state deactivation followed by initiator fragment and monomer/polymer termination by peroxy radical formation. Oxygen inhibition is limited in the presence of proton donors, DH, like amines and thiols, which react with peroxy radicals to form propagating species.

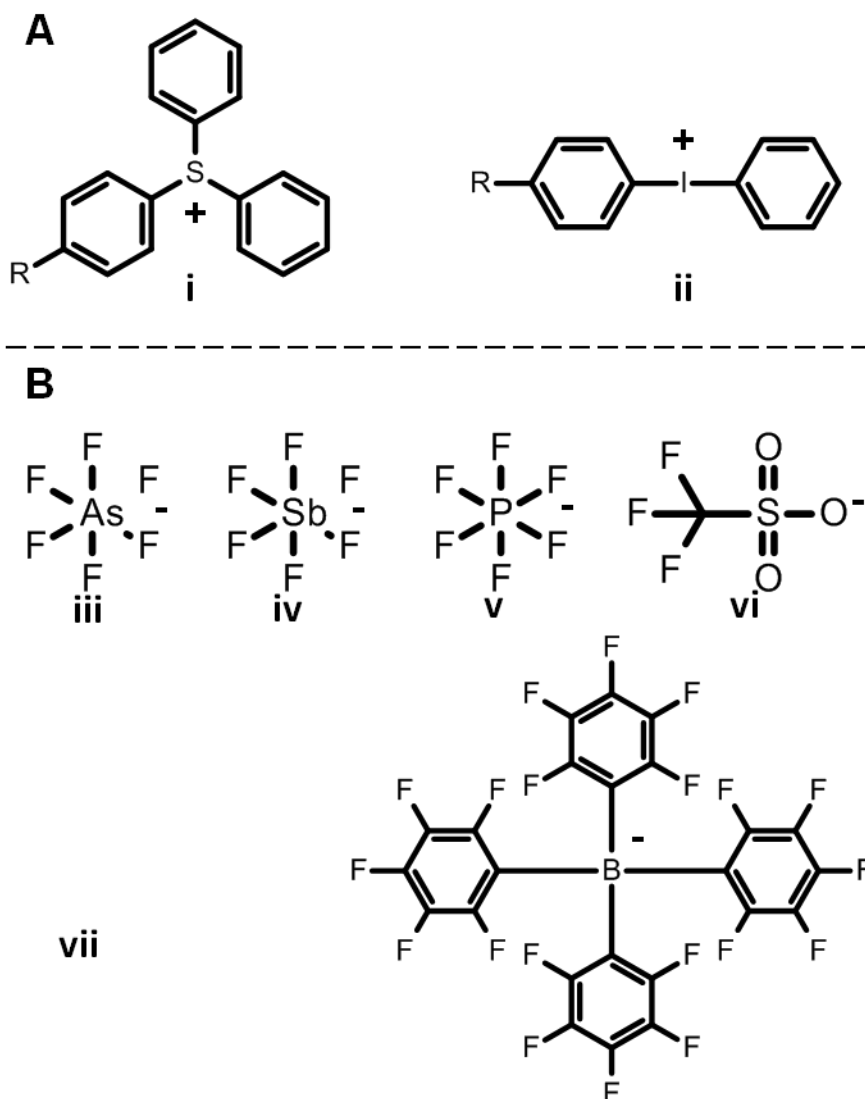


Figure 1.7: Cationic photoinitiator components. A Cations i) Triarylsulfonium, TAS; ii) diaryliodonium, DAI. B Anions: iii) hexafluoroarsenate,  $\text{AsF}_6^-$ ; iv) hexafluoroantimonate,  $\text{SbF}_6^-$ ; v) hexafluorophosphate,  $\text{PF}_6^-$ ; vi) triflate; vii) tetrakis(pentafluorophenyl)borate.

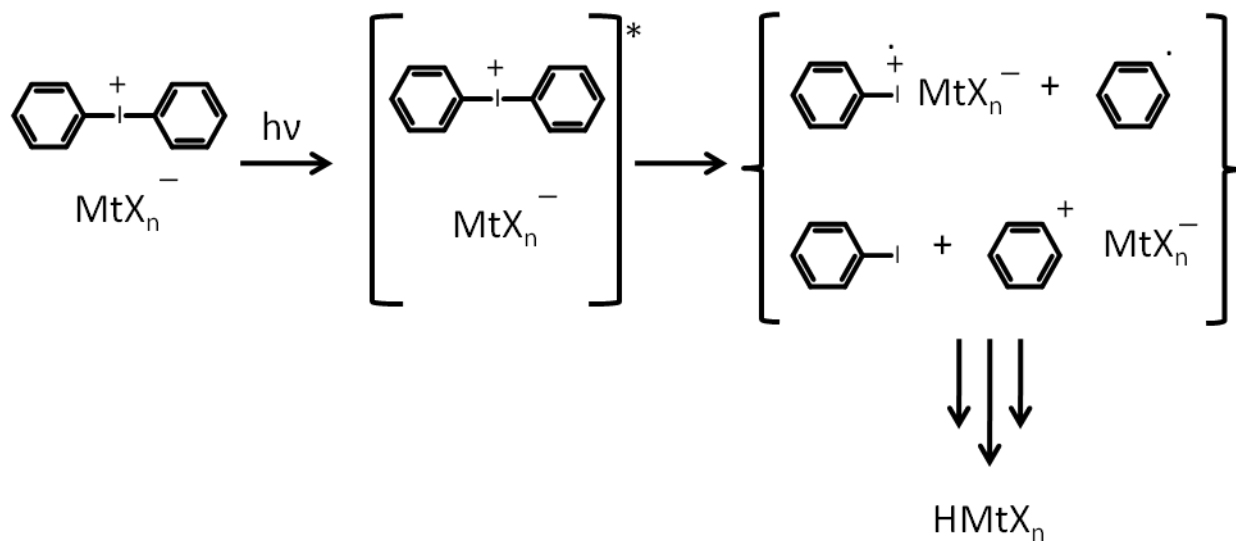


Figure 1.8: Photo-acid generation by direct photolysis of DAI. HMtX<sub>n</sub> is a very strong Bronsted acid produced from reactions between various photolysis products of DAI.

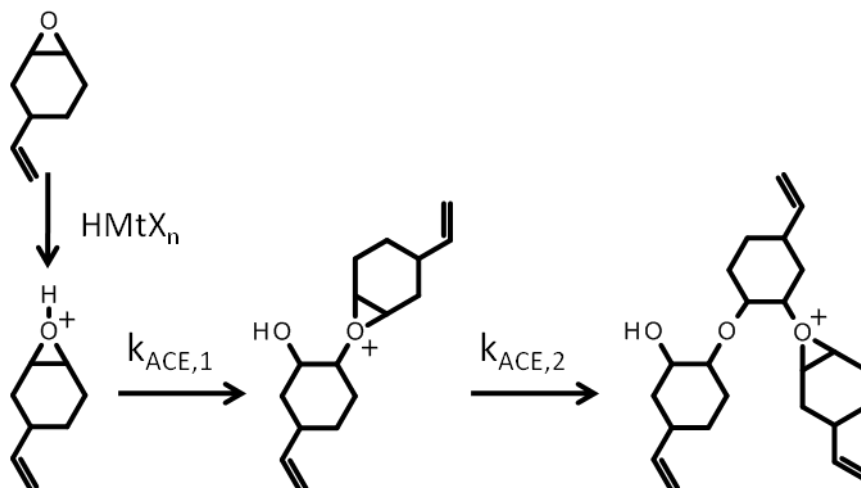


Figure 1.9: Cationic chain propagation of VCM by the ACE mechanism: Monomer protonation and formation of a secondary oxonium ion, followed by formation of tertiary oxonium ion.

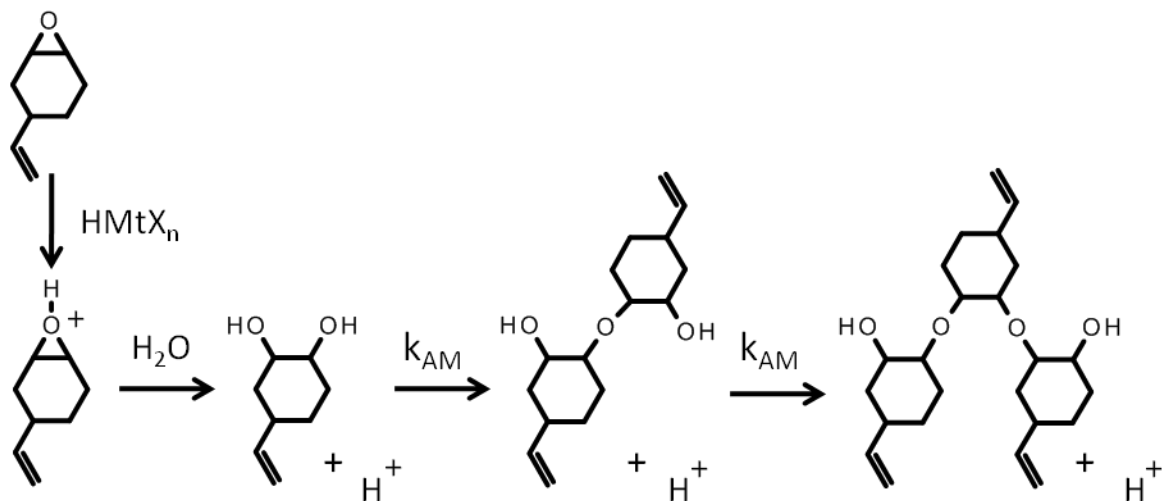


Figure 1.10: Cationic propagation of VCM by the AM mechanism with water as the CTA. Monomer protonation, formation of secondary oxonium ion and reaction with CTA to produce organic hydroxyls and regenerate acid.

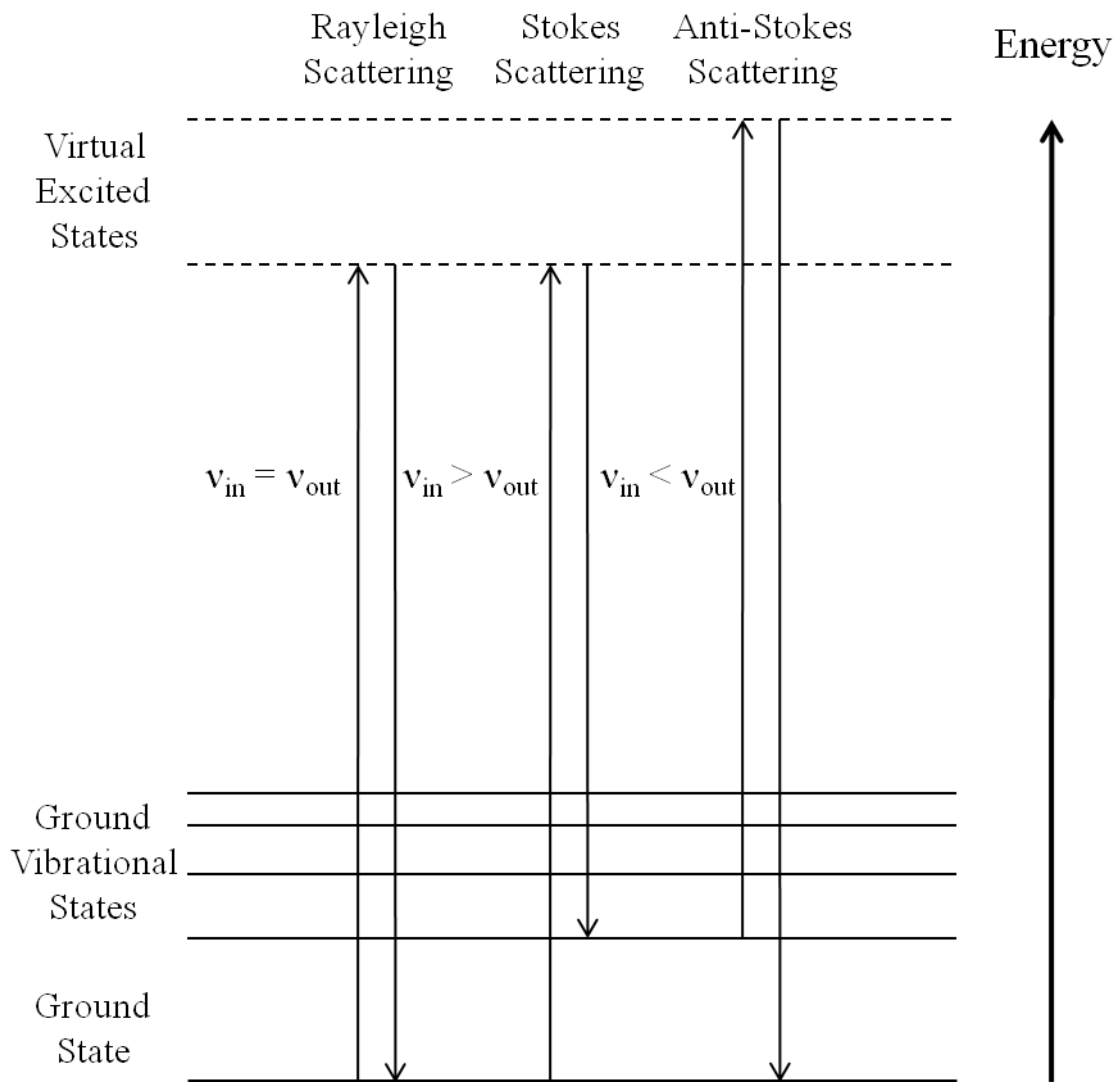


Figure 1.11: Energy-level diagram illustrating the different types of light scattering modes.



### Notes

- (1) Koleske, J. V. *Radiation Curing of Coatings*; ASTM International: West Conshohocken, PA, 2002; Vol. 1, pp 244.
- (2) Fouassier, J. *Photoinitiation, Photopolymerization, and Photocuring*; Hanser/Gardner Publications, Inc.: Cincinnati, OH, 1995; , pp 375.
- (3) Kloosterboer, J. "Network Formation by Chain Crosslinking Photopolymerization and its Applications in Electronics" *Advances in polymer science* **1988**, *84*, 1.
- (4) Bowman, C. N.; Kloxin, C. "Toward an Enhanced Understanding and Implementation of Photopolymerization Reactions" *AIChE Journal* **2008**, *54*, 2775-2795.
- (5) Decker, C. "Photoinitiated Crosslinking Polymerization." *Progress in Polymer Science* **1996**, *21*, 593-650.
- (6) Rutsch, W.; Dietliker, K.; Leppard, d.; Koehler, M.; Misev, L.; Kolczak, U.; Rist, G. "Recent developments in photoinitiators." *Progress in Organic Coatings* **1996**, *27*, 227-239.
- (7) Crivello, J. V.; Lam, J. H. W. "Diaryliodonium Salts. A New Class of Photoinitiators for Cationic Polymerization." *Macromolecules* **1977**, *10*, 1307-1315.
- (8) Crivello, J. V. "The discovery and development of onium salt cationic photoinitiators." *Journal of Polymer Science Part A: Polymer Chemistry* **1999**, *37*, 4241-4254.
- (9) Dietliker, K.; Jung, T.; Studer, K.; Benkhoff, J. "Photolatent Tertiary Amines A New Technology Platform for Radiation Curing" *CHIMIA International Journal for Chemistry* **2007**, *61*, 655-660.
- (10) Decker, C.; Moussa, K. "Photopolymerization of multifunctional monomers in condensed phase." *Journal of Applied Polymer Science* **1987**, *34*, 1603-1618.
- (11) Moussa, K.; Decker, C. "Light-Induced Polymerization of New Highly Reactive Acrylic-Monomers" *Journal of Polymer Science Part A: Polymer Chemistry* **1993**, *31*, 2197-2203.
- (12) Jansen, J. F. G. A.; Dias, A. A.; Dorschu, M.; Coussens, B. "Fast Monomers: Factors Affecting the Inherent Reactivity of Acrylate Monomers in Photoinitiated Acrylate Polymerization." *Macromolecules* **2003**, *36*, 3861-3873.
- (13) Andrzejewska, E. "Photopolymerization kinetics of multifunctional monomers." *Progress in Polymer Science* **2001**, *26*, 605-665.

- (14) Timpe, H. J.; Ulrich, S.; Decker, C.; Fouassier, J. P. "Photoinitiated polymerization of acrylates and methacrylates with decahydroacridine-1,8-dione/onium salt initiator systems." *Macromolecules* **1993**, *26*, 4560-4566.
- (15) Jakubiak, J.; Allonas, X.; Fouassier, J.; Sionkowska, A.; Andrzejewska, E.; Linden, L. "Camphorquinone-amines photoinitiated systems for the initiation of free radical polymerization" *Polymer* **2003**, *44*, 5219.
- (16) Groenenboom, C. J.; Hageman, H. J.; Overeem, T.; Weber, A. J. M. "Photoinitiators and photoinitiation. 3. Comparison of the photodecompositions of alpha - methoxy- and alpha ,alpha -dimethoxydeoxybenzoin in 1,1-diphenylethylene as model substrate." *Makromolekulare Chemie* **1982**, *183*, 281-292.
- (17) Anderson, D.; Davidson, R.; Elvery, J. "Thioxanthenes: Their fate when used as photoinitiators" *Polymer* **1996**, *37*, 2477.
- (18) Gou, L.; Ophem, B.; Scranton, A. B. "The effect of oxygen in free radical photopolymerization." *Recent Research Developments in Polymer Science* **2004**, *8*, 125.
- (19) Odian, G. *Principles of Polymerization (Fourth Edition)*; John Wiley and Sons: Hoboken, NJ, 2004; .
- (20) Oxman, J. D.; Jacobs, D. W.; Trom, M. C.; Sipani, V.; Ficek, B.; Scranton, A. B. "Evaluation of initiator systems for controlled and sequentially curable free-radical/cationic hybrid photopolymerizations." *Journal of Polymer Science Part A: Polymer Chemistry* **2005**, *43*, 1747-1756.
- (21) Kloosterboer, J.; Vandehei, G.; Boots, H. "Inhomogeneity During the Photopolymerization of Diacrylates - DSC Experiments and Percolation Theory" *Polymer communications* **1984**, *25*, 354.
- (22) Boots, H.; Kloosterboer, J.; Vandehei, G.; Pandey, R. "Inhomogeneity During The Bulk-Polymerization of Divinyl Compounds - Differential Scanning Calorimetry Experiments and Percolation Theory" *British polymer journal* **1985**, *17*, 219.
- (23) Hoyle, C. E.; Lee, T. Y.; Roper, T. "Thiol-enes: Chemistry of the past with promise for the future." *Journal of Polymer Science Part A: Polymer Chemistry* **2004**, *42*, 5301-5338.
- (24) Cramer, N. B.; Davies, T.; O'Brien, A. K.; Bowman, C. N. "Mechanism and Modeling of a Thiol-Ene Photopolymerization." *Macromolecules* **2003**, *36*, 4631-4636.

- (25) Cramer, N. B.; Reddy, S. K.; O'Brien, A. K.; Bowman, C. N. "Thiol-Ene Photopolymerization Mechanism and Rate Limiting Step Changes for Various Vinyl Functional Group Chemistries." *Macromolecules* **2003**, *36*, 7964-7969.
- (26) Senyurt, A. F.; Wei, H.; Hoyle, C. E.; Piland, S. G.; Gould, T. E. "Ternary Thiol-Ene/Acrylate Photopolymers: Effect of Acrylate Structure on Mechanical Properties." *Macromolecules* **2007**, *40*, 4901-4909.
- (27) Senyurt, A. F.; Hoyle, C. E.; Wei, H.; Piland, S. G.; Gould, T. E. "Thermal and Mechanical Properties of Cross-Linked Photopolymers Based on Multifunctional Thiol-Urethane Ene Monomers." *Macromolecules* **2007**, *40*, 3174-3182.
- (28) O'Brien, A. K.; Bowman, C. N. "Modeling the effect of oxygen on photopolymerization kinetics." *Macromolecular Theory and Simulations* **2006**, *15*, 176-182.
- (29) Cai, Y.; Jessop, J. L. P. "Decreased oxygen inhibition in photopolymerized acrylate/epoxide hybrid polymer coatings as demonstrated by Raman spectroscopy." *Polymer* **2006**, *47*, 6560-6566.
- (30) Gou, L.; Opheim, B.; Scranton, A. B. *In Methods to overcome oxygen inhibition in free radical photopolymerizations*. Chemistry of Synthetic High Polymers; 2006; , pp 301-310.
- (31) Decker, C.; Jenkins, A. "Kinetic Approach of Oxygen Inhibition in Ultraviolet-Induced and Laser-Induced Polymerizations" *Macromolecules* **1985**, *18*, 1241-1244.
- (32) Carioscia, J. A.; Schneidewind, L.; O'Brien, C.; Ely, R.; Feeser, C.; Cramer, N.; Bowman, C. N. "Thiol-norbornene materials: approaches to develop high Tg thiol-ene polymers." *Journal of Polymer Science Part A: Polymer Chemistry* **2007**, *45*, 5686-5696.
- (33) Crivello, J. V.; JO, K. "Propenyl Ethers I The Synthesis of Propenyl Ether Monomers" *Journal of Polymer Science Part A: Polymer Chemistry* **1993**, *31*, 1473-1482.
- (34) Crivello, J. V.; JO, K. "Propenyl Ethers II Study of the Photoinitiated Cationic Polymerization of Propenyl Ether Monomers" *Journal of Polymer Science Part A: Polymer Chemistry* **1993**, *31*, 1483-1491.
- (35) Hartwig, A. "Influence of moisture present during polymerisation on the properties of a photocured epoxy resin" *International Journal of Adhesion and Adhesives* **2002**, *22*, 409-414.

- (36) Brzezinska, K.; Szymanski, R.; Kubisa, P.; Penczek, S. "Activated monomer mechanism in cationic polymerization. I: Ethylene oxide, formulation of mechanism" *Die Makromolekulare Chemie Rapid Communications* **1986**, *7*, 1-4.
- (37) Sipani, V.; Scranton, A. B. "Dark-cure studies of cationic photopolymerizations of epoxides: Characterization of the active center lifetime and kinetic rate constants" *Journal of Polymer Science Part A: Polymer Chemistry* **2003**, *41*, 2064-2072.
- (38) Sipani, V.; Kirsch, A.; Scranton, A. B. "Dark cure studies of cationic photopolymerizations of epoxides: Characterization of kinetic rate constants at high conversions." *Journal of Polymer Science Part A: Polymer Chemistry* **2004**, *42*, 4409-4416.
- (39) Jancovicova, V.; Brezova, V.; Ciganek, M.; Cibulkova, Z. "Photolysis of diaryliodonium salts (UV/Vis, EPR and GC/MS investigations)." *Journal of Photochemistry and Photobiology, A: Chemistry* **2000**, *136*, 195-202.
- (40) Decker, C. "Photoinitiated cationic polymerization of epoxides" *Polymer International* **2001**, *50*, 986-997.
- (41) Crivello, J. V.; Falk, B.; Zonca, M. R., Jr "Study of cationic ring-opening photopolymerizations using optical pyrometry." *Journal of Applied Polymer Science* **2004**, *92*, 3303-3319.
- (42) Bulut, U.; Crivello, J. V. "Investigation of the Reactivity of Epoxide Monomers in Photoinitiated Cationic Polymerization." *Macromolecules* **2005**, *38*, 3584-3595.
- (43) Kubisa, P.; Bednarek, M.; Biedron, T.; Biela, T.; Penczek, S. "Progress in activated monomer polymerization. Kinetics of AM polymerization." *Macromolecular Symposia* **2000**, *153*, 217-226.
- (44) Ghosh, N. N.; Palmese, G. R. "Electron-beam curing of epoxy resins: Effect of alcohols on cationic polymerization." *Bulletin of Materials Science* **2005**, *28*, 603-607.
- (45) Esposito Corcione, C.; Malucelli, G.; Frigione, M.; Maffezzoli, A. "UV-curable epoxy systems containing hyperbranched polymers: Kinetics investigation by photo-DSC and real-time FT-IR experiments." *Polymer Testing* **2009**, *28*, 157-164.
- (46) Sangermano, M.; Malucelli, G.; Bongiovanni, R.; Priola, A.; Harden, A. "Investigation on the effect of the presence of hyperbranched polymers on

- thermal and mechanical properties of an epoxy UV-cured system." *Polymer International* **2005**, *54*, 917-921.
- (47) Sangermano, M.; Bongiovanni, R.; Malucelli, G.; Roppolo, I.; Priola, A. "Siloxane additive as modifier in cationic UV curable coatings" *Progress in organic coatings* **2006**, *57*, 44.
- (48) Cai, Y.; Jessop, J. L. P. "Effect of water concentration on photopolymerized acrylate/epoxide hybrid polymer coatings as demonstrated by Raman spectroscopy" *Polymer* **2009**, *50*, 5409-5413.
- (49) Lin, Y.; Stansbury, J. W. "The impact of water on photopolymerization kinetics of methacrylate/vinyl ether hybrid systems" *Polymers for Advanced Technologies* **2005**, *16*, 195-199.
- (50) Lin, Y.; Stansbury, J. W. "Near-infrared spectroscopy investigation of water effects on the cationic photopolymerization of vinyl ether systems" *Journal of Polymer Science Part A: Polymer Chemistry* **2004**, *42*, 1985-1998.
- (51) Sperling, L. H. "Interpenetrating polymer networks: an overview." *Advances in Chemistry Series* **1994**, *239*, 3-38.
- (52) Sophiea, D.; Klempner, D.; Sendijarevic, V.; Suthar, B.; Frisch, K. C. "Interpenetrating polymer networks as energy-absorbing materials." *Advances in Chemistry Series* **1994**, *239*, 39-75.
- (53) He, Y.; Xiao, M.; Wu, F.; Nie, J. "Photopolymerization kinetics of cycloaliphatic epoxide-acrylate hybrid monomer." *Polymer International* **2007**, *56*, 1292-1297.
- (54) Acosta Ortiz, R.; Sangermano, M.; Bongiovanni, R.; Garcia Valdez, A. E.; Duarte, L. B.; Saucedo, I. P.; Priola, A. "Synthesis of hybrid methacrylate-silicone-cyclohexanepoxide monomers and the study of their UV induced polymerization." *Progress in Organic Coatings* **2006**, *57*, 159-164.
- (55) Decker, C.; Nguyen Thi Viet, T.; Decker, D.; Weber-Koehl, E. "UV-radiation curing of acrylate/epoxide systems." *Polymer* **2001**, *42*, 5531-5541.
- (56) Carioscia, J. A.; Stansbury, J. W.; Bowman, C. N. "Evaluation and control of thiol-ene/thiol-epoxy hybrid networks" *Polymer* **2007**, *48*, 1526-1532.
- (57) Matsushima, H.; Shin, J.; Bowman, C. N.; Hoyle, C. E. "Thiol-Isocyanate-Acrylate Ternary Networks by Selective Thiol-Click Chemistry" *Journal of Polymer Science Part A: Polymer Chemistry* **2010**, *48*, 3255-3264.

- (58) Shin, J.; Matsushima, H.; Comer, C. M.; Bowman, C. N.; Hoyle, C. E. "Thiol-Isocyanate-Ene Ternary Networks by Sequential and Simultaneous Thiol Click Reactions." *Chemistry of Materials* **2010**, *22*, 2616-2625.
- (59) Peeters, S. *In Overview of dual-cure and hybrid-cure systems in radiation curing*. Section Title: Chemistry of Synthetic High Polymers; 1993; Vol. 3, pp 177-217.
- (60) Crivello, J. V. "Benzophenothiazine and benzophenoxazine photosensitizers for triarylsulfonium salt cationic photoinitiators" *Journal of Polymer Science Part A: Polymer Chemistry* **2008**, *46*, 3820-3829.
- (61) Nelson, E.; Scranton, A. B. "In situ Raman spectroscopy for cure monitoring of cationic photopolymerizations of divinyl ethers" *Journal of Raman Spectroscopy* **1996**, *27*, 137-144.
- (62) Dursun, C.; Degirmenci, M.; Yagci, Y.; Jockusch, S.; Turro, N. J. "Free radical promoted cationic polymerization by using bisacylphosphine oxide photoinitiators: substituent effect on the reactivity of phosphinoyl radicals." *Polymer* **2003**, *44*, 7389-7396.
- (63) Durmaz, Y. Y.; Moszner, N.; Yagci, Y. "Visible Light Initiated Free Radical Promoted Cationic Polymerization Using Acylgermane Based Photoinitiator in the Presence of Onium Salts." *Macromolecules (Washington, DC, United States)* **2008**, *41*, 6714-6718.
- (64) Crivello, J. V.; Rajaraman, S.; Mowers, W. A.; Liu, S. "Free radical accelerated cationic polymerizations." *Macromolecular Symposia* **2000**, *157*, 109-119.
- (65) Crivello, J. V. "A new visible light sensitive photoinitiator system for the cationic polymerization of epoxides." *Journal of Polymer Science Part A: Polymer Chemistry* **2009**, *47*, 866-875.
- (66) Crivello, J. V. "Radical-Promoted Visible Light Photoinitiated Cationic Polymerization of Epoxides." *Journal of Macromolecular Science Part A: Pure and Applied Chemistry* **2009**, *46*, 474-483.
- (67) Magwood, L. Evaluation of the physical property evolution of the hybrid acrylate/epoxide photopolymerization system, University of Iowa, University of Iowa, 2009.
- (68) Raman, C.; Krishnan, K. "A new type of secondary radiation" *Nature* **1928**, *121*, 501.
- (69) Raman, C. "A change of wave-length in light scattering" *Nature* **1928**, *121*, 619.

- (70) Lewis, I. *Handbook of Raman Spectroscopy*; Marcel Dekker: New York, 2001; , pp 1054.
- (71) Xue, G. "Laser Raman spectroscopy of polymeric materials." *Progress in Polymer Science* **1994**, *19*, 317-388.
- (72) Xue, G. "Fourier transform Raman spectroscopy and its application for the analysis of polymeric materials." *Progress in Polymer Science* **1997**, *22*, 313-406.
- (73) Chalmers, J. *Handbook of Vibrational Spectroscopy*; J. Wiley: New York, 2002; Vol. 1, pp 3862.
- (74) Crandall, E. W. "Spectroscopic analysis using the near-infrared region of the electromagnetic spectrum" *Journal of chemical education* **1987**, *64*, 466.
- (75) Menard, K. *Dynamic Mechanical Analysis: A Practical Introduction*; CRC Press: Boca Raton, FL, 2008; , pp 218.

## CHAPTER 2

### OBJECTIVES

Epoxide monomers can be polymerized by two mechanisms, cationic and anionic, and as neat homopolymers or in concert with radical polymerizations. Epoxide systems cured via cationic mechanisms are used in photopolymerization systems because of the commercially available photoinitiation systems and the propagation mechanisms that do not interfere with the free radical polymerization of acrylate monomers (anionic epoxide polymerizations copolymerize with acrylate monomers). The kinetics and final material properties can be influenced by initiating systems, chain transfer agent (CTA) type and concentration, and mobility limitations due to additional polymer formation in hybrid epoxide-acrylate systems. In order to clarify the reaction details and properties of materials formed from epoxide-containing resins and acrylate resins, several objectives were pursued. The realization of these objectives aids in the development of efficient photopolymerization techniques and materials that ameliorate the effects of atmospheric factors, such as oxygen and water.

1. Determine key variable in tuning physical properties in both acrylate and epoxide photopolymerization systems. By varying CTA type and amount in formulations for various epoxide monomers, correlations were made between the size and functionality of the CTA and the  $T_g$ , crosslink density and gel fraction of epoxide photopolymers. After synthesizing a novel, bio-based acrylate oligomer, property-tuning capabilities in commercial formulations were determined via reactive diluent type and amount.
2. Characterize the kinetics of cationic epoxide polymerization with regard to the secondary propagation (AM mechanism). Epoxide resins were polymerized and studied kinetically using real-time Raman spectroscopy and real-time infrared



spectroscopies. The AM mechanism was studied via CTA:epoxide formulations and found to increase the polymerization rate and epoxide conversion, in general.

3. Determine the effects of different curing conditions on polymerization kinetics and physical properties. Dual initiator systems (photo-acid generators combined with free-radical generators) were applied to various neat epoxide and epoxy-acrylate systems. The free-radical initiator selection affected the final conversion and rates of polymerization of each species (epoxide and acrylate). The surface of epoxide polymers was found to be affected by humidity levels. The final properties were found to be unstable for high  $T_g$  epoxide materials unless a annealing process was added to the curing protocol.

The project focused mainly on epoxide materials using the bicycloaliphatic epoxide monomer EEC as a model compound for study. In Chapter 3, the kinetics of epoxide photopolymerization were studied via real-time mid-IR and real-time near-IR spectroscopies. Water was formulated in quantitative amounts, and epoxide conversion profiles, water consumption profiles, and alkyl hydroxyl production profiles were obtained. The profound effect of water on epoxide conversions stimulated further interest in other CTAs (organic alcohols) that were investigated for Chapter 4. Epoxide conversion profiles were obtained via Raman spectroscopy, and DMA profiles were obtained from polymers formed from EEC:alcohol formulations. Chapters 5 and 6 present the effects of curing conditions on epoxide polymer physical properties. Epoxide resins were cured in both dry and humid atmospheres, and the surface hardness was analyzed via atomic force microscopy, demonstrating that humid atmospheres do result in lower surface hardness. Epoxide resins were also cured by light alone and with additional heat treatments, or annealing steps. The properties, as measured via DMA, were found to be unstable without annealing the epoxide polymers. Chapter 7 provides further characterization of the AM mechanism through the study of the grafting of epoxide

monomers on well-defined hydroxyl-containing acrylate polymers. In addition, GPC was used to characterize the molecular weight of the polymers. In Chapter 8, dual free-radical and cationic photoinitiators were studied in neat epoxide and hybrid acrylate-epoxide materials. Chapter 9 overviews the kinetics and physical properties of acrylate-based resins, which were formulated with a specially synthesized renewable acrylate oligomer.

Epoxide resins not only are free from oxygen inhibition that plagues acrylate chemistries, but can also provide a broad range of reactivities and physical properties through careful selection of materials and process parameters. The understanding of these key variables that affect the kinetics and physical properties of epoxide resins provides guidelines for product design and future applications in the field of photopolymerization.

## CHAPTER 3

### EPOXIDE KINETICS IN WATER CONTAINING FORMULATIONS

#### 3.1 Introduction

Photopolymerization has been used widely in coatings, adhesives, and inks, as well as in medical applications such as dental filling composites. This widespread use is due to the high level of spatial and temporal control inherent to photopolymerization and the associated energy and material savings.<sup>1-3</sup> In order to further reduce cost and broaden the applicability of photopolymerization, hybrid resin systems have been developed by combining acrylates with epoxides or other cationic monomers.<sup>3-5</sup> The unique curing capabilities of these systems result in a high degree of cure for acrylate in ambient atmospheric conditions. To optimize the use of these hybrid systems for practical applications, it is essential to obtain a quantitative understanding of and the factors that influence each component in the system. The epoxide monomers used in this research, like most cationically polymerizable monomers, are affected by atmospheric moisture. The work presented in this paper strives to clarify kinetic effects of water on these epoxide monomers.

Water has been shown to affect cationic photopolymerization in several ways. Water can induce decomposition of the photoinitiator,<sup>6</sup> but it can also participate in propagation reactions and consequently impact the final polymer properties.<sup>7,8</sup> In a system containing only epoxide monomers, the propagation reaction proceeds via the active chain end (ACE) mechanism, as shown in Fig. 1.9. If nucleophilic species are introduced to the system a secondary reaction pathway becomes available. This pathway is referred to as the activated monomer (AM) mechanism, as shown in Fig. 1.10.<sup>9,10</sup> These two reaction pathways are not kinetically equivalent. The relative reactivity of the initiating molecules and the active centers with the monomer and other nucleophilic species, water, alcohols or other functional groups in the system, will factor into the

prevalence of one of the two reaction mechanisms. Thus, the measured rate of epoxide consumption should be indicative of the pathway that dominates the overall cationic curing process. Additionally, polymers resulting from the respective reaction mechanisms will differ in structure and therefore in properties. For example, increasing amounts of water have been shown to reduce the average molecular weight of linear polymers and the hardness of cross-linked polymers.<sup>7,8</sup>

In this study, the conversion of epoxide monomer and consumption of water were monitored by real-time mid-infrared (RT-MIR), and real-time near-infrared (RT-NIR) spectroscopy. The RT-MIR technique has been used widely in monitoring rapid photopolymerizations due to its short data acquisition time, ability to monitor multiple functional groups simultaneously, and high resolution.<sup>3,11,12</sup> The use of RT-NIR spectroscopy has been limited due to less spectral information available in the NIR region and lower molar absorptivities which then require much more sample volume to obtain reasonable signals. The advantage of RT-NIR spectroscopy in this research is the higher resolution of bands associated with water vibrations and O-H bonds of other species, such as alcohols and carboxylic acids.<sup>13</sup>

## 3.2 Experimental

### 3.2.1 Materials

3,4-Epoxy cyclohexylmethyl-3,4-epoxycyclohexanecarboxylate (EEC, Aldrich) was the epoxide monomer used in this study (Fig. 3.1). The water concentration in this material was determined by a standard addition method to be 0.07 mol H<sub>2</sub>O/L. Additional distilled water was added to the formulations to reach the target concentrations. Five formulations were prepared ranging from 0.07 to 1.43 moles H<sub>2</sub>O/ L. The cationic photoinitiator used was an iodonium type photo-acid generator (PC-2506, Polyset Company). All materials were used as received. All formulations were prepared to contain an initiator concentration of 8 mmol/L.

### 3.2.2 Methods

#### 3.2.2.1 RT-MIR Spectroscopy

RT-MIR spectra were collected using a FT-IR spectrometer (Thermo Nicolet 670 Nexus) with a KBr beam splitter and a MCT/B detector to determine epoxide conversion with respect to time. The sample solutions were sandwiched between a pair of NaCl plates with 15 micron spacers used to ensure a constant path length for each sample. The spectra contained sample absorbance from 600-4000  $\text{cm}^{-1}$ . The photopolymerization of the formulations was initiated using a 100 W high pressure mercury lamp (Acticure® Ultraviolet/Visible spot cure system, EXFO Photonic Solutions, Inc.) equipped with a fiber optic port to deliver the light dose. The full spectrum irradiance used in these experiments was measured to be 50  $\text{mW}/\text{cm}^2$  using a radiometer (Cole-Parmer). The conversion of epoxide was calculated using the peak height of the 750  $\text{cm}^{-1}$  band (Fig. 3.2) in Eq. 3.1:

$$\text{Epoxide fractional conversion} = 1 - A_{760}(t)/A_{760}(0) \quad 3.1$$

where  $A_{760}(0)$  is the peak height before polymerization and  $A_{760}(t)$  is the peak height and time  $t$  during the polymerization.

Every sample formulation was illuminated for 3 min while spectra were collected. Additionally a “long-term” experiment was performed to monitor post-exposure curing, referred to as “dark cure,” as well as the persistence of different functional groups. In this experiment, spectra of the formulations were collected with illumination for 10 min and then without illumination for 110 min.

#### 3.2.2.2 RT-NIR Spectroscopy

RT-NIR spectra were collected using the same FT-IR spectrometer to determine water consumption over time. The spectra contained absorbance values for 4000-6200  $\text{cm}^{-1}$ . The sample volume required for strong absorbance signals was much greater for the

NIR samples. Therefore, a custom glass sample holder was crafted in house and consisted of a 2.5 cm inner diameter cap with a well depth of about 1.5mm. The sample holder contained a sample volume of 1.0 cm<sup>3</sup> for each experiment. The peak height of 5226 cm<sup>-1</sup> (Fig. 3.3) was used to calculate the fractional consumption of water in Eq. 3.2:

$$\text{Water fractional consumption} = 1 - A_{5226}(t)/A_{5226}(0) \quad 3.2$$

where  $A_{5226}(0)$  is the peak height before polymerization and  $A_{5226}(t)$  is the peak height at time  $t$  during the polymerization.

The “long-term” experiment was performed to investigate the persistence of the hydroxyl functional groups. In this experiment, spectra of the formulations were collected with illumination for 10 min and then without illumination for 110 min.

### 3.3 Results and Discussion

EEC produces highly cross-linked polymer networks upon photopolymerization. Often the conversion of EEC is limited due to the early onset of gelation, resulting in trapped active centers that cannot react further due to diffusion limitations. As shown in Fig. 3.4, the epoxide conversion is indeed affected by increased water concentration. The slowest rate of polymerization and lowest ultimate conversion was observed in the formulation with no added water (i.e., [H<sub>2</sub>O] = 0.07 mol/L). As the water concentration increased, a more pronounced induction period was observed. Additionally, with increasing water content, there was an enhanced final conversion.

RT-NIR experiments of the same EEC formulations produced similar results as observed with the RT-MIR experiments. As shown in Fig. 3.5, the higher the water content, the greater the induction time; however, all formulations ultimately resulted in complete consumption of the water present. The induction time for water consumption was approximately half of that observed with the respective epoxide conversion profiles. Each formulation with added water (i.e., [H<sub>2</sub>O] > 0.07 mol/L) showed a pronounced acceleration in reaction after the induction period, both in water consumption and in

epoxide conversion. The rate acceleration in water consumption appears consistently after the epoxide conversion reaches 3-5%.

During the “long-term” experiments (Fig. 3.6 and 3.7) the alkyl hydroxyl peak increased in intensity as the water peak disappeared during the reaction. Also, there was measurable “dark cure” of the epoxide during the last 110 min. For example, the conversion for the formulation with the highest concentration of water (i.e.,  $[\text{H}_2\text{O}] = 1.43$  mol/L) was about 49% just as the lamp was shuttered and approximately 54% at the end of the 2-h experiment. These results also demonstrated the persistence of hydroxyl content throughout the reaction.

### 3.4 Conclusions

This work demonstrates that RT-NIR spectroscopy can be used to determine the moisture content of monomers accurately, as well as the rate of water consumption during the polymerization. Together, the RT-MIR and RT-NIR experiments show a distinct kinetic dependence of epoxide reaction on the amount of water present. These results indicate that the AM mechanism dominates in the presence of water. The amount of alkyl hydroxyls produced has a direct relationship to the amount of water present in the system. Additionally, the “long-term” study shows that the hydroxyl content is constant once the water in the system is consumed. This persistent hydroxyl concentration further confirms the AM mechanism as shown in Scheme 1b. For every water molecule reacting with an activated monomer, one or two alkyl hydroxyl groups are produced, depending on whether the oxygen of the activated monomer is bound to a carbon or hydrogen, respectively. For every alkyl hydroxyl reacting with an activated monomer bound to hydrogen, there is no net change in the amount of hydroxyls present.

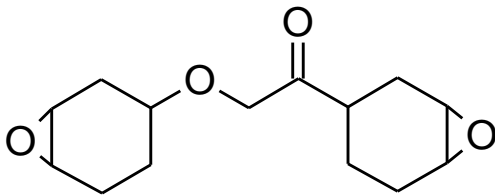


Figure 3.1: Molecular structure of epoxide monomer EEC.



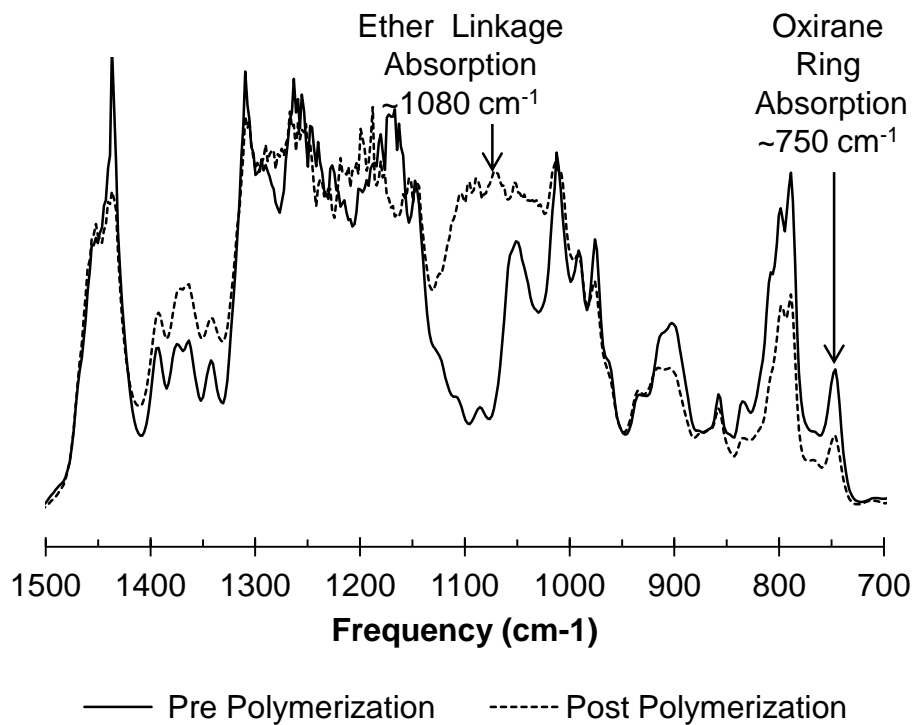


Figure 3.2: Characteristic MIR spectral bands of epoxide monomer EEC before and after photopolymerization. Reactive epoxide band is located at 760 cm<sup>-1</sup>, and the band for ether linkages formed by polymerization are located at 1080 cm<sup>-1</sup>.

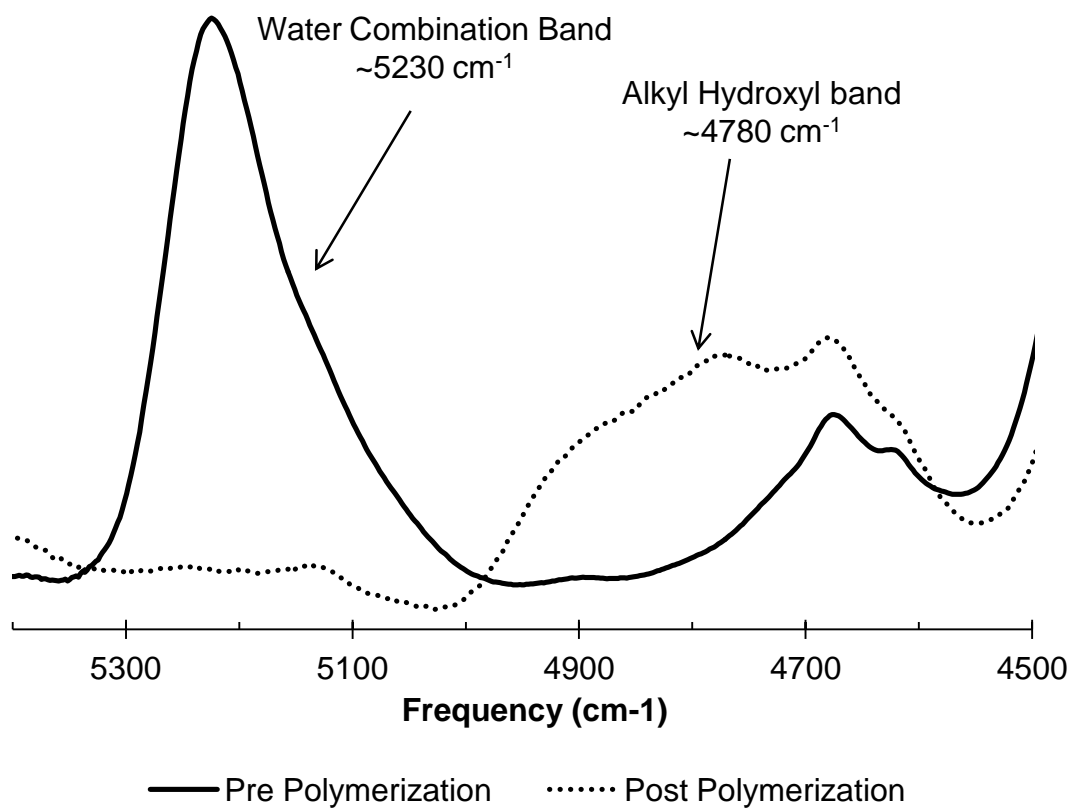


Figure 3.3: Characteristic NIR spectral bands of water and alkyl hydroxyl groups changing during the cationic ring-opening photopolymerization of EEC. The peak frequency of water is located at  $5226\text{ cm}^{-1}$  and of the alkyl hydroxyl groups at  $4778\text{ cm}^{-1}$ .

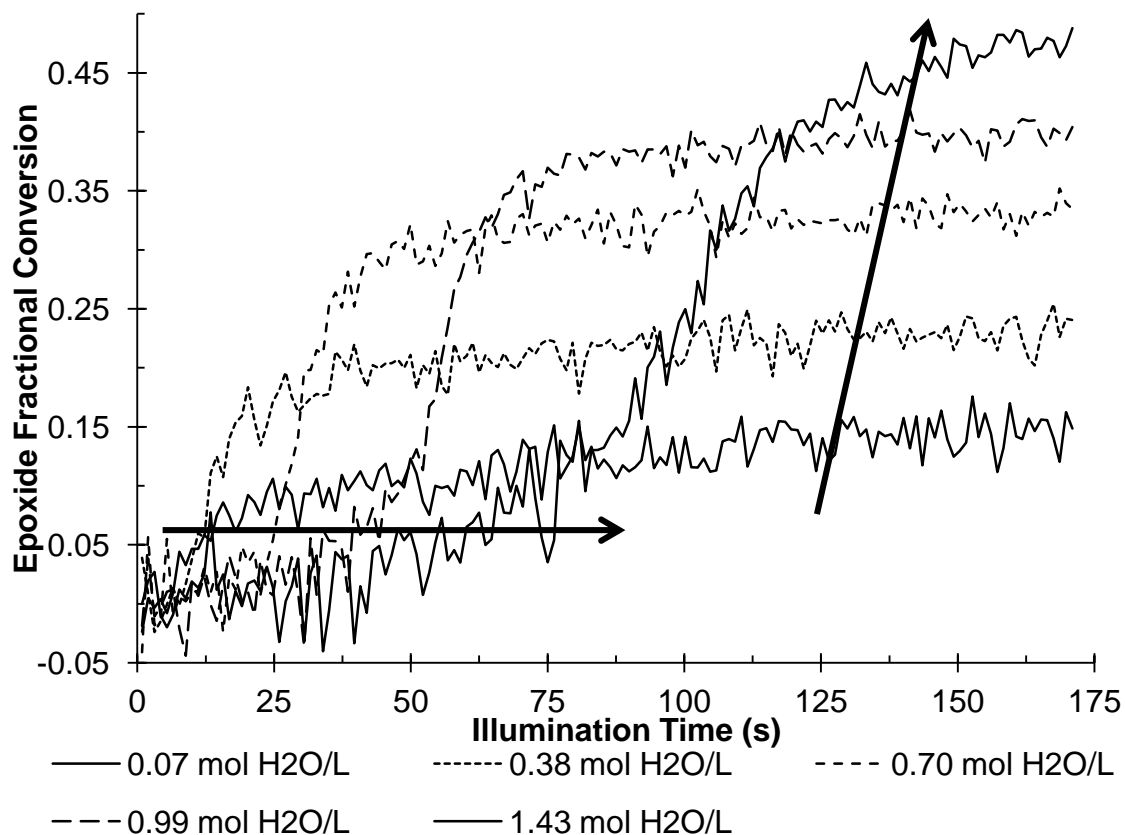


Figure 3.4: Epoxide conversion profiles obtained from RT-MIR spectra for the cationic ring-opening photopolymerization of EEC formulations containing varying concentrations of water. Arrows indicate increased induction time and conversion with increasing water concentration.

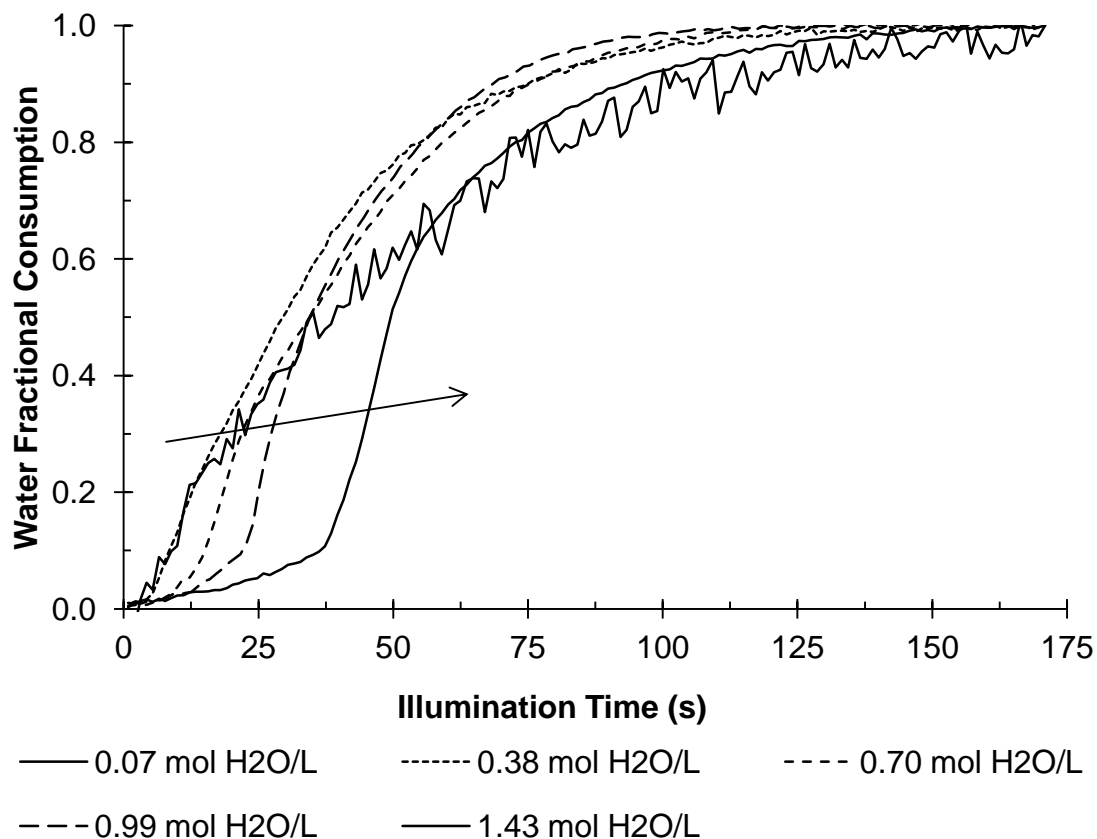


Figure 3.5: Water consumption profiles obtained from RT-NIR spectra for the cationic ring-opening photopolymerization of EEC formulations containing varying concentrations of water. The arrow indicates increased induction time with increased water concentration.

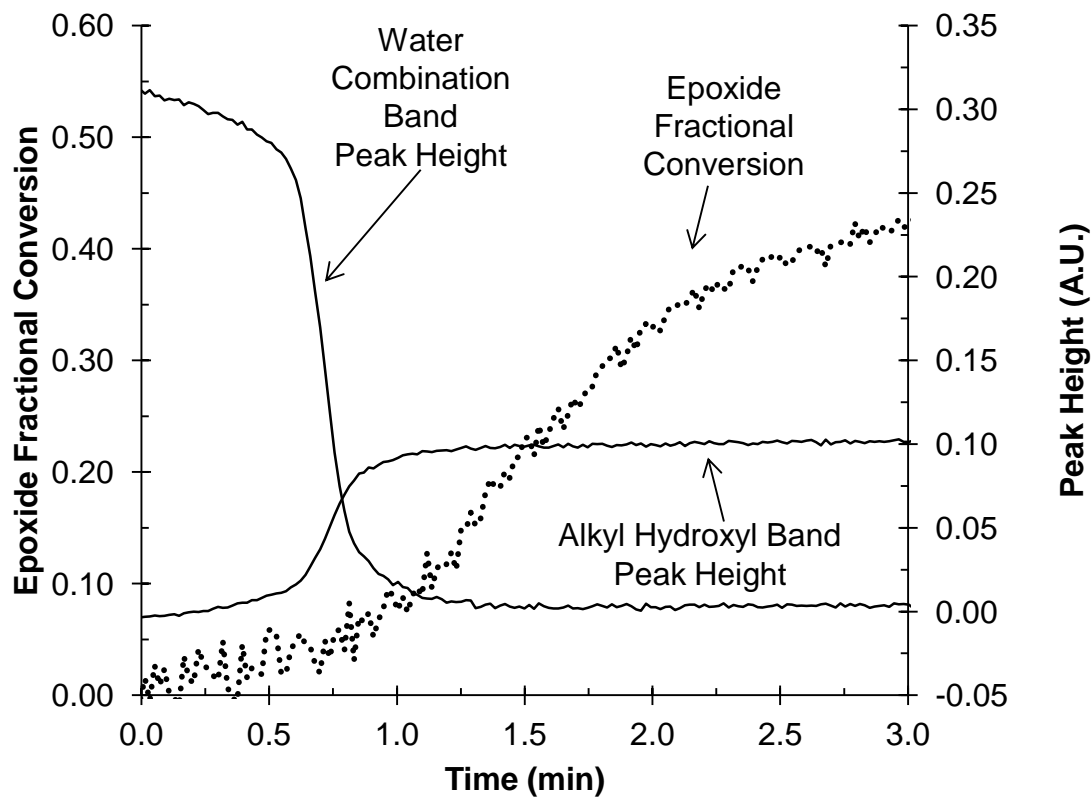


Figure 3.6: Overlaid NIR and MIR experiments during the the cationic ring-opening photopolymerization of EEC formulation containing 1.43 mol H<sub>2</sub>O/L. Water consumption and hydroxyl production obtained from RT-NIR experiments, and epoxide conversion obtained from RT-MIR experiments.

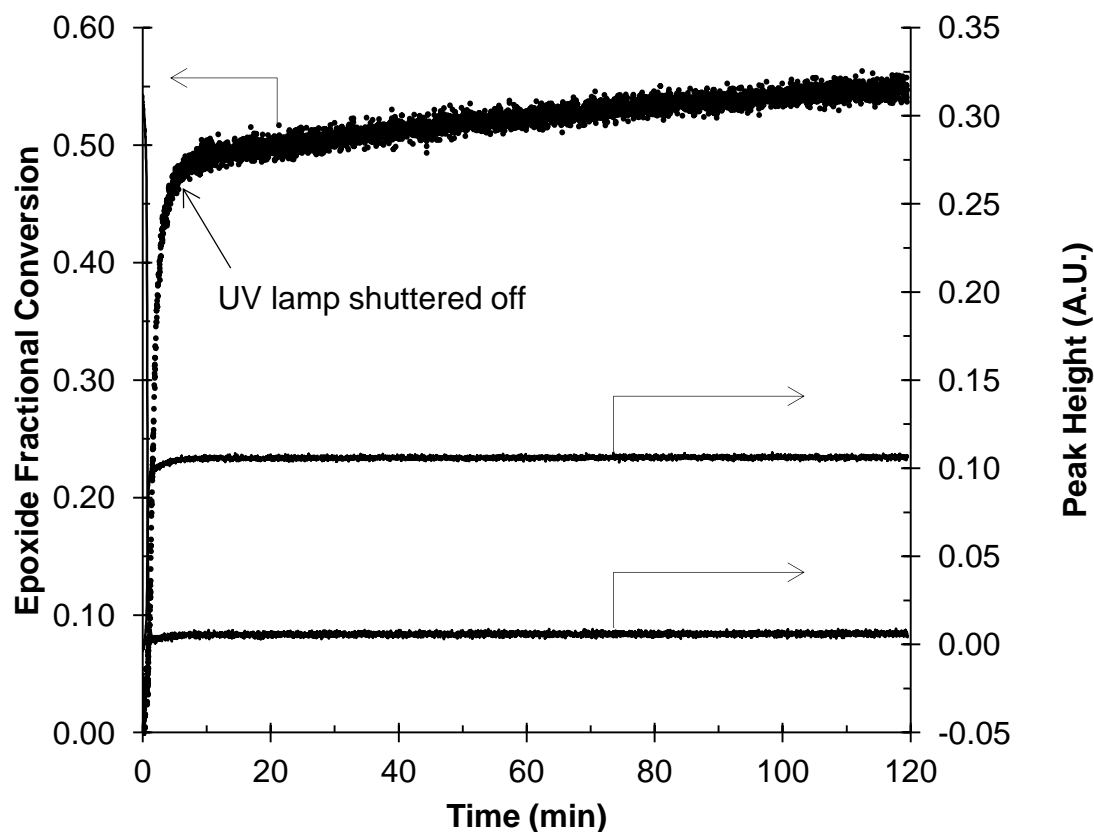


Figure 3.7: Long term study of the cationic ring-opening photopolymerization of EEC formulation containing 1.43 mol H<sub>2</sub>O/L: illumination started at  $t = 0$  and stopped at  $t = 10$  min. Water consumption and hydroxyl production obtained from RT-NIR experiments, and epoxide conversion obtained from RT-MIR experiments.

### Notes

- (1) Fouassier, J. *Photoinitiation, Photopolymerization, and Photocuring*; Hanser/Gardner Publications, Inc.: Cincinnati, OH, 1995; , pp 375.
- (2) Koleske, J. V. *Radiation Curing of Coatings*; ASTM International: West Conshohocken, PA, 2002; Vol. 1, pp 244.
- (3) Decker, C. "Photoinitiated Crosslinking Polymerization." *Progress in Polymer Science* **1996**, *21*, 593-650.
- (4) Cai, Y.; Jessop, J. L. P. "Decreased oxygen inhibition in photopolymerized acrylate/epoxide hybrid polymer coatings as demonstrated by Raman spectroscopy." *Polymer* **2006**, *47*, 6560-6566.
- (5) Lin, Y.; Stansbury, J. W. "The impact of water on photopolymerization kinetics of methacrylate/vinyl ether hybrid systems" *Polymers for Advanced Technologies* **2005**, *16*, 195-199.
- (6) Hartwig, A.; Harder, A.; Lühring, A.; Schröder, H. "(9-Oxo-9H-fluoren-2-yl)-phenyliodonium hexafluoroantimonate(V) – a photoinitiator for the cationic polymerisation of epoxides" *European Polymer Journal* **2001**, *37*, 1449-1455.
- (7) Ghosh, N. N.; Palmese, G. R. "Electron-beam curing of epoxy resins: Effect of alcohols on cationic polymerization." *Bulletin of Materials Science* **2005**, *28*, 603-607.
- (8) Decker, C. "Photoinitiated cationic polymerization of epoxides" *Polymer International* **2001**, *50*, 986-997.
- (9) Cai, Y.; Jessop, J. L. P. "Effect of water concentration on photopolymerized acrylate/epoxide hybrid polymer coatings as demonstrated by Raman spectroscopy" *Polymer* **2009**, *50*, 5409-5413.
- (10) Lin, Y.; Stansbury, J. W. "Near-infrared spectroscopy investigation of water effects on the cationic photopolymerization of vinyl ether systems" *Journal of Polymer Science Part A: Polymer Chemistry* **2004**, *42*, 1985-1998.
- (11) Cramer, N. B.; Bowman, C. N. "Kinetics of thiol-ene and thiol-acrylate photopolymerizations with real-time Fourier transform infrared" *Journal of Polymer Science Part A: Polymer Chemistry* **2001**, *39*, 3311-3319.
- (12) Crivello, J. V.; Varlemann, U. "Mechanistic study of the reactivity of 3,4-epoxycyclohexylmethyl 3',4'-epoxycyclohexanecarboxylate in photoinitiated cationic polymerizations." *Journal of Polymer Science Part A: Polymer Chemistry* **1995**, *33*, 2473-2486.

- (13) Crandall, E. W. "Spectroscopic analysis using the near-infrared region of the electromagnetic spectrum" *Journal of Chemical Education* **1987**, *64*, 466-467.



CHAPTER 4  
CHAIN TRANSFER AGENTS IN CATIONIC  
PHOTOPOLYMERIZATION OF A BIS-CYCLOALIPHATIC EPOXIDE  
MONOMER: KINETIC AND PHYSICAL PROPERTY EFFECTS

4.1 Introduction

Photopolymerization is a rapid and robust method for the production of polymer thin films.<sup>1,2</sup> Cationic photopolymerization has many positive features that make it an attractive alternative to free-radical-based polymerization in photocured coatings, sealants, and adhesives. One distinct advantage is the lack of oxygen inhibition, which is a major problem for acrylate-based resins.<sup>3-6</sup> Cationic active-center lifetimes are on the order of seconds to days, as opposed to fractions of seconds for radical polymerizations. These long active-center lifetimes allow for continued conversion after the light source has been shuttered off. Thus, the polymer physical properties continue to develop after the initial processing steps are completed.<sup>7-10</sup>

Epoxide monomers may polymerize via cationic mechanisms. One propagation mechanism is called the active chain end (ACE) mechanism (Figure 1.9). The ACE mechanism is similar to other addition mechanisms in that a new monomer reacts directly with the active center (cation) attached to the end of the growing polymer chain, thereby extending the chain length. A secondary propagation pathway is called the activated monomer (AM) mechanism.<sup>11,12</sup> In the AM mechanism, the activated monomer is attacked at the electrophilic carbons on the oxirane ring by a mildly nucleophilic compound, such as water or organic alcohols, and the ring is then opened (Figure 1.10).

The AM mechanism shifts the propagation mechanism from the typical ACE mechanism by transferring the active center away from the growing polymer chain. Therefore, the AM mechanism promotes chain transfer events and affects not only the speed of the polymerization, but also the network structure of the polymer.<sup>13-19</sup> The AM

mechanism has been studied extensively via thermal polymerization of simple oxirane-containing species like epichlorohydrin, ethylene oxide, and propylene oxide monomers. The propagation rate constant for the AM mechanism was determined to be about five fold greater than the propagation rate constant for the ACE mechanism.<sup>20</sup>

3,4-Epoxy cyclohexylmethyl-3',4'-epoxycyclohexane carboxylate (EEC) is a commercially available cycloaliphatic epoxide used in photopolymerization formulations. The synthesis of EEC is carried out in two steps from 3-cyclohexene-1-carboxaldehyde. The Tischenko reaction, which couples aldehydes to the corresponding esters, produces the diolefin that is then oxidized through a variety of methods to form the diepoxide, as shown in Figure 4.1.

In this series of reactions, there is potential for alcohols to be introduced to the system either from the aluminum alkoxide catalyst used in the Tischenko reaction or from any epoxide rings that open prematurely during the oxidation and/or subsequent purification steps. EEC is manufactured by multiple companies, and the processing of the material varies. The alcohol content in EEC monomer is likely to fluctuate greatly depending on the degree of process control used by a particular manufacturer and certainly between different manufacturers. The alcohols that are common impurities in this monomer can promote the AM propagation mechanism, which significantly alters the polymerization rate<sup>21</sup> and the physical/mechanical properties of polymer product.<sup>13,14,22</sup>

In addition to alcohol impurities (potentially introduced during monomer synthesis), water vapour in the processing environment can affect polymerization kinetics. When epoxy resins were polymerized in thin films that were open to the air, the film thickness affected the conversion attained during a given illumination period.<sup>5</sup> The final epoxide conversion was observed to increase with decreasing wet film thickness. Likewise, increasing relative humidity in ambient air during thin-film polymerizations led to higher conversion levels for the diepoxide monomer 3,4-epoxycyclohexylmethyl-3',4'-epoxycyclohexane carboxylate.<sup>23</sup> Increases in conversion are likely due to increased

water absorption into the liquid resin film. More water in the film promotes the AM mechanism and leads to increased epoxide conversions.

It is natural to assume that the addition of chain transfer agents (CTA) to epoxy resins, intentional or via contamination will result in higher rates of polymerization. Although this assumption is correct, it is far too simplistic. The amount and type of CTA incorporated into a thermosetting resin are important parameters that influence polymerization kinetics of the resin and the physical and mechanical properties of the final polymer. In this study, the effects of different types and amounts of CTAs are demonstrated for the commercially available thermosetting epoxide monomer EEC.

## 4.2 Experimental

### 4.2.1 Materials

EEC was purchased from Aldrich, and the cationic photoinitiator PC2506, which is an iodonium hexafluoroantimonate type photo-acid generator, was donated by Polyset Company (see Figure 4.2). The CTAs used consisted of monohydroxy and dihydroxy alcohols (see Figure 4.3). Methanol, ethanol, *n*-butanol, *n*-hexanol, *n*-decanol, *n*-dodecanol, phenol, cyclohexanol, ethylene glycol, 1,2-propanediol, 1,4-butanediol, 1,6-hexanediol, *N*-ethyl-diisopropyl amine, and poly(THF) 250 were purchased from Aldrich. *n*-Octanol was purchased from Acros Organics. Poly(THF) 650, 1000, and 2000 were donated by BASF. 2,2,2-Trifluoroethanol (TFE) and 2,2,2-trichloroethanol (TCE) were purchased from TCI. Isopropyl alcohol and *n*-propyl alcohol were purchased from Fisher. All reagents were used as received.

### 4.2.2 Formulations

Formulations were prepared such that the mole ratio of hydroxyl groups to oxirane ranged from 0.0 to 1.0. This ratio was used to normalize the differences in molecular weight and functionality among the different CTAs surveyed in this study. The

photoinitiator concentration was 0.3 wt% of the resin mass (epoxide monomer + CTA mass) for all formulations unless otherwise noted.

### 4.2.3 Methods

#### 4.2.3.1 Kinetics

Epoxide conversions were determined using real-time Raman spectroscopy, which has been described previously.<sup>24,25</sup> Each formulation was injected into 1 mm ID, 25 mm long quartz capillary tube, which was placed in a thermo-stated sample holder. The temperature of the sample holder was maintained at 30°C. UV light ( $300 \text{ nm} < \lambda < 450 \text{ nm}$ ) with an effective irradiance of  $50 \text{ mW/cm}^2$  was delivered to the midpoint of the sample from a 100 W high pressure mercury lamp (Acticure<sup>®</sup> Ultraviolet/Visible spot cure system, EXFO Photonic Solutions, Inc.) via a fiber optic light guide. Raman spectra were collected from the UV-illuminated region every 1 to 1.5 seconds for 5 to 10 minutes of total illumination time using a holographic fiber-coupled stretch probehead (Mark II, Kaiser Optical Systems, Inc.) attached to a modular research Raman spectrograph (HoloLab 5000R, Kaiser Optical Systems, Inc.). As in previously reported studies, ~200 mW from a 785 nm near-infrared laser was delivered to the sample, and the peak area under the reactive band at  $790 \text{ cm}^{-1}$  was integrated and used to calculate the conversion of epoxide rings. The final conversion was determined by averaging the last ten spectra leading up to 300 seconds of illumination. The normalized rate of polymerization ( $R_p/[M]_0$ ) was determined by fitting the conversion profile to a 4-parameter logistic function and then taking the first derivative with respect to time. The maximum of the first derivative of the conversion profile gives the maximum normalized rate of polymerization,  $R_{p,\text{max}}/[M]_0$ .

#### 4.2.3.2 Physical/Mechanical Properties

Polymer specimens were prepared by injecting the formulation resin between two silanized (Rain-X treated) microscope slides. The slides were separated by two 150 micron thick glass coverslips, resulting in a nominal resin thickness of 300 microns. The resin-containing assembly was illuminated by a black light ( $2-5 \text{ mW/cm}^2$ ) for 5 minutes per side to ensure both sides reached high conversion. Then, the assembly was passed twice, once per side, at 3 ft/minute through a belt-driven Fusion curing system (model LC-6B) fixed with an H-bulb. The specimens were stored for 2 weeks and subsequently heated in a convection oven at  $125^\circ\text{C}$  for 1 hour and then  $175^\circ\text{C}$  for 1 hour, allowed to cool to room temperature, and removed from the mold for analysis. This annealing procedure was necessary to prevent continued epoxide reaction during dynamic mechanical analysis (DMA). Since curing conditions for kinetic analysis and DMA specimen preparation are different, no direct correlations between observed conversions and physical properties are expected. The specimens were analyzed by DMA in a TA instruments Q800 dynamic mechanical analyzer. Specimens with approximate dimensions of  $15 \times 5 \times 0.3 \text{ mm}$  were tested in a film tension clamp with a sinusoidal strain of 0.05% applied at a frequency of 1 Hz over a broad temperature range ( $-100 < T < 300^\circ\text{C}$ ). The glass transition ( $T_g$ ) of the materials produced was taken to be the temperature corresponding to the maximum  $\tan \delta$  value.

The gel fraction was determined from polymer bars prepared by pouring formulations into 1 mm deep moulds made of Teflon. The filled moulds were subsequently illuminated and annealed in the same way as DMA specimens. The polymer specimens were massed (1-2 g) and placed in a capped vial with a THF solution containing 3 wt% *N*-ethyl-diisopropylamine. The THF solution serves as a solvent and terminates the polymerization; the amine prevents further cationic polymerization of residual epoxide monomer and THF. After storage for three days, the solvent was decanted, and the polymer was filtered and washed with three portions of THF. Then, the

filter paper and polymer were dried under vacuum, and the remaining polymer was weighed. The gel fraction was calculated using the Eq. 4.1:

$$\text{gel fraction} = W_f / W_i \quad 4.1$$

where  $W_f$  is the final polymer mass and  $W_i$  is the initial polymer mass.

### 4.3 Results and Discussion

#### 4.3.1 Reactivity of Neat EEC

The reactivity of neat EEC under cationic photopolymerization conditions is low (~10% under the conditions in this study, see Figure 4.4). The substructures found in EEC have been studied with respect to reactivity, and the nucleophilicity and basicity of the ester functionality significantly decreases the maximum polymerization rate.<sup>26</sup> In addition to the kinetic effect, the high network density achieved at relatively low conversions severely limits the mobility of polymerized segments and active centers, which limits the rate of polymerization as well as the conversion.

#### 4.3.2 General CTA Effects

The effect of increased CTA concentration in an EEC-based resin is increased conversion (see Figure 4.4 for representative conversion profiles of *n*-octanol and 1,2-propanediol in EEC). In addition to increased conversions, greater induction periods (i.e., the time from illumination to rapid polymerization) are also observed at high CTA levels. Both mono-ol and diol CTAs greatly enhanced epoxide conversion compared to formulations of neat EEC (~10% conversion), with conversions up to 60% and 80% for 1.0 OH eq. from mono-ol and diol CTAs, respectively. Limiting conversions are often observed in photopolymerizations of high  $T_g$  formulations carried out at ambient conditions. As the network develops, it reaches a critical crosslink density above which a glassy, highly vitrified polymer is formed. In the glassy state, propagation is very slow, and conversion increases are not observed in normal reaction times (seconds to

minutes).<sup>27-29</sup> With no CTAs present, EEC reaches the glassy state at low conversions. CTAs decrease the average molecular weight of thermoplastics<sup>30</sup> and the average crosslink density in thermosets and therefore increase the critical conversion. Through this network density depression, higher conversion levels are achieved under ambient photopolymerization conditions. A direct effect of increased CTA concentration in an EEC-based resin is decreased  $T_g$  and rubbery modulus (see Figure 4.5 for representative DMA traces of *n*-octanol and 1,2-propanediol in EEC). The addition of *n*-octanol resulted in a  $T_g$  depression of about 40°C per 0.1 hydroxyl equivalents; whereas, 1,2-propanediol only depressed the  $T_g$  by 15-20°C per 0.1 hydroxyl equivalents. The rubbery modulus is the region of the storage modulus immediately following the glass transition. The modulus value in the rubbery region has been shown to correlate with the crosslink density.<sup>31,32</sup> Neat EEC has a rubbery modulus of approximately 70 MPa, while the *n*-octanol:EEC (0.3 OH eq.) rubbery modulus is only 4-5 MPa. 1,2-Propanediol formulations exhibited similar rubbery modulus depression. The 0.3 eq. formulation had a rubbery modulus of about 20 MPa, and the 0.6 eq. formulation had a rubbery modulus of 4-5 MPa.

In addition to reduction in  $T_g$  and rubbery modulus, CTAs also reduce the gel fraction of the polymer (see Figure 4.6 for representative gel fraction changes of *n*-octanol and 1,2-propanediol in EEC). The addition of *n*-octanol steadily decreased the gel fraction of the polymer from about 100% gel content at 0.1 hydroxyl equivalents to less than 50% gel content at 0.5 hydroxyl equivalents. CTA loadings above 0.5 hydroxyl equivalents from *n*-octanol resulted in a viscous liquid from which gel fraction could not be determined. Conversely, 1,2-propanediol can be formulated up to 0.6 hydroxyl equivalents before dropping below 90% gel content. At the equimolar hydroxyl to oxirane ratio (hydroxyl equivalent = 1.0) with 1,2-propanediol, the gel content was just below 50%.

Differences in functionality cause the lag in gel fraction reduction for diol CTA loadings in comparison with mono-ol CTA loadings. This difference between mono-ols and diols can be illustrated by the hypothetical reaction of these two CTAs with a growing linear polymer chain that has a cationic active center located at its terminus (see Figure 4.7). In the first case, the mono-functional *n*-octanol reacts with the end of the growing polymer chain, producing an octyl-terminated polymer and a free proton. In the second case, the di-functional 1,2-propanediol reacts with the growing polymer chain, producing a hydroxyl-terminated polymer and a free proton. In both cases, the free proton is available for monomer activation, and therefore the net polymerization is not terminated. However, in the first case, the polymer cannot react any further because it has been end capped with the non-reactive octyl group; whereas, in the second case, the polymer can continue to react with other activated monomers because it is hydroxyl terminated. Therefore, CTAs of higher functionality lead to higher molecular weights and higher properties ( $T_g$ , gel fraction and crosslink density) in general. The thermosetting systems studied in this work show increases in network density and gel fraction when diols were formulated in place of mono-ols.

#### 4.3.3 CTA Size: Mono-ols

*n*-Alkyl alcohols ranging from methanol to dodecanol were studied and characterized by the average conversions observed at the end of 300-s illumination, as well as average maximum polymerization rates. The final conversion increased with increasing CTA level, but no relationship between the size of the CTA and the final conversion was found. The maximum rate also showed no dependence on the size or concentration of the CTA used. However, all formulations with CTAs exhibited higher rates of polymerization and conversions than neat EEC.

For a mono-ol series (formulated to 0.3 OH eq.), the  $T_g$  of the polymer decreased as the molecular weight of the CTA increased (see Figure 4.8). Methanol in EEC resulted



in a  $T_g$  around 130°C, while the  $T_g$  of the dodecanol formulation occurred around 80°C. The  $T_g$  reduction is likely due to the plasticizing effect of the alkyl chains that terminate the polymer. Larger alkyl chains provide a greater plasticization effect. The relationship between the  $T_g$  of the polymer and the molecular weight of the mono-functional CTA is non-linear and plateaus at an alkyl chain of about eight carbons in length. The diminishing effect of CTA alkyl chain length is shown in the  $T_g$ 's of dodecanol and octanol, which are approximately the same despite octanol being only two thirds the length of dodecanol. In the chain transfer reaction, an alkyl group is exchanged for the terminal group in place of a secondary hydroxyl group (Figure 1.10). Thus, the chemical similarity between relatively long alkyl groups and shorter alkyl groups in comparison to the much greater chemical difference between shorter alkyl groups and a secondary hydroxyl group results in little difference between the  $T_g$ 's of octanol and dodecanol.

The rubbery plateau of mono-ol containing formulations dropped precipitously in comparison to neat EEC (4-8 MPa vs. ~70 MPa). All of the mono-ol CTAs formulated at 0.3 OH eq. resulted in similar rubbery moduli regardless of the CTA molecular weight. The mono-functional CTAs all have similar nucleophilicities, reaction rates, and final conversion with only small absolute changes in molecular weight to differentiate. The number of chain transfer events induced by the CTA will be the same for all CTAs of this group; therefore, the resulting crosslink density, which is correlated via rubbery modulus, will also be similar.

#### 4.3.4 CTA Size: Di-ols

Diols of varying molecular weights were also formulated and studied under the same conditions and analytical methods as the mono-ol CTAs. The smallest diol studied was 1,2-ethanediol, and the largest was polyTHF 2000. The final conversion increased slightly with increasing CTA molecular weight. In addition, all CTAs were effective in increasing the epoxide conversion compared to neat EEC, indicating that the AM

mechanism took place in all cases. The maximum rate of polymerization decreased dramatically from the 0.3 OH eq. formulation of EEC:1,2-ethanediol, which reacted about eight times faster than the neat EEC, to the EEC:polyTHF 2000 formulations, which reacted at or slightly less than the reaction speed of neat EEC (see Figure 4.9).

The lower rates of polymerization observed with the high molecular weight (MW) diols are likely due to dilution. Only the terminal hydroxyl groups of the diols react and therefore contribute to epoxide conversion. In high MW CTAs, a very high fraction (volume and mass fractions) of the material is nonreactive. In order to load the high MW CTAs to the same OH equivalents as the lower MW CTAs, more mass is required (due to the high equivalent weight). The epoxide species, as well as the hydroxyl groups, are diluted when high MW CTAs are used. The rate of epoxide consumption is proportional to the concentration of epoxide functional groups (as described by the ACE mechanism) and the hydroxyl group concentration (as described by the AM mechanism). The dilution of reactive species therefore decreases the rate of epoxide conversion.

The large size differences of the diols studied produced a broad range in physical properties (see Figure 4.10). The glass transition temperatures of the polymers formed from diol formulations were lower than neat EEC, which is around 230°C, and the  $T_g$  could be tuned by selecting the appropriately sized CTA. The lowest  $T_g$  measured was approximately -20°C, and the highest was approximately 170°C, corresponding to the polyTHF 2000 and 1,2-ethanediol formulations, respectively. However, the diols did not depress the  $T_g$  as much as their mono-ol analogs. For instance, at 0.3 hydroxyl equivalents from 1,2-ethanediol, the  $T_g$  was 170°C, while the ethanol formulation exhibited a much lower  $T_g$  of 115°C. For butanols, 1,4-butanediol gave a  $T_g$  of 160°C, while the *n*-butanol formulation produced a  $T_g$  of 100°C. In addition, although the rubbery plateau of all diol formulations was lower than that for neat EEC, the rubbery plateau was generally greater than that of mono-ol formulations (rubbery modulus > 18 MPa for diol formulations vs. 4-8 MPa for mono-ol formulations). PolyTHF 1000 and

2000 had rubbery moduli approaching mono-ol values (11 and 8 MPa, respectively) as shown in Figure 4.10. Since the height of the rubbery plateau is directly related to the crosslink density, the higher rubbery moduli of the diol formulations further supports that higher functionality CTAs retain higher properties of crosslinking resins and is consistent with the comparison of  $T_g$ 's and gel fractions of 1,2-propanediol and *n*-octanol discussed previously. The exceptionally low rubbery moduli of polyTHF 1000 and 2000 are observed because a high mass fraction of low  $T_g$  material was used as CTAs; whereas, low MW diols did not require as much material to reach the normalized OH concentration of 0.3 eq. Thus, a hard, rigid polymer or a soft, rubbery polymer may be formed via judicious selection of EEC:CTA formulation.

#### 4.3.5 Variation in Nucleophilicity: Sterics

According to the AM mechanism, the hydroxyl groups of the CTA attack the protonated monomer, as shown in Figures 1.9 and 1.10. The mono-ol and diol CTAs showed no significant differences in polymerization rates except for dilution effects. All of the mono-ols and diols discussed thus far are primary alcohols and therefore have similar nucleophilicities. In order to understand the effect of substituent groups attached to CTAs, primary, secondary, and tertiary alcohols were selected for study.

The primary and secondary alcohols had similar conversions and polymerization rates, while the tri-substituted *t*-butanol had lower conversions and rates that were nearly the same as those for neat EEC. The similarity between the primary and secondary alcohols as CTAs is not surprising, since only a fraction of the epoxide conversion occurs from the direct reaction between the CTA and the protonated epoxide (direct CTA-epoxide reactions account for up to 30% epoxide conversion in experiments with 0.3 OH eq. formulations). Subsequent propagation reactions occur between the secondary hydroxyl groups produced from the ring opening of protonated monomers. The lower conversions and rates observed in the case of *t*-butanol are attributed to the increased

steric hindrance, which retards the initial ring-opening reactions between the CTA and protonated monomer in comparison to primary and secondary alcohols.

In order to clarify the differences between primary, secondary, and tertiary alcohols as CTAs, EEC was formulated with *n*-butanol, *s*-butanol, and *t*-butanol such that the epoxide to hydroxyl ratio was 1.0. Thus, with such high CTA concentrations, a much larger fraction of the epoxide conversions are attributed to the direct reaction between CTA hydroxyls and protonated monomers. Conversion profiles for EEC in the presence of primary, secondary, and tertiary butanol are shown in Figure 4.11. The *n*-butanol resulted in the steepest conversion profile, followed by *s*-butanol and then *t*-butanol, which was the least reactive CTA. The observed trend is expected, but the behavior of mildly substituted (secondary) alcohols at low concentrations is noteworthy. Only at high levels of steric hindrance and high concentrations is the retarding effect evident in the rate of polymerization.

The  $T_g$ 's of polymer specimens formed from formulations of normal, secondary, or tertiary butanol range from 100°C to 115°C, with *n*-butanol producing the lowest  $T_g$  and *t*-butanol producing the highest. The volume fraction taken up by the CTAs is similar since all three are isomers of butanol; however, the bulkiness of the tri-substituted *t*-butanol, and to some extent *s*-butanol, limits chain-end mobility and reptation, which drive the  $T_g$  up. *n*-Butanol and *s*-butanol show similar rubbery moduli, yet *t*-butanol has a rubbery modulus that is elevated relative to the other butanol isomers studied. The retention of higher crosslinking density further indicates that *t*-butanol is not as effective as a CTA relative to normal and secondary isomers of butanol.

#### 4.3.6 Variation in Nucleophilicity: Electronics

The nucleophilicity of an alcohol can be diminished by steric crowding and electronic effects. In the process of a CTA reacting with a protonated epoxide monomer, the lone pair of electrons attacks the protonated epoxide carbons (which have a partial

positive charge due to the oxygen being protonated). Substituents on the CTA can withdraw the electrons from the hydroxyl group (via induction or resonance) and reduce the charge and nucleophilicity of the CTA. CTAs with low nucleophilicities (lower pKa's)<sup>33</sup> are less reactive than more nucleophilic CTAs and therefore produce lower maximum polymerization rates and conversions. Phenol [pKa ~ 10]; 2,2,2-trifluoroethanol (TFE) [pKa ~ 11]; and 2,2,2-trichloroethanol (TCE) [pKa ~ 12] were studied in comparison with ethanol [pKa ~ 16] and cyclohexanol [pKa ~ 18] to examine these electronic effects.<sup>34-36</sup> The hydroxyl on a phenol molecule will deposit some of its electron density into the  $\pi$  system of the benzene ring via resonance. The hydroxyl groups of TFE and TCE lose electron density via induction from the highly electronegative trifluoro and trichloro groups. All three of these CTAs have reduced electron density at the hydroxyl group, which reduces the nucleophilicity and reactivity of these particular CTAs in comparison to their aliphatic analogs (i.e., ethanol and cyclohexanol). In addition to lower nucleophilicity, phenol, TFE, and TCE all have lower pK<sub>a</sub>s and are more acidic than their aliphatic analogs. Therefore, phenol, TFE, and TCE will be further referenced as acidic CTAs.

Formulations with the acidic CTAs yielded very low final conversions and maximum rates of epoxide conversion (see Figure 4.12). While formulations containing the aliphatic analogs produced conversion levels 2-3 times greater than neat EEC, the acidic CTAs had conversions comparable to neat EEC. The maximum rate for ethanol formulations was much greater than all other CTAs studied here. The maximum rate for cyclohexanol formulations was similar to those with acidic CTAs. However, the

relatively high conversion of cyclohexanol formulations demonstrates that the maximum rate was sustained much longer than those for neat EEC or the acidic CTAs formulations, even though it was much lower compared to that of the ethanol formulations.

Polymers formulated with EEC and the acidic CTAs or their aliphatic analogs had similar  $T_g$ 's (110-120°C). The CTAs are of similar size except phenol and cyclohexanol, which are bulkier. The larger size of phenol and cyclohexanol should promote lower  $T_g$  values, according to what was observed in the case of mono-ols, but this effect is offset by the bulky rings in these two CTAs, which promote higher  $T_g$  values, as observed in the case of *t*-butanol. However, the rubbery moduli vary between the acidic CTAs and aliphatic analogs. Polymers formulated with the aliphatic alcohols have very low rubbery moduli (5-10 MPa), similar to those with mono-ols. Polymers formulated with the acidic CTAs have higher rubbery moduli (20-60 MPa), which indicate materials with higher crosslink density. Since the acidic CTA concentrations were comparable to the other formulations studied, they have lower efficacies as CTAs.

#### 4.4 Conclusion

Various alcohols were selected and studied as CTAs in the cationic crosslinking epoxide polymerization of EEC. Increasing the concentration of the CTA in a given formulation generally produces greater conversions and polymerization rates. Multifunctional CTAs were found to retain the high properties ( $T_g$ , crosslink density, and gel fraction) of the neat crosslinking resin more fully than the monofunctional CTAs. The size of monofunctional CTAs had minimal effects on conversion and polymerization rates, but reduced the  $T_g$ . Diols also produced lower  $T_g$  materials with increasing CTA size. However, as the size of the diol increased, the increase in the rate of polymerization was less due to dilution effects. High epoxide conversion was obtained without respect to the size of the CTA. Two groups of CTAs with lower nucleophilicities resulted in lower reactivity with the epoxide: (1) alcohols with high steric shielding near the active hydroxyl group and (2) alcohols with acidic hydroxyl groups arising from low electron density around the active hydroxyl groups via resonant and/or inductive effects. In

general, CTAs can be used to tune the properties of epoxy resins over a very broad range of  $T_g$ 's and crosslink densities through selection of CTA alkyl chain length.

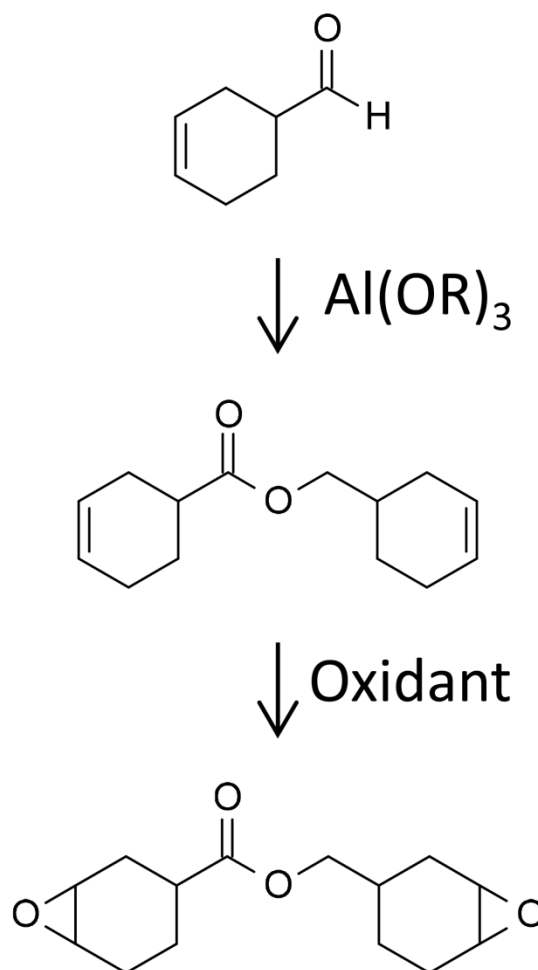


Figure 4.1: Synthesis of EEC carried out via aldehyde coupling (Tischenko reaction) followed by oxidation/epoxidation.



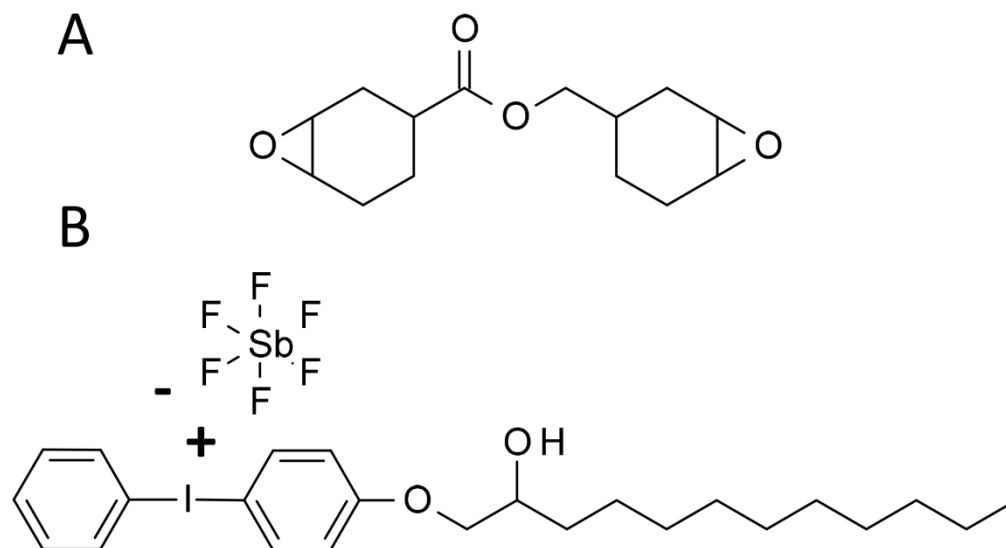


Figure 4.2: Chemical structures of (A) the di-epoxide monomer(EEC) and (B) the cationic photoinitiator (PC2506) used in this study.

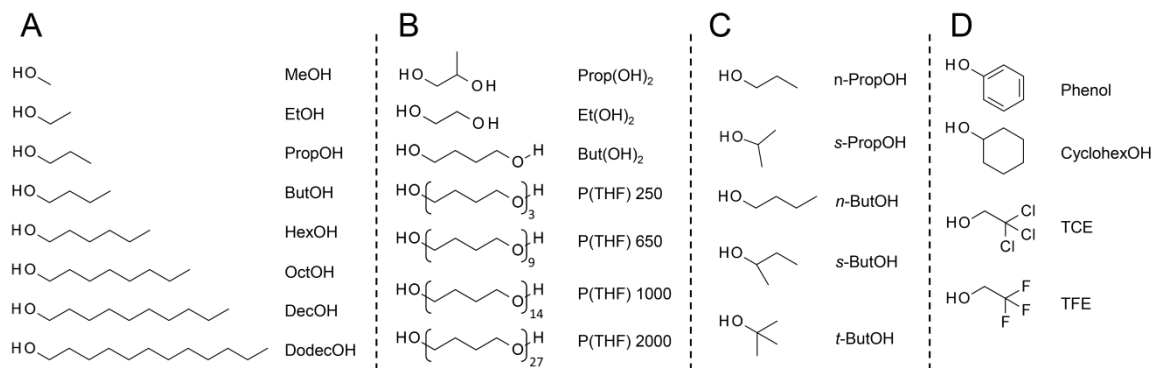


Figure 4.3: Chemical structures of CTAs used in this study. From top to bottom: (A) Mono-ols: methanol, ethanol, n-propanol, n-butanol, n-hexanol, n-octanol, n-decanol, and n-dodecanol; (B) diols: 1,2-propanediol, 1,2-ethanediol, 1,4-butanediol, polyTHF 250, polyTHF 650, polyTHF 1000, and polyTHF 2000; (C) primary, secondary, and tertiary CTAs: n-propanol, s-propanol, n-butanol, s-butanol, t-butanol; (D) acidic CTAs and aliphatic analogs: phenol, cyclohexanol, 2,2,2-trifluoroethanol, and 2,2,2-trichloroethanol.

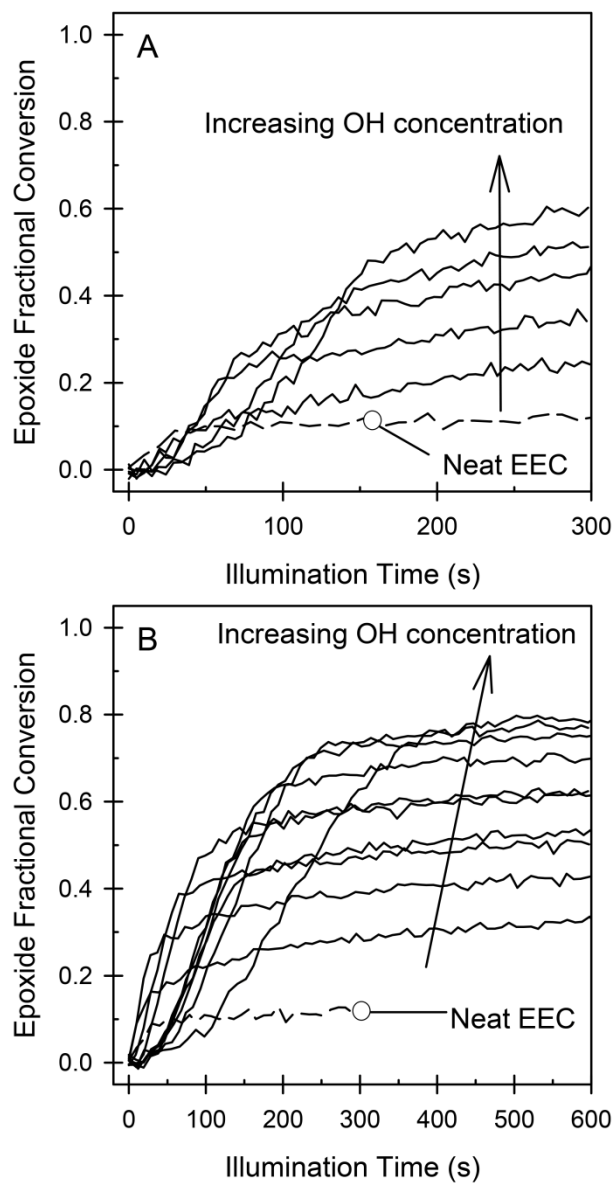


Figure 4.4: Epoxide conversion profiles. Formulations varied in increments of 0.1 OH equivalents from neat EEC (dashed line) to 0.5 OH equivalents from n-octanol (A) and 1.0 OH equivalents from 1,2-propanediol (B).

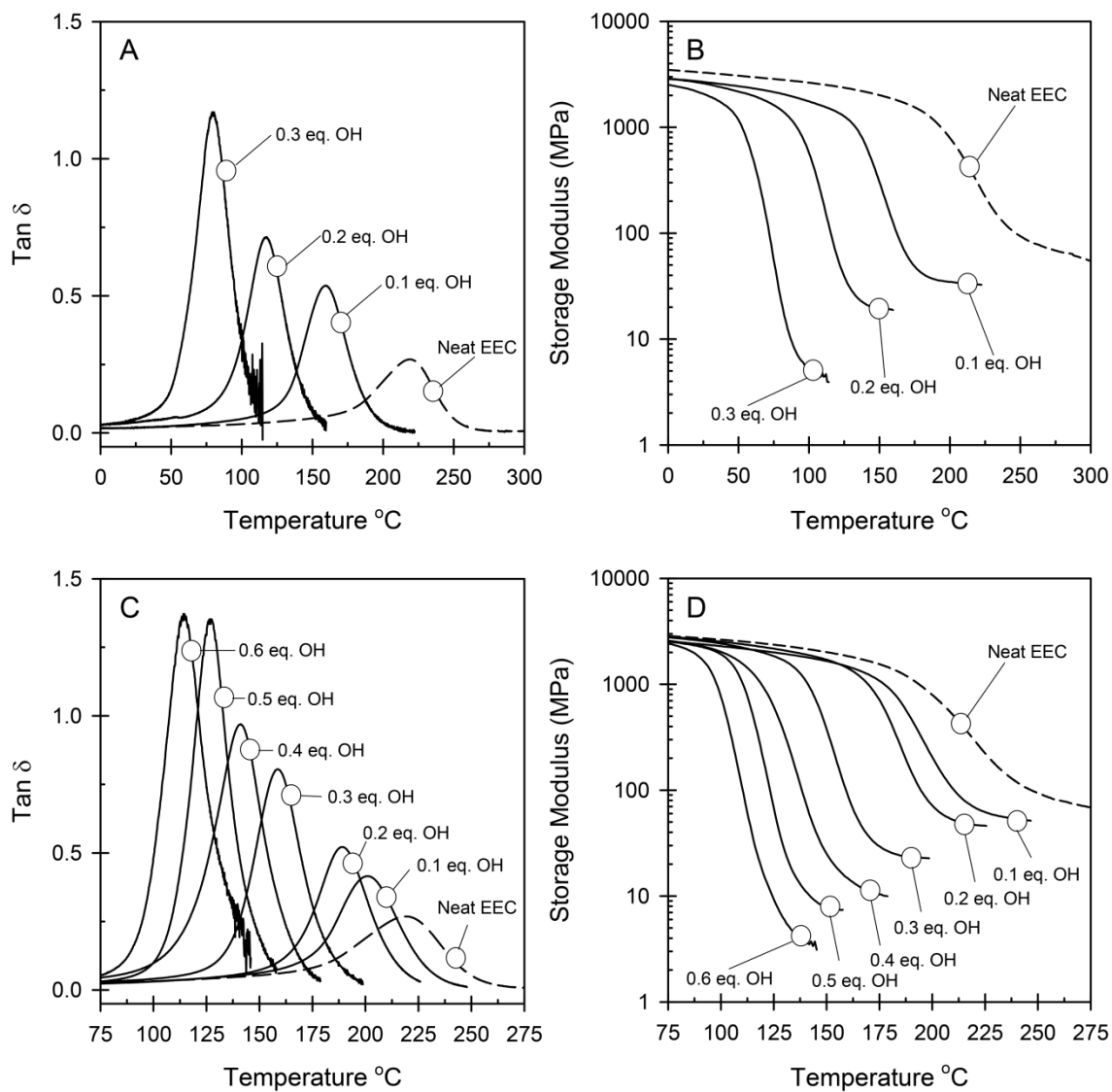


Figure 4.5: DMA traces showing the tan  $\delta$  (left) and the storage modulus (right) for EEC formulations containing n-octanol (A and B) or 1,2-propanediol (C and D) as CTA. Polymer specimens were annealed before measurements.

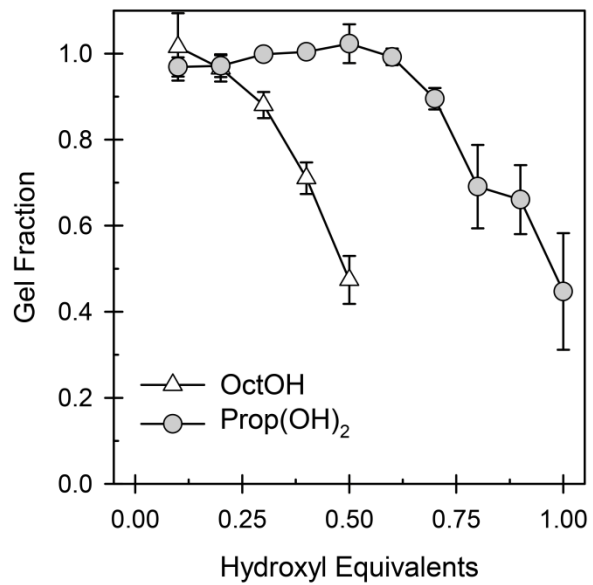


Figure 4.6: Gel fraction data for polymers prepared from EEC:octanol (open triangles) and EEC:1,2-propanediol (filled circles) formulations.

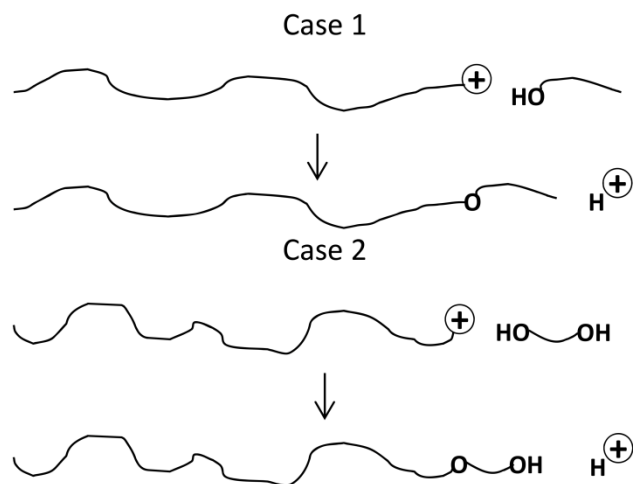


Figure 4.7: A comparison of a propagating cationic active center reacting with two types of CTAs (Case 1: a mono-ol, Case 2: a diol).

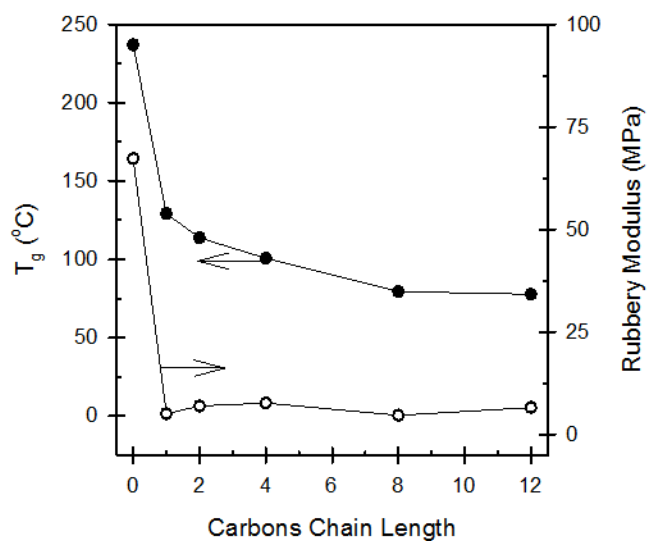


Figure 4.8: Glass transition temperature (filled circles) and rubbery modulus (open circles) of polymers prepared from EEC:- mono-ols formulations as a function of the carbon chain length of aliphatic alcohols used as CTAs. All formulations contained 0.3 OH equiv CTA and were photocured and annealed before analysis. Carbon chain length  $\frac{1}{4}$  0 for neat EEC.

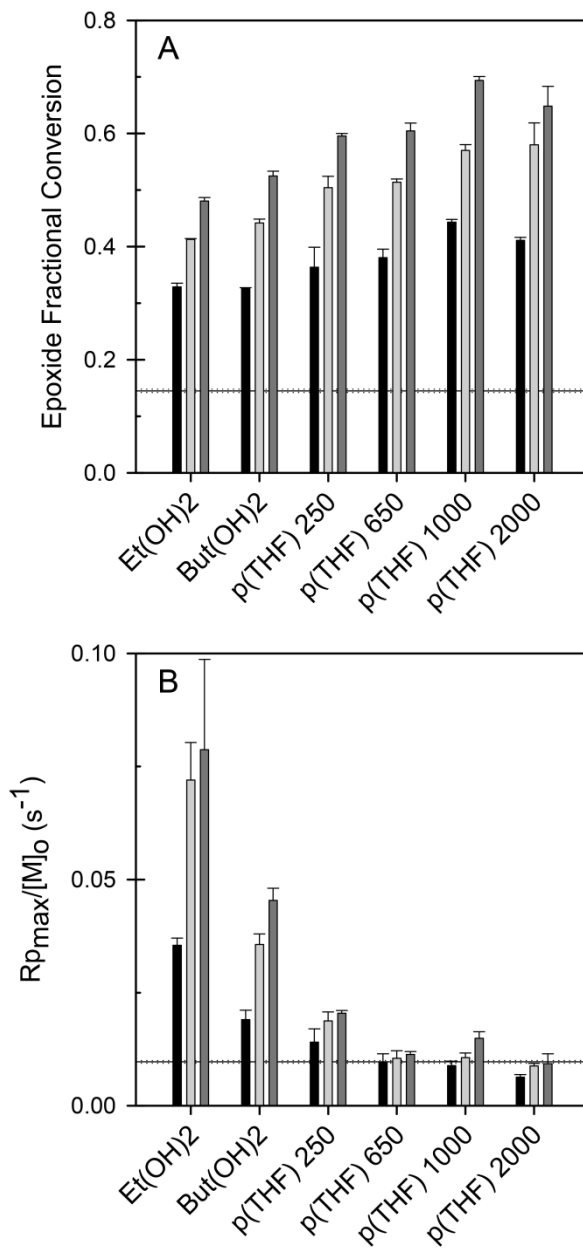


Figure 4.9: Final conversions (A) and maximum rates of epoxide consumption (B) observed in EEC formulated with diols. Each CTA was formulated to 0.1 (black bar), 0.2 (light gray bar), and 0.3 (dark gray bar) OH equivalents. The horizontal line represents the conversion and maximum rate observed in neat EEC.



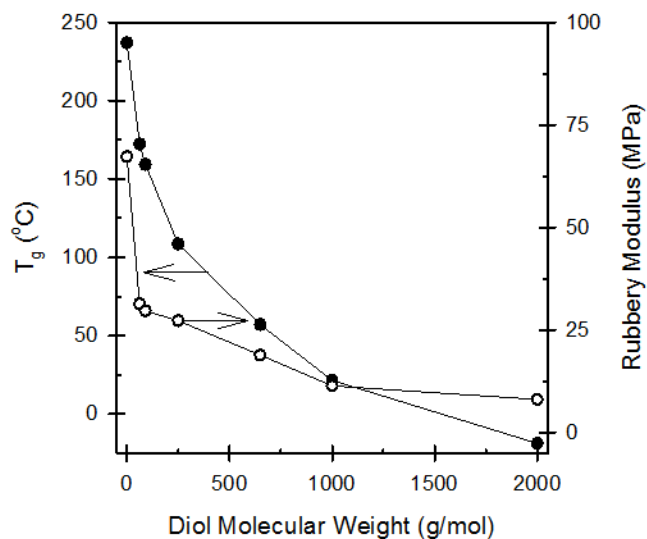


Figure 4.10: Glass transition temperature (filled circles) and rubberystorage modulus (open circles) of polymers prepared from EEC:diol formulations as a function of the molecularweight of the diols used as CTAs. All formulations contained 0.3 OH equiv CTA and were photocured and annealed before analysis. MW  $\frac{1}{4}$  0 for neat EEC.

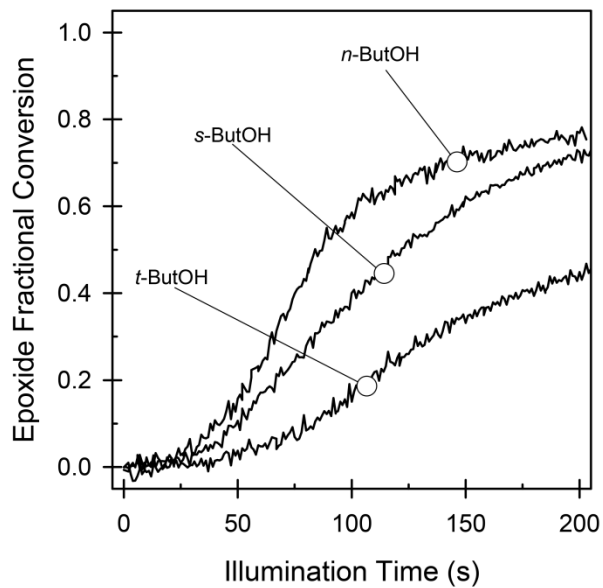


Figure 4.11: Conversion profiles for EEC:(n, s, or t) butanol formulations. The OH concentration was equal to the oxirane concentration in all cases.

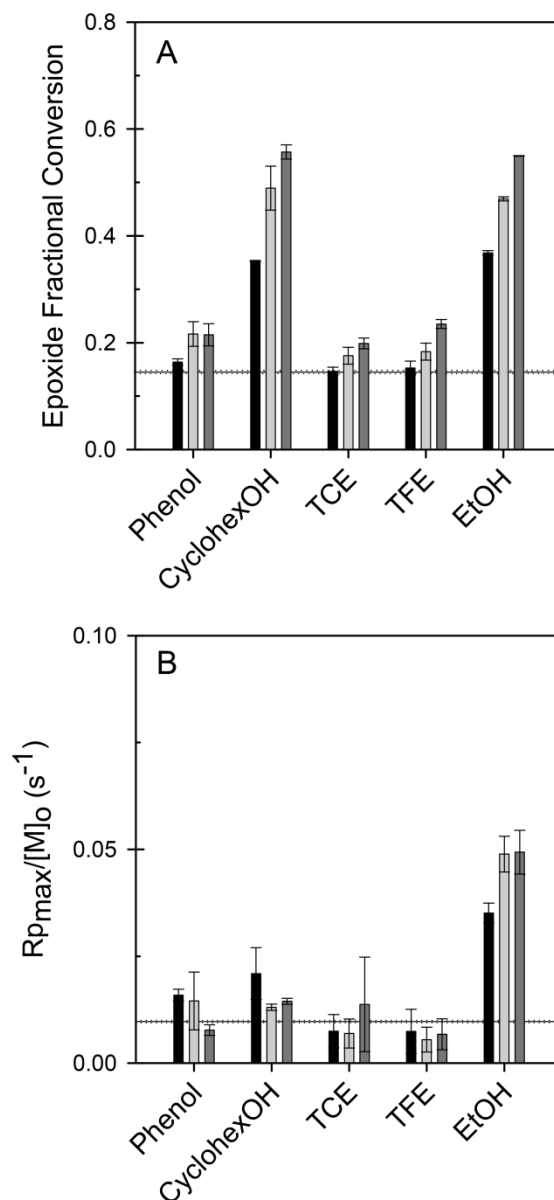


Figure 4.12: Final conversions (A) and maximum rates of epoxide consumption (B) observed in EEC formulated with acidic CTAs and their aliphatic analogs. Each CTA was formulated to 0.1 (black bar), 0.2 (light gray bar), and 0.3 (dark gray bar) OH equivalents. The horizontal line represents the conversion and maximum rate observed in neat EEC.

Notes

- (1) Fouassier, J. *Photoinitiation, Photopolymerization, and Photocuring*; Hanser/Gardner Publications, Inc.: Cincinnati, OH, 1995; , pp 375.
- (2) Koleske, J. V. *Radiation Curing of Coatings*; ASTM International: West Conshohocken, PA, 2002; Vol. 1, pp 244.
- (3) Crivello, J. V.; Lam, J. H. W. "Diaryliodonium Salts. A New Class of Photoinitiators for Cationic Polymerization." *Macromolecules* **1977**, *10*, 1307-1315.
- (4) Crivello, J. V. "The discovery and development of onium salt cationic photoinitiators." *Journal of Polymer Science Part A: Polymer Chemistry* **1999**, *37*, 4241-4254.
- (5) Decker, C.; Moussa, K. "Kinetic-Study of the Cationic Photopolymerization of Epoxy Monomers" *Journal of Polymer Science Part A: Polymer Chemistry* **1990**, *28*, 3429-3443.
- (6) Decker, C. "Photoinitiated cationic polymerization of epoxides" *Polymer International* **2001**, *50*, 986-997.
- (7) Nelson, E.; Scranton, A. B. "In situ Raman spectroscopy for cure monitoring of cationic photopolymerizations of divinyl ethers" *Journal of Raman Spectroscopy* **1996**, *27*, 137-144.
- (8) Nelson, E.; Jacobs, J.; Scranton, A. B.; Anseth, K.; Bowman, C. N. "Photo-differential Scanning Calorimetry Studies of Cationic Polymerizations of Divinyl Ethers" *Polymer* **1995**, *36*, 4651-4656.
- (9) Sipani, V.; Scranton, A. B. "Dark-cure studies of cationic photopolymerizations of epoxides: Characterization of the active center lifetime and kinetic rate constants" *Journal of Polymer Science Part A: Polymer Chemistry* **2003**, *41*, 2064-2072.
- (10) Sipani, V.; Kirsch, A.; Scranton, A. B. "Dark cure studies of cationic photopolymerizations of epoxides: Characterization of kinetic rate constants at high conversions." *Journal of Polymer Science Part A: Polymer Chemistry* **2004**, *42*, 4409-4416.
- (11) Kubisa, P.; Bednarek, M.; Biedron, T.; Biela, T.; Penczek, S. "Progress in activated monomer polymerization. Kinetics of AM polymerization." *Macromolecular Symposia* **2000**, *153*, 217-226.
- (12) Kubisa, P.; Penczek, S. "Cationic activated monomer polymerization of heterocyclic monomers." *Progress in Polymer Science* **2000**, *24*, 1409-1437.

- (13) Crivello, J. V.; Conlon, D. A.; Olson, D. R.; Webb, K. K. "The Effects of Polyols as Chain Transfer Agents and Flexibilizers in Photoinitiated Cationic Polymerization" *Journal of Radiation Curing* **1986**, 3-9.
- (14) Hartwig, A.; Sebald, M. "Preparation and properties of elastomers based on a cycloaliphatic diepoxide and poly(tetrahydrofuran)" *European polymer journal* **2003**, 39, 1975.
- (15) Hartwig, A.; Koschek, K.; Lühring, A.; Schorsch, O. "Cationic polymerization of a cycloaliphatic diepoxide with latent initiators in the presence of structurally different diols" *Polymer* **2003**, 44, 2853.
- (16) Sangermano, M.; Bongiovanni, R.; Malucelli, G.; Roppolo, I.; Priola, A. "Siloxane additive as modifier in cationic UV curable coatings" *Progress in organic coatings* **2006**, 57, 44.
- (17) Ortiz, R.; Lopez, D.; Cisneros, M.; Valverde, J.; Crivello, J. V. "A kinetic study of the acceleration effect of substituted benzyl alcohols on the cationic photopolymerization rate of epoxidized natural oils" *Polymer* **2005**, 46, 1535-1541.
- (18) Sangermano, M.; Bongiovanni, R.; Priola, A.; Pospiech, D. "Fluorinated alcohols as surface-active agents in cationic photopolymerization of epoxy monomers" *Journal of polymer science. Part A, Polymer chemistry* **2005**, 43, 4144-4150.
- (19) Sangermano, M.; Tasdelen, M.; Yagci, Y. "Photoinitiated curing of mono- and bifunctional Epoxides by combination of active chain end and activated monomer cationic polymerization methods" *Journal of polymer science. Part A, Polymer chemistry* **2007**, 45, 4914-4920.
- (20) Biedron, T.; Brzezinska, K.; Kubisa, P.; Penczek, S. "Macromonomers by Activated Polymerization of Oxiranes - Synthesis and Polymerization" *Polymer International* **1995**, 36, 73-80.
- (21) Crivello, J. V.; Liu, S. "Photoinitiated cationic polymerization of epoxy alcohol monomers" *Journal of polymer science. Part A, Polymer chemistry* **2000**, 38, 389-401.
- (22) Ghosh, N. N.; Palmese, G. R. "Electron-beam curing of epoxy resins: Effect of alcohols on cationic polymerization." *Bulletin of Materials Science* **2005**, 28, 603-607.
- (23) Hartwig, A.; Schneider, B.; Lühring, A. "Influence of moisture on the photochemically induced polymerisation of epoxy groups in different chemical environment" *Polymer* **2002**, 43, 4243-4250.

- (24) Cai, Y.; Jessop, J. L. P. "Decreased oxygen inhibition in photopolymerized acrylate/epoxide hybrid polymer coatings as demonstrated by Raman spectroscopy." *Polymer* **2006**, *47*, 6560-6566.
- (25) Cai, Y.; Jessop, J. L. P. "Effect of water concentration on photopolymerized acrylate/epoxide hybrid polymer coatings as demonstrated by Raman spectroscopy" *Polymer* **2009**, *50*, 5409-5413.
- (26) Crivello, J. V.; Varlemann, U. "Mechanistic study of the reactivity of 3,4-epoxycyclohexylmethyl 3',4'-epoxycyclohexanecarboxylate in photoinitiated cationic polymerizations." *Journal of Polymer Science Part A: Polymer Chemistry* **1995**, *33*, 2473-2486.
- (27) Decker, C.; Moussa, K. "Photopolymerization of multifunctional monomers in condensed phase." *Journal of Applied Polymer Science* **1987**, *34*, 1603-1618.
- (28) Scherzer, T.; Decker, U. "The effect of temperature on the kinetics of diacrylate photopolymerizations studied by Real-time FTIR spectroscopy" *Polymer* **2000**, *41*, 7681.
- (29) Ye, S.; Cramer, N.; Bowman, C. N. "Relationship between Glass Transition Temperature and Polymerization Temperature for Cross-Linked Photopolymers" *Macromolecules* **2011**, *44*, 490-494.
- (30) Odian, G. *Principles of Polymerization (Fourth Edition)*; John Wiley and Sons: Hoboken, NJ, 2004; .
- (31) Menard, K. *Dynamic Mechanical Analysis: A Practical Introduction*; CRC Press: Boca Raton, FL, 2008; , pp 218.
- (32) Murayama, T. *Dynamic Mechanical Analysis of Polymeric Material*; Elsevier Scientific Publishing Company: New York, 1978; Vol. 1, pp 231.
- (33) Anslyn, E. V.; Dougherty, D. A. *Modern Physical Organic Chemistry*; University Science Books: Sausalito, California, 2006; , pp 1099.
- (34) Wade, L. G. *Organic Chemistry*; Pearson Education Inc.: Upper Saddle River, NJ, 2006; , pp 1262.
- (35) Ballinger, P.; Long, F. "Acid ionization Constants of Alcohols. I. Trifluoroethanol in the Solvents H<sub>2</sub>O and D<sub>2</sub>O" *Journal of the American Chemical Society* **1959**, *81*, 1050-1053.
- (36) Ballinger, P. "Acid Ionization Constants of Alcohols. II. Acidities of Some Substituted Methanols and Related Compounds<sup>1, 2</sup>" *Journal of the American Chemical Society* **1960**, *82*, 795.

## CHAPTER 5

### THE INFLUENCE OF HUMIDITY ON SURFACE MODULUS OF PHOTO-CURED EPOXY COATINGS

#### 5.1 Introduction

Cationically cured epoxy coatings and adhesives are an important class of materials that serve as alternatives to the commonly used (meth)acrylate resins. Cationic polymerization is used in instances where inert gases or ultra-high illumination intensities are not feasible because oxygen (which inhibits free-radical polymerizations) has no effect on cationic polymerization.<sup>1-3</sup> Although oxygen does not affect cationic polymerization of epoxy resins, humidity can and does.<sup>4-6</sup> Water, through the activated monomer (AM) mechanism,<sup>7</sup> acts as a chain transfer agent in epoxy systems, which results in lower polymer properties, specifically cross-link density and glass transition temperature ( $T_g$ ).<sup>8</sup> If a formulation has been optimized for dry conditions and is then used under humid conditions, the effects of water may negatively impact the performance of the material, even to the point of material failure. In this study, we used atomic force microscopy (AFM) to show the extent of damage humid-curing conditions can have on the surface hardness of an epoxy resin. The surface of the cured materials will be impacted the greatest by atmospheric factors (water vapor in this case) because the surface interacts with the atmosphere directly, while the bulk of the resin is insulated from the atmosphere.

#### 5.2 Experimental

##### 5.2.1 Materials

An epoxy silicone monomer (PC-1000, Polyset Company) was chosen for this study as it displays high reactivity and high polymer properties, such as cross-link density and  $T_g$ , upon photocuring. The monomer was formulated with *n*-decanol (Sigma Aldrich)

at concentrations such that the ratio of hydroxyl to oxirane rings was equal to 0.1. The alcohol was used as a chain transfer agent to reduce the cross-link density and  $T_g$  of the neat resin to one that is less brittle and easier to handle. The photo-acid generator (PC-2506, Polyset Company) was formulated at 0.3 wt% relative to the resin mass (monomer + alcohol). All materials were used as received and are shown in Figure 5.1.

The liquid resins were poured into 1 mm deep, cup-style Teflon molds and placed inside an in-house fabricated humidity control chamber fitted with a quartz window. Polymer specimens were prepared using a 100 W high pressure mercury lamp (Acticure<sup>®</sup> Ultraviolet/Visible spot cure system, EXFO Photonic Solutions, Inc.). The UV light ( $300 \text{ nm} < \lambda < 450 \text{ nm}$ ), with an effective irradiance of  $50 \text{ mW/cm}^2$ , was directed at the sample, through the quartz window, for 400 seconds. In the first case, dry nitrogen gas was flowed through Drierite pellets and into the curing chamber; in the second case, the nitrogen gas was bubbled into saturated solutions of  $\text{NaSO}_4$ , resulting in the chamber equilibrating to 93% relative humidity at room temperature. Following photo-curing, the specimens were stored in a drawer at room temperature for 2 weeks and subsequently heated in a convection oven at  $125^\circ\text{C}$  for 1 hour and then  $175^\circ\text{C}$  for 1 hour, allowed to cool to room temperature, and removed from the mold for analysis. This annealing procedure was necessary to prevent continued epoxide reaction during dynamic mechanical analysis (DMA).

### 5.2.2 Methods

The  $T_g$  of the polymer specimens was determined via DMA. The specimens were cut into  $0.3 \times 6 \times 15$  mm sections and fixed in a film tension clamp. The temperature was ramped from  $-25$  to  $200^\circ\text{C}$  while oscillating the strain from 0-0.05% at a frequency of 1 Hz. The  $T_g$  was taken as the maximum of the tan delta profile.

Micro-surface analysis was carried out using AFM. The elastic modulus of an AFM tip was calibrated by deflecting it against a clean glass slide. The polymer specimen



was then imaged under coarse resolution conditions in order to find a flat, defect-free region. The defect-free region was indented by the cantilever 10 times per point, for a total of 3 points. The force applied to the sample was uniquely set for each point (12.5, 10.0, and 8.5  $\mu\text{N}$ ). A high resolution image was then obtained of the indented area. The image was used to determine the penetration depth for each point.

### 5.3 Results and Discussion

The effects of chain transfer agents (CTAs), including organic alcohols and water, in epoxy resins have been studied.<sup>8</sup> In general, increased concentration of CTA leads to increased conversion and maximum rate of polymerization with decreases in cross-link density and  $T_g$ .

The polymers prepared from epoxy silicone monomer formulations are characterized as clear, colorless, highly cross-linked, hard, and high  $T_g$  materials.<sup>9</sup> The tan delta maximum was approximately equal to  $\sim 90$  °C, and the approximate cross-link density, as measured from the rubbery modulus plateau at 150 °C, was  $4.4 \times 10^3$  mol/m<sup>3</sup> (see Figure 5.2).<sup>10,11</sup> It can be expected that significant changes in the degree of cure and crosslink density of the material would be required in order for it to behave as a rubber at room temperature, as opposed to the glass-like behavior it exhibits at full cure. These changes may be induced by the presence of humidity.

Water acting as a CTA decreases the crosslink density and  $T_g$  of a polymer, relative to the same polymer prepared under dry conditions.<sup>6</sup> The low solubility of water in epoxy resins, as well as the high viscosity and rapid photo-curing of epoxy resins, limits the effects of high humidity to the surface and near-surface region. Using AFM, the relative surface hardness of cured epoxy resins was determined for specimens cured under dry and humid conditions, respectively, via indentation experiments (see Figure 5.3).

In both the dry-cured and humid-cured materials, indentations formed from 12.5 and 10.0  $\mu\text{N}$  forces produced similar penetration depths for each sample; while the indentation resulting from the 8.5  $\mu\text{N}$  force was 2-3 times shallower than those from the two higher forces. However, the surfaces of the humid-cured material were sufficiently softened such that the permanent indentation depth was approximately double that of the dry-cured material indentations. The increased indentation depth suggests that the humid-cured polymer surface was much softer relative to the dry-cured material. The available water reduced the cross-link density of the material at the surface via chain transfer reactions, which resulted in a softer surface.

Another qualitative relationship to surface hardness is found in the shape of the force curves obtained during the indentation procedure.<sup>12</sup> Similar to stress-strain profiles, steep curves indicate a high modulus (hard surface), and shallow curves indicate a low modulus (soft surface). The force curves in Figure 5.4 display a distinct difference between the surface modulus of the humid-cured and dry-cured materials, despite the bulk properties of the polymer specimens being similar. The surface is affected by the humidity because the water vapor is initially sorbed on the resin surface. The water may then diffuse into the depths of the resin but much more slowly due to the high viscosity of epoxy resins. Therefore, the highest concentration of water is at the surface, and the highest impact water has on physical properties is observed at the surface.

#### 5.4 Conclusions

The effects of humidity on the bulk polymer properties of cross-linked materials based on photo-cured epoxy silicone monomers were negligible. AFM was used to determine qualitatively the surface hardness of the polymers when cured under dry and humid atmospheres. The apparent surface modulus and therefore hardness were impacted negatively when cured in a humid atmosphere. The decrease in properties due to humidity is explained by the AM mechanism, whereby water at the air-formulation

interface acts as a chain transfer agent and reduces the cross-link density in the surface layer of the cured material relative to polymers cured under dry conditions.

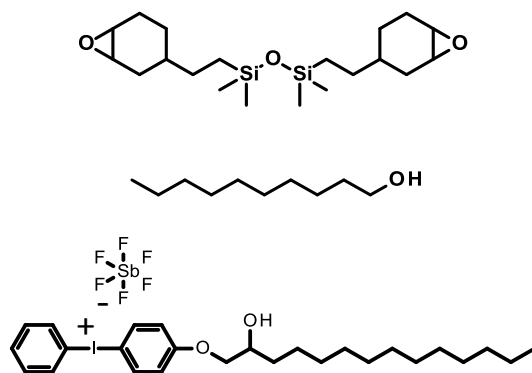


Figure 5.1: Epoxy silicone monomer, PC-1000 (top); chain transfer agent, n-decanol (middle); and photoinitiator PC-2506 (bottom).

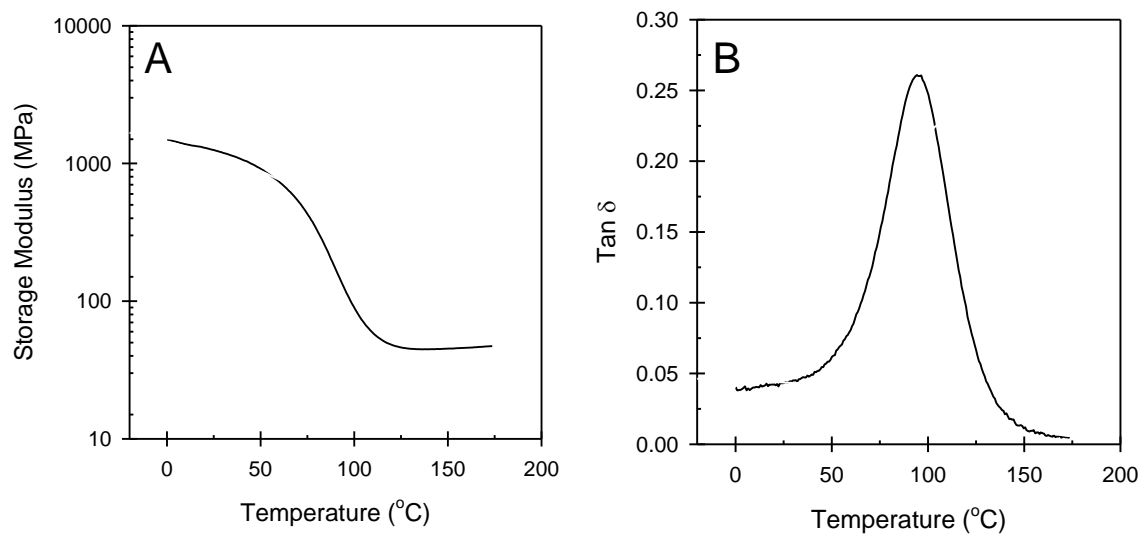


Figure 5.2: Storage modulus (A) and tan delta (B) profiles of a photocured and annealed silicone epoxy formulation.

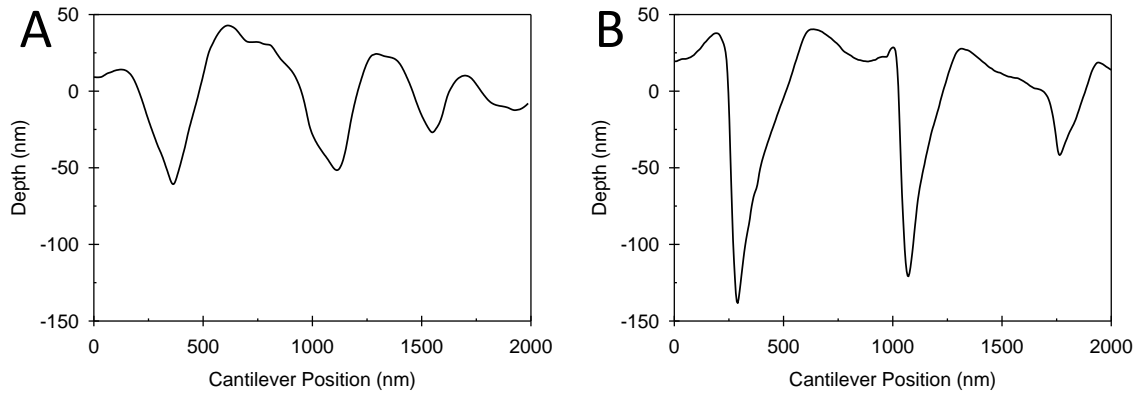


Figure 5.3: Cross sections of the polymer specimens after indentation procedure were acquired. Dry-cured materials are represented in A and humid-cured materials are represented in B. Indentations were obtained by applying 12.5, 10.0, and 8.5  $\mu\text{N}$  from left to right.

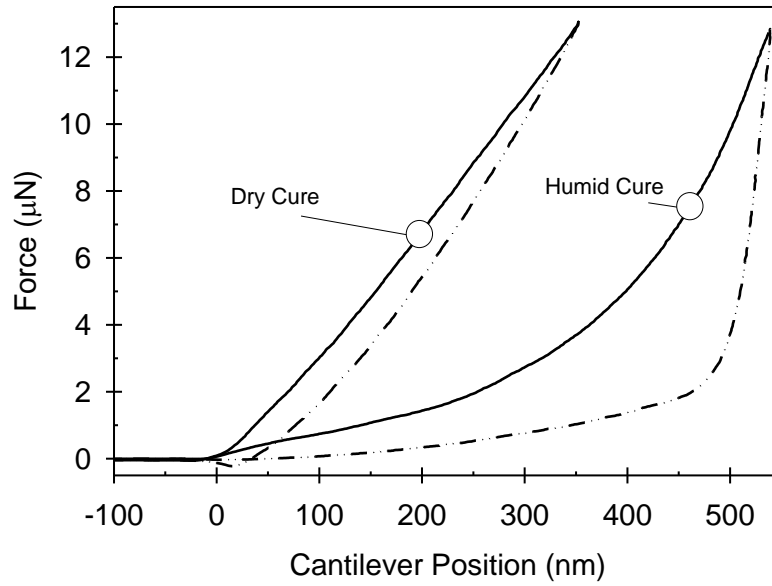


Figure 5.4: Force curves obtained during the indentation procedure via AFM. Solid traces represent the penetration step and the dashed lines represent the retraction step.

### Notes

- (1) Gou, L.; Opheim, B.; Scranton, A. B. "The effect of oxygen in free radical photopolymerization." *Recent Res. Dev. Polym. Sci.* **2004**, *8*, 125.
- (2) Decker, C.; Moussa, K. "Kinetic-Study of the Cationic Photopolymerization of Epoxy Monomers" *J. Polym. Sci. , Part A: Polym. Chem.* **1990**, *28*, 3429-3443.
- (3) Decker, C. "Photoinitiated cationic polymerization of epoxides" *Polym. Int.* **2001**, *50*, 986-997.
- (4) Hartwig, A.; Schneider, B.; Lühring, A. "Influence of moisture on the photochemically induced polymerisation of epoxy groups in different chemical environment" *Polymer* **2002**, *43*, 4243-4250.
- (5) Esposito Corcione, C.; Malucelli, G.; Frigione, M.; Maffezzoli, A. "UV-curable epoxy systems containing hyperbranched polymers: Kinetics investigation by photo-DSC and real-time FT-IR experiments." *Polym. Test.* **2009**, *28*, 157-164.
- (6) Cai, Y.; Jessop, J. L. P. "Effect of water concentration on photopolymerized acrylate/epoxide hybrid polymer coatings as demonstrated by Raman spectroscopy" *Polymer* **2009**.
- (7) Brzezinska, K.; Szymanski, R.; Kubisa, P.; Penczek, S. "Activated monomer mechanism in cationic polymerization. I: Ethylene oxide, formulation of mechanism" *Die Makromolekulare Chemie.Rapid communications* **1986**, *7*, 1-4.
- (8) Dillman, B.; Jessop, J. L. P. "Chain transfer agents in cationic photopolymerization of a bis-cycloaliphatic epoxide monomer: Kinetic and physical property effects" *J. Polym. Sci. , Part A: Polym. Chem.* **2013**.
- (9) Jang, M.; Crivello, J. "Synthesis and cationic photopolymerization of epoxy-functional siloxane monomers and oligomers" *Journal of polymer science.Part A, Polymer chemistry* **2003**, *41*, 3056-3073.
- (10) Menard, K. *Dynamic Mechanical Analysis: A Practical Introduction*; CRC Press: Boca Raton, FL, 2008; , pp 218.
- (11) Murayama, T. *Dynamic Mechanical Analysis of Polymeric Material*; Elsevier Scientific Publishing Company: New York, 1978; Vol. 1, pp 231.
- (12) Briscoe, B. J.; Fiori, L.; Pelillo, E. "Nano-indentation of polymeric surfaces" *J. Phys. D: Appl. Phys.* **1998**, *31*, 2395-2405.



CHAPTER 6  
POST ILLUMINATION PROPERTY DEVELOPMENT IN EPOXIDE  
PHOTOPOLYMERS

6.1 Introduction

UV/EB curing is a rapid and energy efficient method used to produce protective coatings, adhesives and sealants, templates for electronic devices, and even biomaterials such as tissue scaffolds.<sup>1-5</sup> A variety of chemical polymerization mechanisms are initiated via radiation curing including free radical (both chain and step polymerization), cationic, and anionic.<sup>6-15</sup> Free-radical polymerization is the most commonly used mechanism in UV/EB curing due to the low cost materials and high rates of polymerization. Cationic polymerization is used at lower volumes; anionic polymerization has been demonstrated to work in research laboratories, but to the author's knowledge has not yet been implemented in industry. Though cationic systems are more costly than the free-radical systems (in terms of monomers and photoinitiators), the use of cationic resins can be economically viable due to the tolerance of atmospheric oxygen.<sup>15</sup> Free-radical systems are inhibited by molecular oxygen in both the active center generation step (via photoinitiation) and the subsequent polymerization.<sup>6,16</sup> Conversely, cationic systems are unaffected by molecular oxygen in both the photoinitiation and polymerization steps.<sup>14,17</sup> The oxygen-tolerating capacity of cationic systems allows for good cure of thin films with hard, fully cured surfaces without the use of expensive purging equipment and inert gases (N<sub>2</sub>, CO<sub>2</sub>, and Ar). Other characteristics that set cationic systems apart include: monomer side reactions with other nucleophilic compounds (water and alcohols) and long-lived active centers (virtually no chemical termination occurs in many systems).<sup>18-26</sup>

The effects of other atmospheric factors and process contaminants that may affect the curing kinetics and the material properties of epoxy resins are important to consider.

The ubiquitous contaminant that is most difficult to control is water. Alcohols may also be introduced during monomer synthesis and purification phases of manufacture.

Epoxydes polymerize by two distinct mechanisms. One mechanism, called the active chain end (ACE) mechanism, is analogous to radical chain polymerization in that the active center is attached to the end of the growing polymer chain and neutral monomers react with the cationic active center to effect polymer chain growth. A second mechanism, called the activated monomer (AM) mechanism, is a chain transfer reaction in which a nucleophilic compound, like water or organic alcohols, react with a cationic active center that opens the epoxide ring, regenerates a hydroxyl group, and ejects a proton.<sup>27,28</sup> The ejected proton then bonds with other nucleophilic species, including neutral monomers that can then react with the hydroxyl group, formed at the terminus of the growing polymer chain, to continue polymer propagation. Representations of the ACE and AM mechanisms are shown in Figures 1.9 and 1.10. The effect of including alcohols or moisture in a formulation leads to promotion of the AM mechanism. When the AM mechanism is the dominant propagation mechanism, the kinetics and the network structure will be different. Our group has studied a variety of alcohols formulated in epoxy resins and observed increasing rates of polymerization, increasing final conversion levels, decreasing glass transition temperatures, and decreasing gel fractions with increasing amounts of CTAs.

## 6.2 Experimental

### 6.2.1 Materials

3,4-Epoxy cyclohexylmethyl-3,4-epoxycyclohexanecarboxylate (EEC, Aldrich) was the epoxide monomer used in this study (Figure 6.1). 1-Dodecanol, 1-butanol, t-butanol, 1,4-butanediol were purchased from Aldrich and used as chain transfer agents (CTA). The photo-acid generator was an iodonium hexafluoroantimonate salt (IHA) manufactured under the trade name PC2506 and donated by Polyset Company. All

formulations were prepared to contain 0.3 wt% IHA. The CTAs were formulated such that the ratio of hydroxyl groups to epoxide ranged from 0.1 to 1.0 in the kinetic experiments and equal to 0.3 for mechanical analysis.

## 6.2.2 Methods

### 6.2.2.1 Mechanical Analysis

Polymer specimens were prepared by injecting the formulation resin between two silanized (Rain-X treated) microscope slides. The slides were separated by two 150 micron thick glass coverslips resulting in a nominal resin thickness of 300 microns. The resin containing assembly was illuminated by a black light (about 2-5 mW/cm<sup>2</sup>) for 5 min per side then passed twice, once per side, through a belt-driven Fusion curing system fitted with a H-bulb at 3 ft/min. The specimens were stored for 2 weeks, after which they were either immediately removed from the mold for analysis or heated in a convection oven at 125°C for 1 hour, 175°C for 1 hour, allowed to cool to room temperature, and then removed from the mold for analysis. The specimens were analyzed by dynamic mechanical analysis (DMA) in a TA instruments Q800 dynamic mechanical analyzer. Specimens of approximate dimensions (15 x 5 x 0.3 mm) were tested in a film tension clamp with a sinusoidal strain of 0.05% applied at a frequency of 1 Hz over a broad temperature range (-100 < T < 300°C). The glass transition ( $T_g$ ) of the materials produced was taken to be the temperature corresponding to the maximum  $\tan \delta$  value.

## 6.3 Results and Discussion

### 6.3.1 Mechanical Analysis

The cured resins formulated with CTAs yielded a range of glass transition temperatures depending on the CTA type, relative concentration, and curing protocol. We have limited the results reported here to four CTAs, all formulated at 0.3 hydroxyl equivalents (i.e., the ratio of hydroxyl to epoxide is equal to 0.3). The polymers were

synthesized via photopolymerization; half of the specimens were analyzed via DMA, while the other half were annealed and then analyzed via DMA. In handling and preparing the specimens for mechanical analysis, it was observed that the specimens that were not annealed (i.e., photocured only) were more prone to fracture and premature failure. The authors do not have a working hypothesis that explains this behavior. More interesting is the mechanical analysis for the photocured-only specimens. DMA data for four different CTAs in EEC, both for photocured-only and annealed specimens are shown in Figures 6.2 and 6.3. With every CTA, excepting dodecanol, the photocured-only specimens show multimodal behavior in the  $\tan \delta$  plots and have abnormal storage modulus profiles that show two distinct transitions. The DMA profiles for n-butanol suggest a degree of phase segregation in the material that is removed via the annealing process. The optical clarity of the samples and the increased symmetry of the  $\tan \delta$  peaks after annealing imply another mechanism must explain the apparent multimodal behavior.

The DMA data for 1,4-butanediol and t-butanol also show a disparity between the two curing protocols, but offer a second more likely mechanism for the apparent multimodal mechanical behavior. In the storage modulus plots (see Figure 6.3a and 6.3c), the modulus increases after passing through the first apparent transition. The only reason that the modulus should rise so dramatically at increasing temperatures is if the network is changing via increased conversion through thermally-activated dark polymerization. All of the photocured-only specimens show a  $\tan \delta$  maximum or shoulder centered near 70°C. The maximum glass transition for resins of this type cured at room temperature appears to be approximately 70°C.<sup>29</sup> The cationic systems studied here have very long-lived active centers. Once the DMA increases the sample temperature above the initial glass transition temperature, developed via photocuring, the active centers are effectively released from the once glassy matrix and will continue to react with unreacted monomer. The reaction will continue to proceed until the monomer is consumed or the network

develops to a vitrified state that traps the active centers and prevents further crosslinking and polymerization reactions. In the case that the maximum glass transition temperature for a given formulation is exceeded, the monomer will be consumed and stable physical properties will be achieved despite the “living” characteristics of the active centers.

#### 6.4 Conclusions

In this study the utility of CTAs are demonstrated as kinetic enhancers and transition temperature modulators. It is also shown that, despite the good air-curing qualities of cationic systems, other complications must be understood and controlled through processing. Although this research used very long times to thermally anneal, or cure, the specimens post-illumination, it is likely that shorter annealing times may result in similar properties. Further work in process optimization is required to quantify the minimum annealing time for materials with stable physical properties and good, non-brittle mechanical properties.

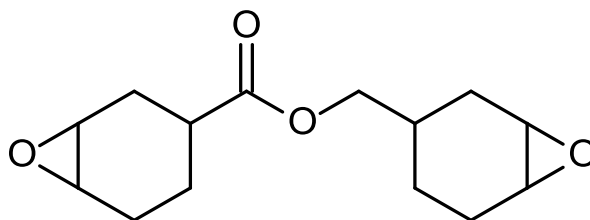


Figure 6.1: Molecular structure of epoxide monomer EEC.

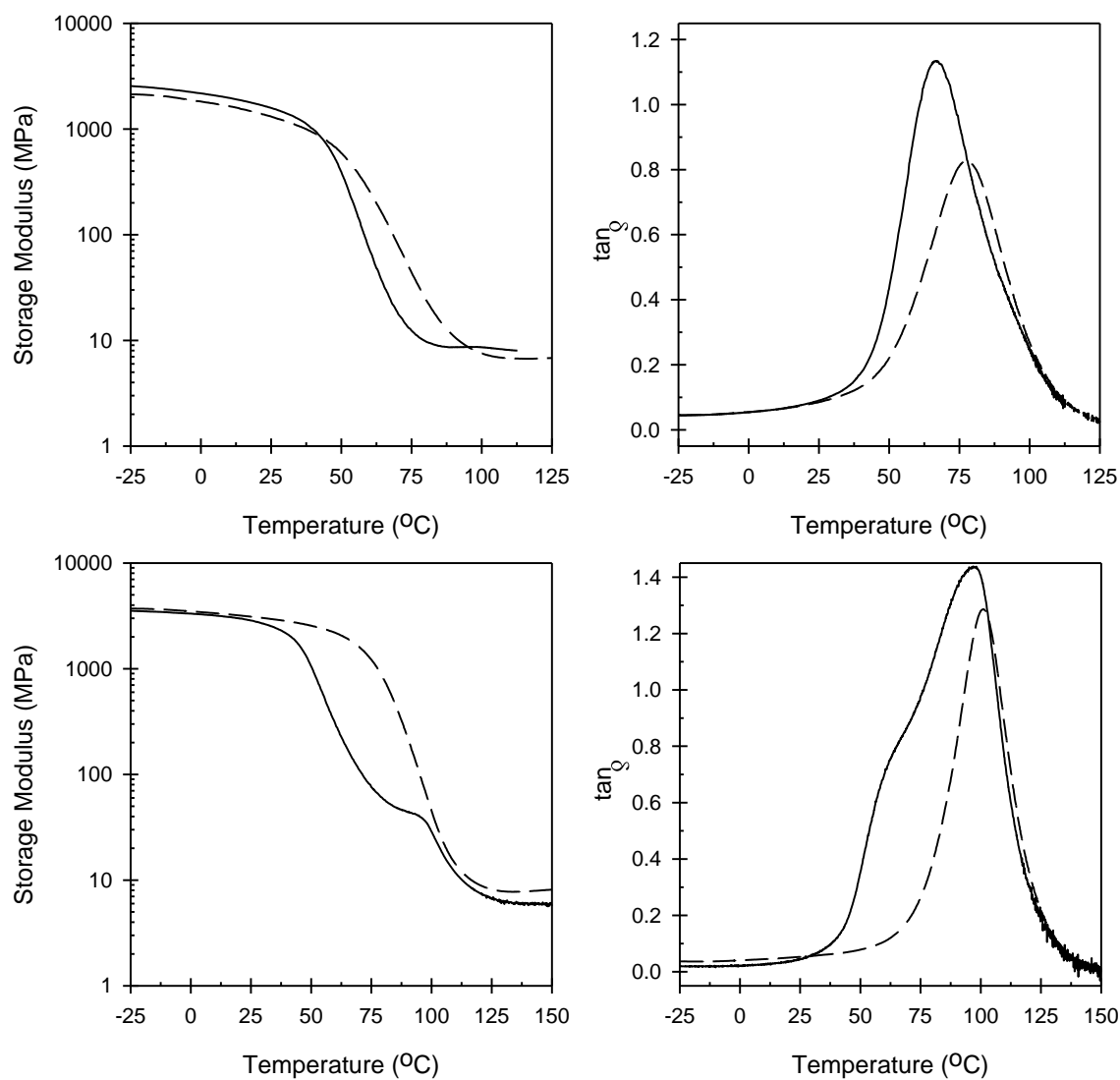


Figure 6.2: Storage modulus and  $\tan \delta$  profiles obtained from EEC formulations with dodecanol (A,B), and n-butanol (C,D) as CTAs. Solid lines represent data collected from specimens that were photocured and the dashed lines were obtained from specimens that were photocured and annealed above the glass transition temperature.

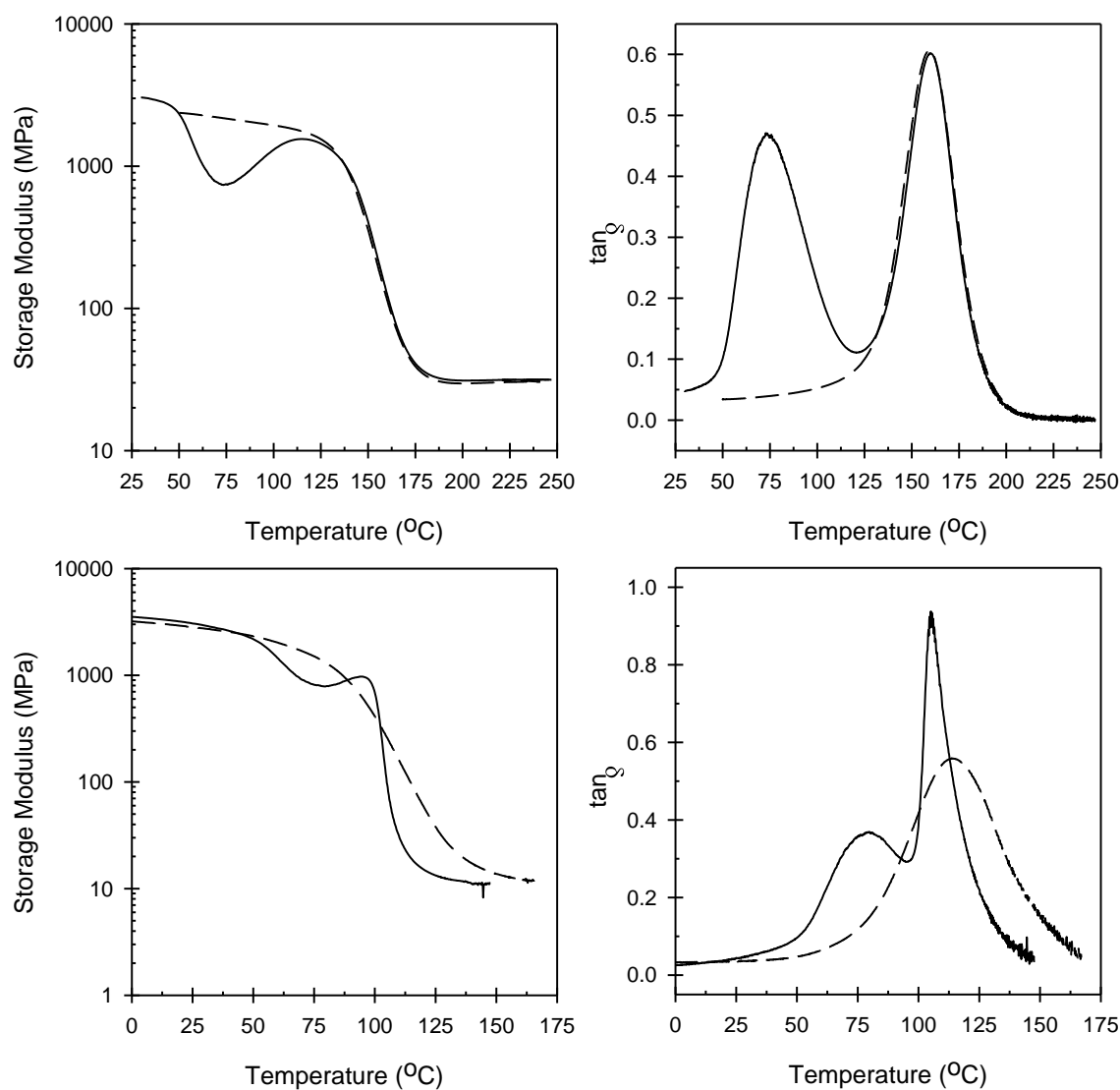


Figure 6.3: Storage modulus and  $\tan \delta$  profiles obtained from EEC formulations with 1,4-butanediol (A,B), and t-butanol (C,D) as CTAs. Solid lines represent data collected from specimens that were photocured and the dotted lines were obtained from specimens that were photocured and annealed above the glass transition temperature.



### Notes

- (1) Fouassier, J. *Photoinitiation, Photopolymerization, and Photocuring*; Hanser/Gardner Publications, Inc.: Cincinnati, OH, 1995; , pp 375.
- (2) Bowman, C.; Kloxin, C. "Toward an Enhanced Understanding and Implementation of Photopolymerization Reactions" *AICHE J.* **2008**, *54*, 2775.
- (3) Kloosterboer, J. "Network Formation by Chain Crosslinking Photopolymerization and its Applications in Electronics" *Advances in polymer science* **1988**, *84*, 1.
- (4) Koleske, J. V. *Radiation Curing of Coatings*; ASTM International: West Conshohocken, PA, 2002; Vol. 1, pp 244.
- (5) Pappas, S. P., Ed.; *Radiation Curing Science and Technology*; Plenum Press: New York, 1992; .
- (6) Decker, C. "Photoinitiated crosslinking polymerization." *Prog. Polym. Sci.* **1996**, *21*, 593-650.
- (7) Dietliker, K.; Huesler, R.; Birbaum, J. -.; Ilg, S.; Villeneuve, S.; Studer, K.; Jung, T.; Benkhoff, J.; Kura, H.; Matsumoto, A.; Oka, H. "Advancements in photoinitiators-Opening up new applications for radiation curing." *Prog. Org. Coat.* **2007**, *58*, 146-157.
- (8) Dietliker, K.; Jung, T.; Studer, K.; Benkhoff, J. "Photolatent Tertiary Amines A New Technology Platform for Radiation Curing" *CHIMIA International Journal for Chemistry* **2007**, *61*, 655-660.
- (9) Rutsch, W.; Dietliker, K.; Leppard, d.; Koehler, M.; Misev, L.; Kolczak, U.; Rist, G. "Recent developments in photoinitiators." *Prog. Org. Coat.* **1996**, *27*, 227-239.
- (10) Kolczak, U.; Rist, G.; Dietliker, K.; Wirz, J. "Reaction Mechanism of Monoacyl- and Bisacylphosphine Oxide Photoinitiators Studied by <sup>31</sup>P-, <sup>13</sup>C-, and <sup>1</sup>H-CIDNP and ESR." *J. Am. Chem. Soc.* **1996**, *118*, 6477-6489.
- (11) Jakubiak, J.; Allonas, X.; Fouassier, J.; Sionkowska, A.; Andrzejewska, E.; Linden, L. "Camphorquinone-amines photoinitating systems for the initiation of free radical polymerization" *Polymer* **2003**, *44*, 5219.
- (12) Groenenboom, C. J.; Hageman, H. J.; Overeem, T.; Weber, A. J. M. "Photoinitiators and photoinitiation. 3. Comparison of the photodecompositions of alpha - methoxy- and alpha ,alpha -dimethoxydeoxybenzoin in 1,1-diphenylethylene as model substrate." *Makromol. Chem.* **1982**, *183*, 281-292.

- (13) Finter, J.; Riediker, M.; Rohde, O.; Rotzinger, B. "Photosensitive systems for microlithography based on organometallic photoinitiators" *Die Makromolekulare Chemie. Macromolecular symposia* **1989**, *24*, 177.
- (14) Crivello, J. V.; Lam, J. H. W. "Diaryliodonium salts. A new class of photoinitiators for cationic polymerization." *Macromolecules* **1977**, *10*, 1307-1315.
- (15) Crivello, J. V. "The discovery and development of onium salt cationic photoinitiators." *J. Polym. Sci., Part A: Polym. Chem.* **1999**, *37*, 4241-4254.
- (16) Andrzejewska, E. "Photopolymerization kinetics of multifunctional monomers." *Prog. Polym. Sci.* **2001**, *26*, 605-665.
- (17) Jancovicova, V.; Brezova, V.; Ciganek, M.; Cibulkova, Z. "Photolysis of diaryliodonium salts (UV/Vis, EPR and GC/MS investigations)." *J. Photochem. Photobiol., A* **2000**, *136*, 195-202.
- (18) Brzezinska, K.; Szymanski, R.; Kubisa, P.; Penczek, S. "Activated monomer mechanism in cationic polymerization. I: Ethylene oxide, formulation of mechanism" *Die Makromolekulare Chemie. Rapid communications* **1986**, *7*, 1-4.
- (19) Biedron, T.; Brzezinska, K.; Kubisa, P.; Penczek, S. "Macromonomers by Activated Polymerization of Oxiranes - Synthesis and Polymerization" *Polym. Int.* **1995**, *36*, 73.
- (20) Hartwig, A. "Influence of moisture present during polymerisation on the properties of a photocured epoxy resin" *Int J Adhes Adhes* **2002**, *22*, 409-414.
- (21) Hartwig, A.; Schneider, B.; Lühring, A. "Influence of moisture on the photochemically induced polymerisation of epoxy groups in different chemical environment" *Polymer* **2002**, *43*, 4243-4250.
- (22) Nelson, E.; Jacobs, J.; Scranton, A.; Anseth, K.; Bowman, C. "Photo-differential Scanning Calorimetry Studies of Cationic Polymerizations of Divinyl Ethers" *Polymer* **1995**, *36*, 4651.
- (23) Nelson, E.; Scranton, A. "In situ Raman spectroscopy for cure monitoring of cationic photopolymerizations of divinyl ethers" *J. Raman Spectrosc.* **1996**, *27*, 137.
- (24) Ficek, B.; Thiesen, A.; Scranton, A. "Cationic photopolymerizations of thick polymer systems: Active center lifetime and mobility" *European polymer journal* **2008**, *44*, 98-105.

- (25) Decker, C.; Moussa, K. "Kinetic-Study of the Cationic Photopolymerization of Epoxy Monomers" *J. Polym. Sci. , Part A: Polym. Chem.* **1990**, *28*, 3429-3443.
- (26) Decker, C. "Photoinitiated cationic polymerization of epoxides" *Polym. Int.* **2001**, *50*, 986-997.
- (27) Kubisa, P.; Bednarek, M.; Biedron, T.; Biela, T.; Penczek, S. "Progress in activated monomer polymerization. Kinetics of AM polymerization." *Macromol. Symp.* **2000**, *153*, 217-226.
- (28) Kubisa, P.; Penczek, S. "Cationic activated monomer polymerization of heterocyclic monomers." *Prog. Polym. Sci.* **2000**, *24*, 1409-1437.
- (29) Ye, S.; Cramer, N.; Bowman, C. "Relationship between Glass Transition Temperature and Polymerization Temperature for Cross-Linked Photopolymers" *Macromolecules* **2011**, *44*, 490-494.

## CHAPTER 7

### EPOXIDE-ACRYLATE HYBRID PHOTOPOLYMERS: FORMATION OF GRAFTED POLYMER NETWORKS

#### 7.1 Introduction

Hybrid epoxide-acrylate photopolymerization affords the unique opportunity to structure polymer networks in time and to engineer advanced material properties. Using light to initiate polymerization rather than heat enables significant savings in energy costs, processing space, and time; solvent-free systems; and increased control over the production of initiating species.<sup>1-4</sup> These hybrid systems are based on formulations that contain both an epoxide moiety, which undergoes cationic ring-opening photopolymerization, and an acrylate moiety, which undergoes free-radical photopolymerization.

Free-radical chain polymerization is most commonly used in current photopolymer industries for its quick cure time and easily modified monomers and oligomers.<sup>1,5</sup> However, free-radical polymerization is subject to oxygen inhibition, shrinkage, and shrinkage stress.<sup>5-8</sup> In contrast, cationic chain polymerization is relatively slow and affected by moisture.<sup>9</sup> However, it is not inhibited by oxygen and results in little or no shrinkage. In addition, the cationic active centers persist for long times, enabling dark cure.<sup>10</sup>

Through the combination of these two independent reactive systems, hybrid epoxide-acrylate polymers exhibit lower sensitivity to oxygen and moisture and offer advantages such as increased cure speed and improved film-forming properties.<sup>11,12</sup> For example, acrylate coatings exhibit surface tackiness due to oxygen diffusion at the air-monomer interface. However, in the hybrid system, cationic polymerization becomes the dominant route of conversion at the sample surface, resulting in tack-free coatings.<sup>11</sup>

These hybrid systems also show promise of abating free-radical-polymerization-induced shrinkage by sequencing the epoxide and acrylate reactions to mitigate shrinkage stress.

This ability to sequence the two independent reactions with a large selection of available monomers also allows for greater control over property tuning in a hybrid system. Careful control of the independent reactions in a hybrid system is required; otherwise, the first reaction can limit the second by vitrification or topological restraint and thus affect monomer conversion.<sup>13</sup> Another opportunity to develop physical properties in hybrid systems is the formation and alteration of polymer networks.<sup>1,3</sup> In interpenetrating networks (IPNs), distinct polymer systems are joined only through co-entanglement. When each network is independently cross-linked, a full-IPN results (Figure 7.1).<sup>14</sup> A semi-IPN is the entanglement of a cross-linked polymer network and a linear polymer. The cross-linking density of IPNs can affect polymer properties as well as phase separation (the separation of polymers caused by a lack of mutual solubility). The cross-linking density of each polymer can be controlled by adding chain transfer agents and/or altering the functionality of the monomer.<sup>13,15-17</sup>

Hybrid formulations can also be designed to create grafted polymer networks (GPNs). GPNs form when the two polymers are not only co-entangled, but are also covalently bonded together. Covalent bonds between polymers is achieved by the addition of a secondary functional group to one monomer, which is able to react with the second monomer. Hybrid monomers, such as 3,4-epoxy-cyclohexyl-methyl methacrylate (METHB), contain both an epoxide and an acrylate moiety to provide the link between the two polymer systems formed in an epoxide-acrylate hybrid polymerization.<sup>11</sup>

However, unique attributes of the cationic polymerization provide an opportunity to form GPNs and reduce phase separation in epoxide-acrylate hybrid systems without the addition of a hybrid monomer. Cationic active centers can form a polymer chain through either an active chain end (ACE) mechanism or an activated monomer (AM) mechanism.<sup>18,19</sup> The ACE mechanism is a propagation reaction in the traditional sense in

that the polymer chain grows through the addition of a monomer to the cationic active center at one end. The AM mechanism is a chain transfer reaction in which water or an organic alcohol reacts with the cationic active center, capping the growing chain with a hydroxyl group and releasing a proton that can start a new polymer chain. Including hydroxyl-containing acrylates in the hybrid formulation facilitates the AM mechanism for the epoxides and results in the covalent bonding of the epoxide polymer system to the acrylate polymer system. Controlling the dominance of one mechanism with respect to the other provides an effective means to tune GPN properties based on the concentration of epoxide and hydroxyl groups and the reactivity of the cationic active centers.

In this work, GPNs are demonstrated by grafting epoxide polymer chains onto hydroxylated acrylate polymer chains via the AM mechanism. The extent of AM propagation vs ACE propagation is investigated via gel permeation chromatography (GPC) or grafted polyacrylates that vary in the degree of hydroxylation. The polyacrylates are also formulated in crosslinking resins to determine the effectiveness of “specialty” CTAs in epoxide formulations.

## 7.2 Experimental

### 7.2.1 Materials

Sodium hydride (60% dispersion in mineral oil), carbon disulfide, 1-dodecanethiol, and chloroacetonitrile were purchased from Acros Organics. Cyclohexene oxide, butyl acrylate, chloroform-d (the solvent used for <sup>1</sup>H NMR spectroscopic analysis), polyTHF 250, diethyl ether, and azobisisobutyronitrile (AIBN) were purchased from Sigma Aldrich. 4-Hydroxybutyl acrylate was donated by BASF. PC-2506 (diaryliodonium cationic photoinitiator) and PC-1000 (diepoxide monomer) were donated by Polyset Company. All materials were used as received.

### 7.2.1.1 RAFT Agent

Sodium hydride (1.723 g, 43.08 mmol) was placed in a three neck flask. The mineral oil was extracted from sodium hydride by washing with three 10 mL portions of hexane via syringe under nitrogen. The three neck flask was placed in an ice bath and fitted with a pressure equalizing addition funnel containing 1-dodecanethiol (7.7083 g, 38.1 mmol), diluted with diethyl ether (20 mL), which was added over a period of 10 minutes. A bright yellow precipitate was observed and stirred for 30 minutes. Carbon disulfide (3.1129 g, 40.9 mmol) was then added via the addition funnel. A bright green precipitate was formed and then filtered to obtain sodium trithiocarbonate. Chloroacetonitrile (1.2389 g, 16.4 mmol) was added to the trithiocarbonate/diethyl ether slurry and stirred for approximately 3 hours. The yellow solution was dried over anhydrous sodium sulfate. The solvent was then removed via rotary evaporation, and yellow oil was obtained. Upon cooling to room temperature, the product (RAFT agent) formed a waxy solid. NMR spectra of the product were collected, confirming an approximate yield of 55%.

### 7.2.1.2 RAFT Polymers

Two butyl acrylate polymers were synthesized via reversible addition-fragmentation chain-transfer (RAFT) polymerization, which is a controlled radical polymerization method. The first was neat poly(butyl acrylate). Butyl acrylate (12.1485 g, 94.8 mmol), RAFT agent (0.4006 g, 1.3 mmol), and AIBN (0.0223 g, 0.1 mmol) were added to a 50 mL round bottom flask and stirred until dissolved. The contents were purged with nitrogen for 5 minutes and then plunged into a 65 °C water bath for 2 hours. After the 2 hours, the solution was opened to the air and cooled with an ice bath to quench the reaction. The same procedure was used to prepare the second butyl acrylate polymer: poly(butyl acrylate-ran-4-hydroxy butyl acrylate). Here, butyl acrylate (10.9463 g, 85.4 mmol), 4-hydroxybutyl acrylate (1.3844 g, 9.6 mmol), RAFT agent (0.4006 g, 1.3

mmol), and AIBN (0.0207 g, 0.1 mmol) were stirred in a 50 mL round bottom flask and polymerized.

The solutions gelled, and NMR spectroscopy confirmed that very high conversions were obtained (>90%). The polymer was poured into a cold methanol/water (70:30) mixture (500 mL), the liquid was decanted, and the polymer product was allowed to degas for about 3 days. Following this procedure, no unreacted monomer was detected via NMR spectroscopy.

#### 7.2.1.3 Linear Epoxide Polymers

Linear polyethers were synthesized via thermal polymerization. Thermal conditions were chosen over photocuring conditions due to the volatility of the cyclohexene oxide monomer. The epoxide monomer was polymerized under three conditions. In Condition A, cyclohexene oxide (5.0328 g, 51.3 mmol), cationic photoinitiator (0.3780 g, 0.5 mmol), and chloroform (10 mL) were mixed. In Condition B, cyclohexene oxide (5.0502 g, 51.5 mmol), poly(butyl acrylate) (0.5160 g), cationic photoinitiator (0.3738 g, 0.5 mmol), and chloroform (10 mL) were mixed. In Condition C, cyclohexene oxide (5.0505 g, 51.5 mmol), poly(butyl acrylate-ran- 4-hydroxy butyl acrylate) (0.4999 g), cationic photoinitiator (0.3703 g, 0.5 mmol), and chloroform (10 mL) were mixed. The three mixtures were heated in a water bath under reflux for 24 hours. After polymerization, the solvent was removed via rotary evaporation, and the polymers were analyzed via GPC.

#### 7.2.1.4 Cross-linked Epoxide Polymers

Three formulations were prepared for cross-linked polymer synthesis. Formulation A was composed of diepoxide monomer (5.0021 g, 13.4 mmol) and cationic photoinitiator (0.1948 g, 26.1 mmol). Formulation B was composed of diepoxide monomer (5.0019 g, 13.4 mmol), cationic photoinitiator (0.1925 g, 25.8 mmol), and poly(butyl acrylate) (0.4892 g). Formulation C was composed of diepoxide monomer



(5.0164 g, 13.5 mmol), cationic photoinitiator (0.1932 g, 0.3 mmol), and poly(butyl acrylate-ran-4-hydroxy butyl acrylate) (0.5071 g). After mixing, each formulation was placed in glass molds prepared from silanized (Rain-x treated) glass slides, which were separated by a double thickness of 150  $\mu\text{m}$  glass cover slips. The molds were placed under a low intensity black light for 5 minutes per side. Then, each resin-filled glass mold was passed, twice on each side, through a belt-driven Fusion curing system (model LC-6B), which was fixed with an irradiator (model 1300MB) comprised of an aluminum reflector and a high intensity Hg lamp (H-bulb). The belt speed was 9 ft/min (0.05 m/s), delivering a UV exposure of  $\sim 3.5 \text{ J/cm}^2$  per run. The samples were placed in an oven at 150  $^\circ\text{C}$  for 2 hours. This annealing procedure ensured no additional epoxide reaction during dynamic mechanical analysis. The resulting polymers were stored in the dark at room temperature for 24 hours prior to analysis. For comparison, formulations of the diepoxide and varying amounts of polyTHF 250 (a CTA studied previously<sup>20</sup>) were prepared similarly.

## 7.2.2 Methods

### 7.2.2.2 Gel Permeation Chromatography

GPC using chloroform as the mobile phase (1.0 mL/min) was performed at room temperature. A Waters 515 HPLC pump was used for GPC. Four Waters columns (styragel HR2, HR4, HR4, and HR6) were used in series. Polystyrene standards with molecular weights of 4,950 g/mol; 10,850 g/mol; 28,500 g/mol; and 70,600 g/mol were diluted with chloroform to concentrations of approximately 1 g/L. Chromatograms of the standards were collected using a refractive index detector (RID). Five different linear polymer samples were diluted to approximately 10 g/L with chloroform and analyzed by GPC: Condition A, Condition B, Condition C, neat poly(butyl acrylate), and poly(butyl acrylate-ran-4-hydroxy butyl acrylate).

### 7.2.2.3 Dynamic Mechanical Analysis

Specimens for dynamic mechanical analysis (DMA) were prepared from the synthesized cross-linked polymers. The polymers were removed from the glass molds, and specimens were cut to approximate dimensions of 15 x 5 x 0.3 mm. A TA Instruments Q800 dynamic mechanical analyzer was used to characterize the thermo-mechanical properties of the polymer specimens. Samples were placed in a vertical film tension clamp and ramped from -100 to 250 °C at a heating rate of 3 °C/min and a 1 Hz sinusoidal strain of 0.05%. The glass transition temperature ( $T_g$ ) was taken as the temperature corresponding to the  $\tan \delta$  maximum.

## 7.3 Results and Discussion

### 7.3.1 Demonstration of Grafting via GPC

Three different linear polymers were formed and analyzed independently via GPC. The linear poly(cyclohexene oxide) (poly(CHO)) was the product of thermally initiated cationic polymerization and is shown in Figure 7.2. The two other linear polymers were polyacrylates synthesized via RAFT polymerization. One was prepared from neat butyl acrylate monomer, and the other was prepared from a 10:1 mol ratio of butyl acrylate and 4-hydroxybutyl acrylate. Subsequent to RAFT polymerization, the polyacrylates were endcapped with parts of the RAFT agent used to synthesize the materials (see Figure 7.3). GPC traces (see Figure 7.4) show that the polyacrylates have a narrow distribution centered around an elution time of 15.2 min. Molecular weight distributions of the polyacrylates are stable. The molecular weight could only increase in these materials if the polymers were heated above ~60 °C in the presence of acrylate monomer; however, all excess monomer was removed after the initial synthesis. Poly(CHO) resulted in a broad distribution asymmetrically centered around an elution time of ~17 min. The distribution associated with poly(CHO) is presumed to be largely

formed from ACE propagation since no chain transfer agent was introduced to the system.

According to the AM mechanism, the hydroxyl groups on the poly(BA-ran-HBA) copolymer may react with protonated epoxide monomers during the polyether synthesis. The reaction of the HBA hydroxyl groups with epoxide monomers results in a ring-opening event that regenerates a hydroxyl group. This hydroxyl group may react with another protonated monomer, resulting in graft propagation. The experiments wherein the epoxide monomer was polymerized in the presence of the different polyacrylates demonstrate this process. When polymerized in the presence of poly(BA), the GPC trace of the product shows a similar broad elution distribution as for neat poly(CHO) with the addition of a small shoulder around the same elution time as the original poly(BA) (15.2 min). The small shoulder indicates that the poly(BA) was indeed inert since no changes in molecular weight were observed. Alternatively, when the epoxide was polymerized in the presence of poly(BA-ran-HBA), a bimodal distribution with a new peak centered around 13.5 min was observed. The decrease in elution time for this peak indicates an increase in molecular weight from the original poly(BA-ran-HBA) material. There is no shoulder at 15.2 min, indicating all of the poly(BA-ran-HBA) has been grafted to some extent. The broad distribution associated with the neat cyclohexene oxide polymerization and the ACE mechanism remains, which indicates that the two reaction mechanisms occur in parallel. Hydroxyl groups promote the AM mechanism, but not to the exclusion of the ACE mechanism.

### 7.3.2 Physical/Mechanical Properties

The polymer networks formed from cross-linking epoxide resins with the polyacrylates as additives were characterized using DMA (Figure 7.5). For formulations containing the diepoxide and poly(BA), a semi-IPN will be formed since the ACE mechanism is predominant. However, for formulations containing the diepoxide and

poly(BA-ran-HBA), a full-GPN will be formed since there are multiple hydroxyl sites on each polyacrylate through which chain transfer (via the AM mechanism) can occur. For these covalently bonded networks, a narrower tan delta peak is expected (indicating less phase separation). The DMA data support this visualization of the polymer networks: the material containing the random copolymer gave a narrower glass transition region and a lower  $T_g$  than the material containing poly(BA). These findings are consistent with the general trends observed in epoxide formulations containing CTAs.<sup>20</sup> However, the decrease in  $T_g$  and narrowing of the tan delta peak are less pronounced than in formulations containing lower molecular weight CTAs. High functionality CTAs ( $\text{OH} \geq 2$  per molecule) have been shown to depress the physical properties ( $T_g$  and cross-link density) of the parent resin less drastically than mono-functional CTAs. Since poly(BA-ran-HBA) is a very high functionality CTA, the properties changed minimally.

In Figure 7.6, DMA data are presented for cross-linking epoxide resins with polyTHF 250 as an additive. Again, since both ACE and AM mechanisms take place in these formulations, covalent bonds are formed between the diepoxide and polyTHF 250, which is a high molecular weight diol. These formulations exhibit more typical physical properties for epoxide formulations containing CTAs: as the concentration of polyTHF 250 doubles, the  $T_g$  decreases by roughly 50 °C. The rubbery modulus, which is proportional to the crosslink density,<sup>21,22</sup> also decreases with increasing polyTHF 250 concentration. In addition, increasing the wt% of polyTHF 250 in the formulation results in a narrower tan delta peak, indicating a more homogeneous network. Low molecular weight, low functionality CTAs promote a great deal of chain transfer reactions, which delays vitrification, increases the active center mobility, and decreases the ultimate cross-link density. High molecular weight CTAs (such as the poly(BA-ran-HBA) studied here) affect polymer properties less than low molecular weight CTAs and behave more like a polymer blend or a semi-IPN.

#### 7.4 Conclusions

A trithiocarbonate-type RAFT agent was synthesized and used to produce narrow molecular weight acrylate polymers, poly(BA) and poly(BA-ran-HBA). During the thermal cationic polymerization of cyclohexene oxide, poly(BA) was inert; however, poly(BA-ran-HBA) facilitated grafting of epoxide monomers via the AM mechanism. GPC analysis confirmed grafting and also showed that the AM and ACE mechanisms occurred in parallel.

Cross-linked polymers were formed from diepoxide resins containing the polyacrylates, but only small differences in mechanical behavior were observed between formulations with poly(BA) or poly(BA-ran-HBA). Both polyacrylates reduced the T<sub>g</sub> of the material in comparison to the neat diepoxide resin; however, less phase separation was observed with poly(BA-ran-HBA). The similarities in the physical properties of the two systems suggest semi-IPNs and GPNs may be comparable. In addition, formulations of the diepoxide with polyTHF 250 (a low molecular weight CTA) were photopolymerized. The polyTHF 250 concentration had a large impact on the resulting polymer T<sub>g</sub> and cross-linking density and provides further opportunities to tune polymer network properties. Future work is planned to quantify the grafting efficiency in these types of systems and to characterize more fully the GPN-forming systems.

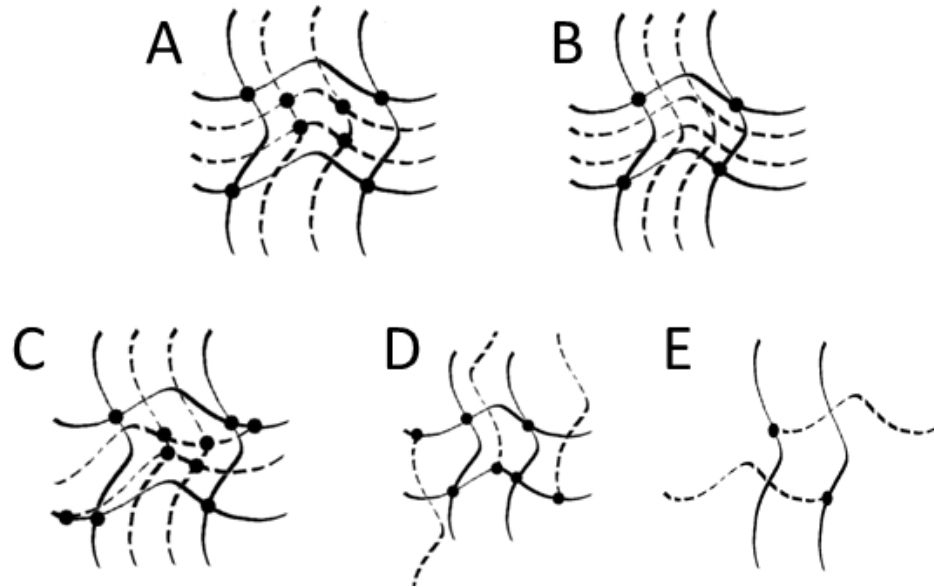


Figure 7.1: Network structures formed from hybrid polymerizations: (A) full-IPN, Polymers 1 and 2 are cross-linked; (B) semi-IPN, Polymer 1 is cross-linked, Polymer 2 is linear; (C) full-GPN, Polymers 1 and 2 are cross-linked and grafting occurs; (D) semi-GPN, Polymer 1 is cross-linked, Polymer 2 is grafted to Polymer 1; (E) GP, Polymer 1 is linear, Polymer 2 is grafted to Polymer 1.

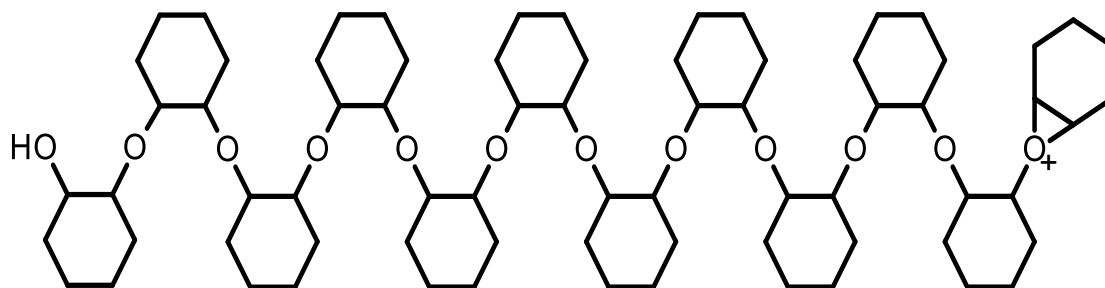


Figure 7.2: Molecular structure of the polyether formed via ACE propagation of cyclohexene oxide.

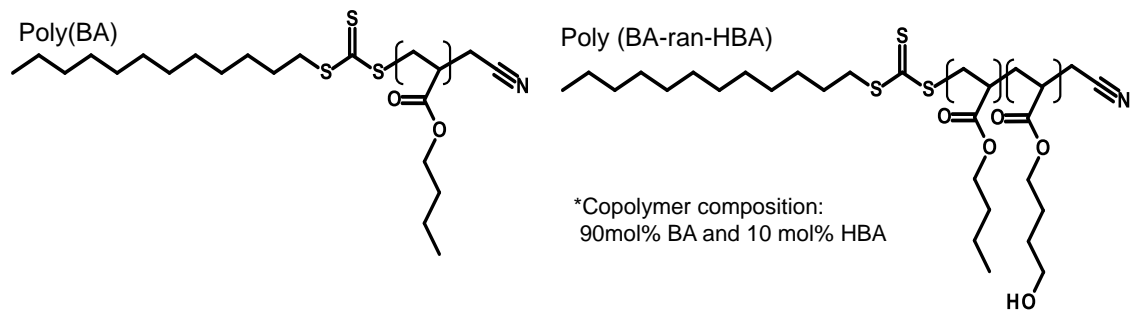


Figure 7.3: Molecular structure of the polyacrylates formed via RAFT polymerization. The butyl acrylate homopolymer (poly(BA)) is *left* and the random copolymer of butyl acrylate and 4-hydroxybutyl acrylate (poly(BA-ran-HBA)) *right*.



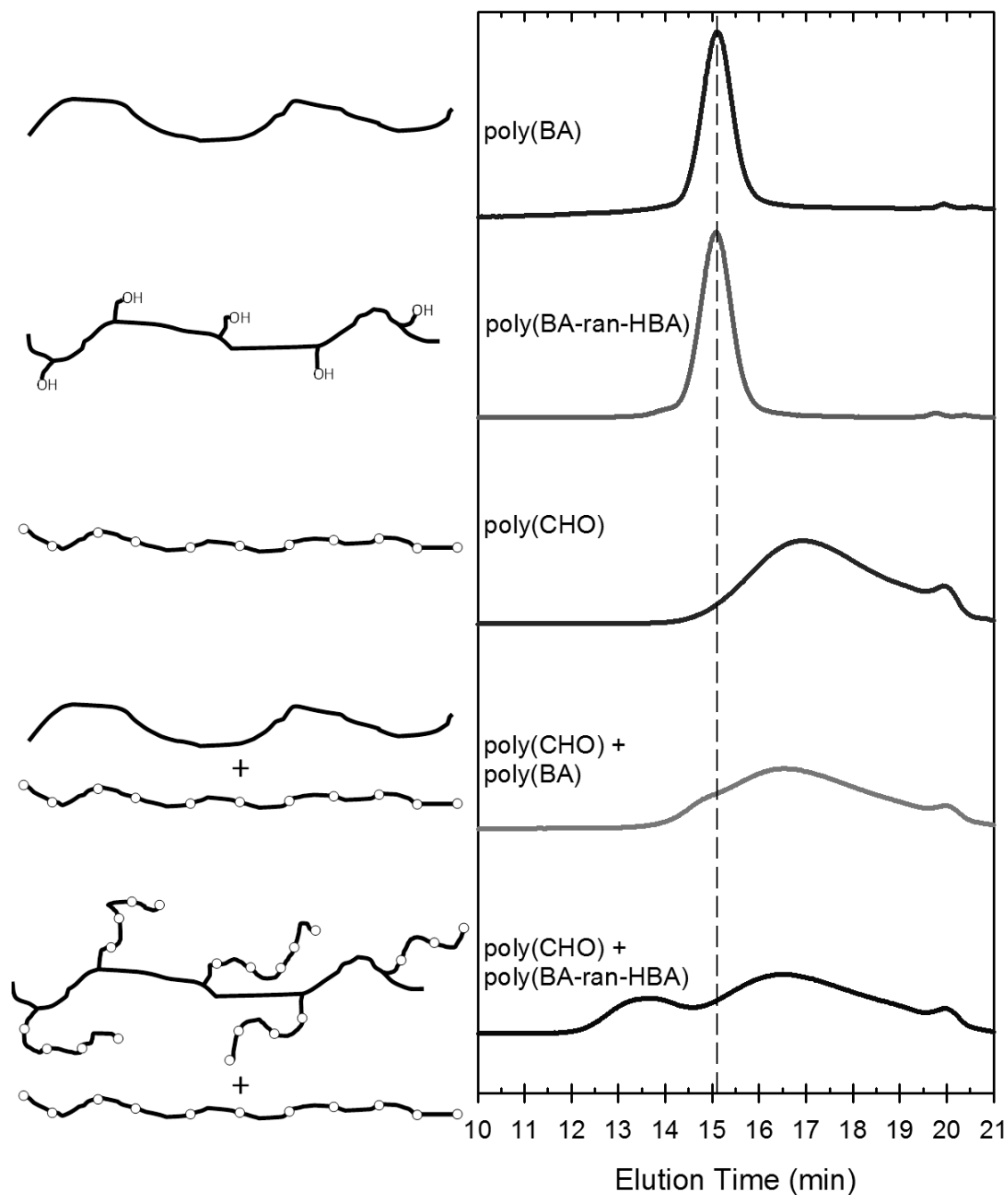


Figure 7.4: GPC traces of linear polyacrylates, linear polyethers, polymer blends, and grafted polymers. The polymer blends were formed by polymerizing cyclohexene oxide in the presence of poly(BA) or poly(BA-ran-HBA), not by simply mixing the polymer products. Depictions of polymers on the left include solid lines for polyacrylates, and solid lines broken by unfilled circles for polyethers.

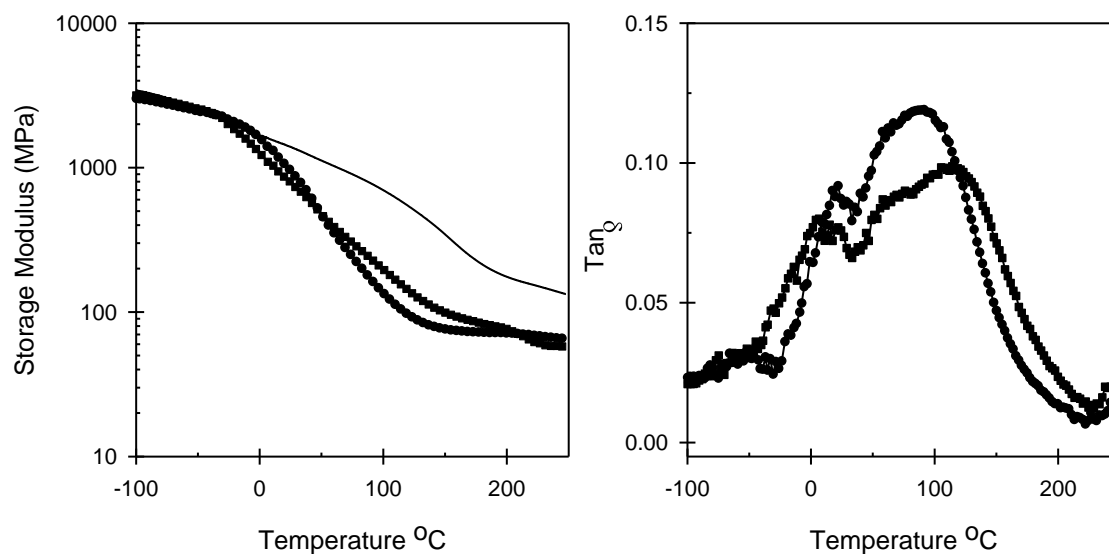


Figure 7.5: DMA traces showing the storage modulus (left) and the tan delta (right) for formulations of neat diepoxide monomer (*solid line*) and diepoxide with poly(BA) (*squares*) or poly(BA-ran-HBA) (*circles*). Polyacrylates were 30 wt% of the epoxide monomer mass. Polymer specimens were annealed before measurements..

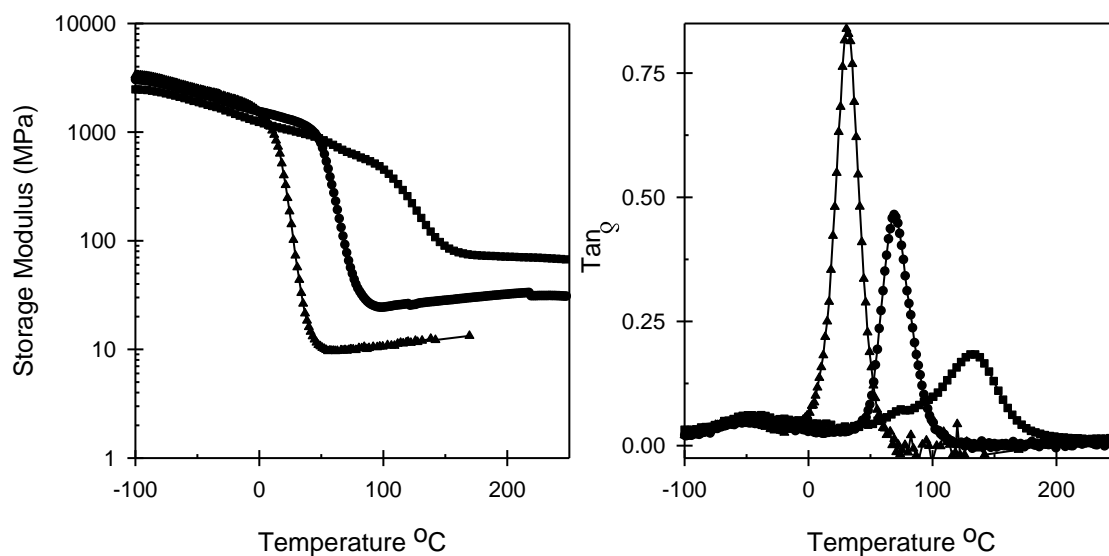


Figure 7.6: DMA traces showing the storage modulus (left) and the tan delta (right) for formulations of diepoxide monomer and polyTHF 250. PolyTHF 250 mass was equal to 0 wt% (*solid line*), 7 wt% (*squares*), 15 wt% (*circles*), and 30 wt% (*triangles*) of the epoxide monomer mass. Polymer specimens were annealed before measurements.

### Notes

- (1) Odian, G. *Principles of Polymerization (Fourth Edition)*; John Wiley and Sons: Hoboken, NJ, 2004; .
- (2) MS Salim *Overview of UV Curable Coatings*; DR Randell, Ed.; Radiation Curing of Polymers II; The Royal Society of Chemistry: Cambridge, 1991; .
- (3) Fouassier, J. *Photoinitiation, Photopolymerization, and Photocuring*; Hanser/Gardner Publications, Inc.: Cincinnati, OH, 1995; , pp 375.
- (4) Pappas, S. P. *Radiation curing: science and technology*; Springer: 1992; .
- (5) Decker, C. "Photoinitiated Crosslinking Polymerization." *Progress in Polymer Science* **1996**, *21*, 593-650.
- (6) Davidson, C. L.; Feilzer, A. J. "Polymerization shrinkage and polymerization shrinkage stress in polymer-based restoratives" *Journal of dentistry* **1997**, *25*, 435-440.
- (7) Anseth, K. S.; Bowman, C. N.; Peppas, N. A. "Polymerization kinetics and volume relaxation behavior of photopolymerized multifunctional monomers producing highly crosslinked networks" *Journal of Polymer Science Part A: Polymer Chemistry* **1994**, *32*, 139-147.
- (8) Andrzejewska, E. "Photopolymerization kinetics of multifunctional monomers." *Progress in Polymer Science* **2001**, *26*, 605-665.
- (9) Rajaraman, S. K.; Mowers, W. A.; Crivello, J. V. "Interaction of Epoxy and Vinyl Ethers During Photoinitiated Cationic Polymerization" *Journal of Polymer Science Part A: Polymer Chemistry* **1999**, *37*, 4007-4018.
- (10) Nelson, E.; Jacobs, J.; Scranton, A. B.; Anseth, K.; Bowman, C. N. "Photo-differential Scanning Calorimetry Studies of Cationic Polymerizations of Divinyl Ethers" *Polymer* **1995**, *36*, 4651-4656.
- (11) Cai, Y.; Jessop, J. L. P. "Decreased oxygen inhibition in photopolymerized acrylate/epoxide hybrid polymer coatings as demonstrated by Raman spectroscopy." *Polymer* **2006**, *47*, 6560-6566.
- (12) Cai, Y.; Jessop, J. L. P. "Effect of water concentration on photopolymerized acrylate/epoxide hybrid polymer coatings as demonstrated by Raman spectroscopy" *Polymer* **2009**, *50*, 5409-5413.

- (13) Dean, K.; Cook, W. "Effect of curing sequence on the photopolymerization and thermal curing kinetics of dimethacrylate/epoxy interpenetrating polymer networks" *Macromolecules* **2002**, *35*, 7942-7954.
- (14) Sperling, L. H. "Interpenetrating polymer networks: an overview." *Advances in Chemistry Series* **1994**, *239*, 3-38.
- (15) Cook, W.; Chen, F.; Ooi, S.; Moorhoff, C.; Knott, R. "Effect of curing order on the curing kinetics and morphology of bisGMA/DGEBA interpenetrating polymer networks" *Polymer International* **2006**, *55*, 1027-1039.
- (16) Dean, K.; Cook, W.; Zipper, M.; Burchill, P. "Curing behaviour of IPNs formed from model VERs and epoxy systems I amine cured epoxy" *Polymer* **2001**, *42*, 1345-1359.
- (17) Jansen, B.; Rastogi, S.; Meijer, H.; Lemstra, P. "Rubber-modified glassy amorphous polymers prepared via chemically induced phase separation. 4. Comparison of properties of semi- and full-IPNs, and copolymers of acrylate-aliphatic epoxy systems" *Macromolecules* **1999**, *32*, 6290-6297.
- (18) Yagci, Y. "Photoinitiated cationic polymerization of unconventional monomers" *Macromolecular symposia* **2006**, *240*, 93-101.
- (19) Biedron, T.; Brzezinska, K.; Kubisa, P.; Penczek, S. "Macromonomers by Activated Polymerization of Oxiranes - Synthesis and Polymerization" *Polymer International* **1995**, *36*, 73-80.
- (20) Dillman, B.; Jessop, J. L. P. "Chain transfer agents in cationic photopolymerization of a bis-cycloaliphatic epoxide monomer: Kinetic and physical property effects" *Journal of Polymer Science Part A: Polymer Chemistry* **2013**, *51*, 2058-2067.
- (21) Menard, K. *Dynamic Mechanical Analysis: A Practical Introduction*; CRC Press: Boca Raton, FL, 2008; , pp 218.
- (22) Murayama, T. *Dynamic Mechanical Analysis of Polymeric Material*; Elsevier Scientific Publishing Company: New York, 1978; Vol. 1, pp 231.

## CHAPTER 8

### DUAL PHOTOINITIATION SYSTEMS IN EPOXIDE MONOMERS AND HYBRID ACRYLATE-EPOXIDE SYSTEMS

#### 8.1 Introduction

Photopolymerization has been demonstrated as a rapid and robust method for the production of polymer thin films.<sup>1,2</sup> Applications of this technology include protective coatings, inks, dental restoratives, adhesives, photolithography, and fiber optic cladding. Commonly used (meth)acrylate monomers are inhibited by molecular oxygen.<sup>3-5</sup> Oxygen inhibition severely limits the use of acrylates in thin film applications without high initiator concentrations, the aid of expensive and cumbersome inerting techniques, or the inclusion of amines or thiol monomers in the formulation.<sup>6</sup> Epoxides, polymerized by a cationic chain polymerization mechanism, offer an alternative to acrylate chemistries because they are not affected by atmospheric oxygen.<sup>7</sup>

In general, epoxide monomers react at slower speeds than acrylates. In order to effectively substitute acrylate monomers in commercial resins, the reactivity of epoxides must be increased. One method has been to increase the initiation rate by adding free-radical generators to the photoinitiation systems. The addition of free-radical photoinitiators in epoxide systems can enhance the rate of polymerization of the epoxide species through radical promoted cationic polymerization (RPCP).<sup>8-10</sup> The RPCP mechanism requires the high reduction potential of diphenyliodonium cations to convert oxidizable free radicals to cationic species (see Figure 8.1).<sup>11</sup> Literature reports have demonstrated the oxidation of phosphinoyl radicals<sup>11,12</sup> from various bisacylphosphine oxides and 2,4,6-trimethylbenzoyl-diphenyl-phosphine oxide; germyl radicals<sup>13</sup> from acylgermane; the  $\alpha,\alpha$ -dimethoxybenzyl radical<sup>12</sup> from 2,2-dimethoxyphenyl acetophenone; silyl radicals;<sup>14-17</sup> and radicals formed from the abstraction of the labile hydrogens on benzyl and vinyl ethers to form carbon-centered cations.<sup>18-21</sup> Carbon-

centered cations can increase the reaction speed of epoxide polymerization by directly converting a neutral epoxide monomer to a tertiary oxonium ion. With a normal proton-centered cation, a neutral monomer is first converted to a secondary oxonium ion and only after a neutral monomer attacks the secondary oxonium ion is it converted to a tertiary oxonium ion. For some monomers, the conversion of a secondary oxonium ion to a tertiary oxonium ion is rate limiting; therefore, the RPCP method can increase the polymerization rate in otherwise low reactivity monomers.<sup>12</sup> Also, free-radical photoinitiators have red-shifted absorption spectra, relative to typical photo-acid generators. When photo-acid generators and free-radical photoinitiators are combined, the breadth of wavelengths that are effective in initiating polymerization by direct photolysis of the photo-acid generators and via the RPCP mechanism is greater, presumably resulting in a higher rate of active center production and ultimately higher rates of polymerization.

In this work, the ultimate conversion and the conversion profiles of neat epoxide monomers, as well as hybrid acrylate-epoxide systems, was studied by changing the initiating systems. While keeping the concentration and type of photo-acid generator constant for all systems, the photo-radical generator was changed to determine the photo-chemical environment best suited for epoxide polymerization in both neat and hybrid systems.

## 8.2 Experimental

### 8.2.1 Materials

Three different epoxide monomers were used: butyl glycidyl ether (BGE), Sigma Aldrich; vinyl cyclohexene monoxide (VCM), Dow Chemical; and 3,4-epoxycyclohexylmethyl-3,4-epoxycyclohexane carboxylate (EEC), Sigma Aldrich. These epoxide monomers were chosen because they vary in reactivity with BGE considered slow to react, EEC reacting at moderate speeds and VCM reacting rapidly.

Two different acrylate monomers were also used: 2-hydroxyethyl acrylate (HEA) and ethylene glycol methyl ether acrylate (EGMEA). The acrylate monomers have high compatibility with the epoxide monomers and were used in hybrid formulations. All monomer chemical structures are shown in Figure 8.2.

Four photo-initiators were used in this study (see Figure 8.3). A di-aryl iodonium salt (PC-2506, Polyset Company) was used as a photoacid generator. The free-radical generators studied include 2,2-dimethoxy-1,2-diphenylethan-1-one (Irgacure 651, Sigma Aldrich); bis-(2,4,6-trimethylbenzoyl)-phenylphosphineoxide (Irgacure 819, Ciba Specialty Chemicals); and diphenyl-(2,4,6-trimethylbenzoyl)phosphine oxide (Lucirin TPO, Ciba Specialty Chemicals). PC-2560 is an iodonium-type acid generator with low molar absorptivities above 325 nm and moderate to high molar absorptivities below 325 nm. Thus, short-wavelength UV radiation is required for the photolysis of PC-2506. Irgacure 651 is a commonly used initiator that has moderate absorptivity around 350 nm and higher absorptivity below 310 nm. Both phosphine oxide initiators have very high molar absorptivities below 425 nm. Irgacure 819 is capable of producing 4 initiating radicals per molecule, and Lucirin TPO produces 2 initiating radicals per molecule. All three of these free-radical initiators have been shown to initiate cationic polymerization via the RPCP mechanism.

#### 8.2.1.1 Formulations

The photo-acid generator PC 2506 was prepared at 0.5 wt% of the liquid resin mass (neat epoxide monomer or the combined mass of the acrylate and epoxide monomers), while radical initiator amounts were varied by molar equivalents relative to the amount of PC2506. In the neat epoxide monomers, the radical initiators were formulated at 0.00, 0.25, and 0.50 molar equivalents.

The hybrid systems were designed to have high compatibility between the acrylate and epoxide domains. The ether groups in EGMEA are compatible with the



oxiranes in the epoxide monomers, as well as the polyethers formed upon epoxide polymerization. The hydroxyl groups on HEA allow for epoxide grafting into the acrylate domains via the AM mechanism.<sup>22</sup> The hybrid systems were equimolar amounts of HEA, EGMEA, and EEC. In the hybrid formulations, the radical initiators were formulated at 0.00, and 0.50 molar equivalents, relative to PC-2506.

## 8.2.2 Methods

### 8.2.2.1 Kinetic Analysis

Epoxide and acrylate conversions were determined using real-time Raman spectroscopy, which has been described previously.<sup>23,24</sup> Each formulation was injected into a 1 mm ID quartz capillary tube, which was placed in a thermo-stated sample holder. The temperature of the sample holder was maintained at 30°C. UV light ( $300 \text{ nm} < \lambda < 450 \text{ nm}$ ) with an effective irradiance of  $150 \text{ mW/cm}^2$  was delivered from a 100 W high pressure mercury lamp (Acticure<sup>®</sup> Ultraviolet/Visible spot cure system, EXFO Photonic Solutions, Inc.) via a fiber optic light guide. Raman spectra were collected every 1 to 1.5 seconds for 5 minutes of total illumination time. The final conversion was determined by averaging the last ten spectra leading up to the end of the experiment. The rate of polymerization can be estimated by the slope of the conversion profile.

### 8.2.2.2 UV-Vis

Initiator absorbance was measured using an Agilent Technologies 8453 UV-Visible Spectrophotometer. The initiators were dissolved at a concentration of  $10^{-4} \text{ mol/L}$  in methanol. The solutions were injected into a glass slide sandwich with an effective optical pathlength of  $150 \mu\text{m}$  (the glass slides were separated by  $150 \mu\text{m}$  thick glass cover slip). Pure methanol was used as a blank in order to establish a baseline. The spectra were taken with each photo-initiator prepared at three concentrations in the Beer's Law regime. The spectra absorbance values were plotted against the photoinitiator

concentration, and the molar absorptivity was calculated from the slope of the best-fit line and plotted against wavelength.

## 8.3 Results and Discussion

### 8.3.1 Kinetic Analysis

#### 8.3.1.1 Neat Epoxide Monomers

In the kinetic analysis, increased rate of active center generation production is presumed to increase the conversion at the end of the Raman experiments. Similarly, the increased active center production is presumed to increase the rate of epoxide polymerization, which may be estimated via the slope of the conversion profile.

The neat epoxide monomers all showed similar sensitivity to the phosphine oxide photoinitiators (see Figure 8.4). The formulations with only PC-2506 and those with PC-2506 and Irgacure 651 showed comparable final conversions in both EEC and BGE. In the systems containing either type of phosphine oxide radical generator (Irgacure 819 or Lucirin TPO), lower final epoxide conversions were observed. The reactivity of VCM is very high, and eventually all formulations were found to have very high conversions. Upon examination of the conversion profiles in the first 60 seconds of illumination, the decrease in rate of polymerization is clearly linked to the phosphine oxide photoinitiators. The formulations containing only PC-2506 and those with Irgacure 651 showed similar reactivity based on the conversion profiles. The systems with Irgacure 819 and Lucirin TPO both showed negligible epoxide conversion over the first 60 seconds.

#### 8.3.1.2 Hybrid Acrylate-Epoxide Systems

The hybrid systems studied were composed of HEA, EGMEA, and EEC in equimolar amounts, resulting in a hydroxyl/oxirane ratio of 0.5. The hybrid formulations formed clear, colorless solid polymers upon polymerization with no indications of phase separation. The Raman signal was clear and well-resolved throughout the entire

polymerization (phase separation and/or volumetric shrinkage manifested via cavities forming between the quartz capillary tube and the polymeric material have proven problematic with regard to Raman spectral resolution in preliminary studies of other hybrid systems (e.g., BGE:HEA)).

The photoinitiation systems with no radical generators showed moderate epoxide conversions (~45%) occurring during 300 seconds of illumination (see Figure 8.5a). Lower rates of epoxide polymerization were observed in comparison to other systems with high hydroxyl/oxirane ratios studied previously.<sup>22</sup> The decrease in the relative polymerization rate was most likely due to the dilution of epoxide monomer in acrylate monomers.

By adding Irgacure 651 as the radical generator, similar epoxide conversion profiles were observed as in the formulations with no radical generator present. In addition to preserving the epoxide reactivity, the acrylate monomer reached quantitative conversion in approximately 100 seconds of illumination (see Figure 8.5b). The hybrid formulations containing Irgacure 819 or Lucirin TPO exhibited extremely high acrylate conversions (quantitative conversion reached just after ~50 seconds of illumination), but the final epoxide conversion and the epoxide polymerization rate were depressed relative to the formulations with no radical photo-initiators and the formulations with Irgacure 651 (see Figures 8.5c and 8.5d). These results were clarified through an understanding of the photoinitiator absorption characteristics discussed below.

### 8.3.2 UV-Vis

UV-Vis absorbance spectra obtained for each of the photoinitiators used in this study reveal why the phosphine oxide type radical generators suppress the epoxide polymerization (see Figure 8.6). PC-2506 absorbs light with wavelengths below 325 nm, meaning the photons in this wavelength range have sufficient energy to produce cationic active centers via direct photolysis of PC-2506. Light greater than 325 nm will not be

absorbed by PC-2506 and, therefore, is not useful in producing active centers via direct photolysis of PC-2506. Both Irgacure 819 and Lucirin TPO have much greater molar absorptivities than PC-2506 at wavelengths less than 425 nm. Irgacure 651 has lower molar absorptivities than PC-2506 for wavelengths less than 325 nm, but greater molar absorptivities for wavelengths greater than 325 nm.

The RPCP mechanism is occurring in all the studied systems with radical photoinitiators present. The high molar absorptivities of Irgacure 819 and Lucirin TPO indicate that they will out-compete PC-2506 in absorbing deep and near-UV photons incident on the resin. Therefore, epoxide photopolymerization is dependent largely on the RPCP initiation mechanism in systems containing the phosphine oxide-type radical generators. The PC-2506:Irgacure 651 systems allow for both direct photolysis and RPCP initiation mechanisms to occur simultaneously. PC-2506 out-competes Irgacure 651 for short wavelength photons (those with sufficient energy for direct photolysis of PC-2506), and Irgacure 651 out-competes PC-2506 for long wavelength photons (only useful in generating cationic active centers via the RPCP mechanism). Epoxide polymerization rates are low in the systems that suppress direct photolysis (formulations with phosphine oxide-type initiators) because a single-step initiation process (direct photolysis of PC-2506) is traded for a multi-step initiation process (RPCP mechanism).

#### 8.4 Conclusions

The competitive and complementary effects of dual initiators that take place in hybrid and neat epoxide systems were investigated. The addition of phosphine oxide radical initiators decreased the epoxide conversion in neat epoxide and hybrid acrylate-epoxide systems. Decreases in conversion were explained by deep-UV photon competition between PC-2506 and the phosphine oxide radical initiators. The negligible increase in epoxide conversion for EEC with Irgacure 651 and the reduced epoxide conversion for EEC with Irgacure 819 and Lucirin TPO showed that the RPCP

mechanism was not significant in neat EEC systems. In neat VCM, the relative rates of polymerization showed the same order for the different photoinitiation systems (PC-2506 > Irgacure 651 > Irgacure 819 = Lucirin TPO). In summary, the study has demonstrated that the polymerization of cycloaliphatic epoxides in neat and hybrid formulations is not enhanced by the RPCP mechanism and underscores the importance of choosing carefully the photoinitiator system to avoid deleterious effects on the conversion of either monomer system. Future work will focus on optimizing PC-2506:Irgacure 651 photoinitiation systems for hybrid acrylate-epoxide resins.

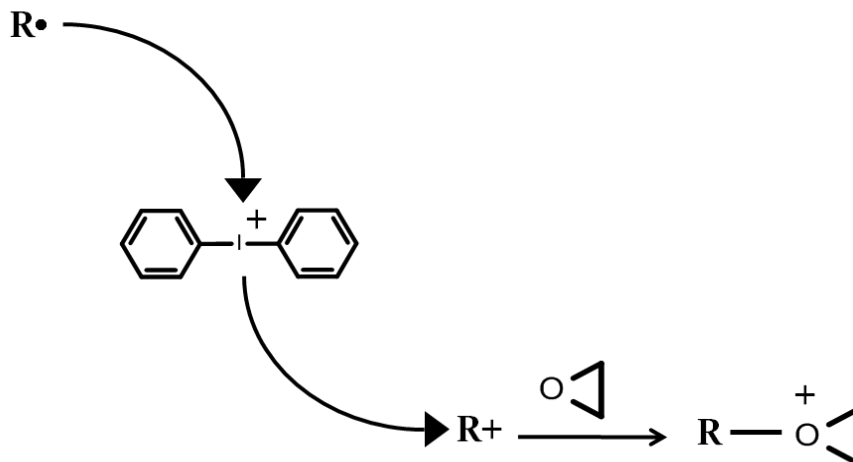


Figure 8.1: A generalized reaction sequence for the production of cationic active centers via the radical promoted cationic polymerization mechanism.

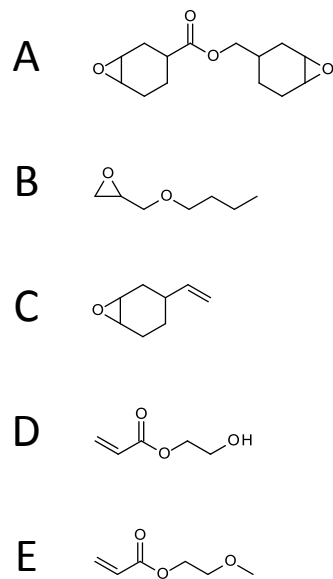


Figure 8.2: Monomer structures: (A) EEC, (B) BGE, (C) VCM, (D) HEA, (E) EGMEA.

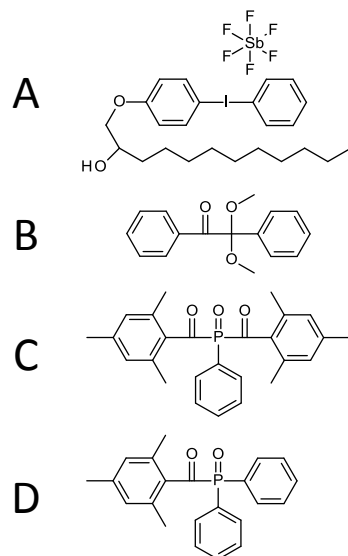


Figure 8.3: Photoinitiator structures: (A) PC-2506, (B) Irgacure 651, (C) Irgacure 819, (D) Lucirin TPO.



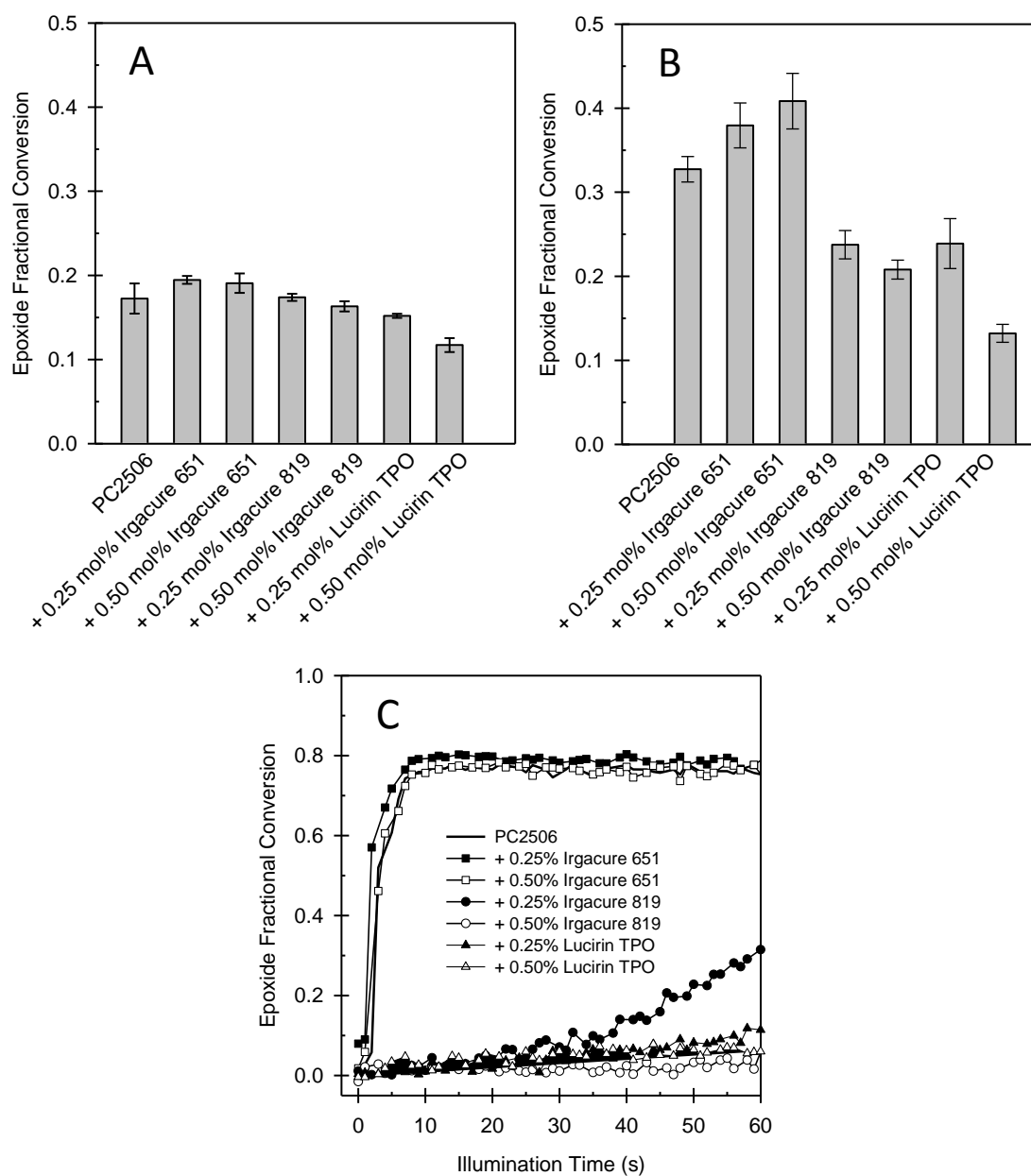


Figure 8.4: Final epoxide conversions of (A) EEC, and (B) BGE and epoxide conversion profiles (C) VCM systems.

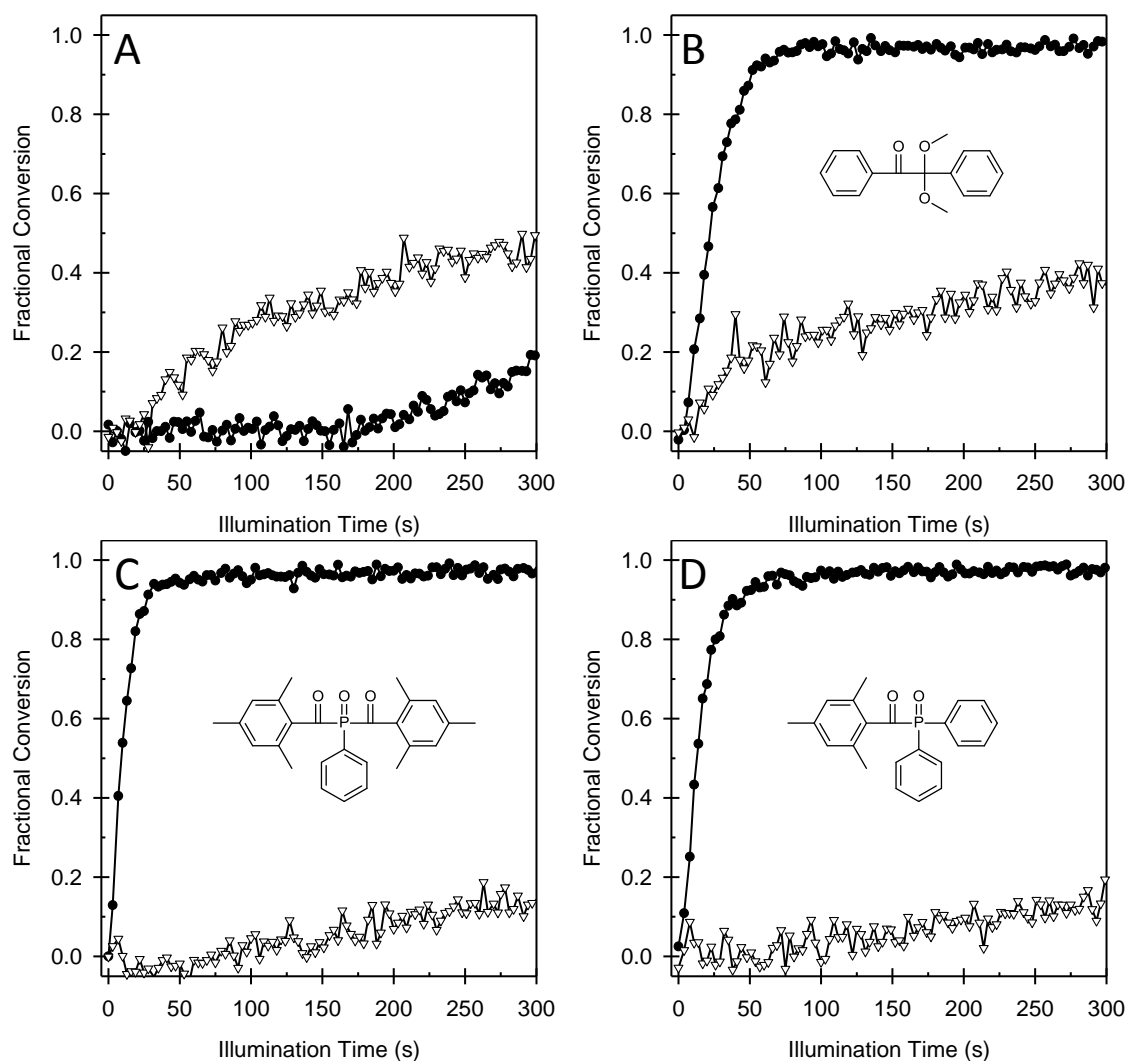


Figure 8.5: Conversion profiles for hybrid acrylate-epoxide systems varying in free-radical initiator: (A) PC-2506 only, (B) PC-2506:Irgacure 651, (C) PC-2506:Irgacure 819, (D) PC-2506:Lucirin TPO. Closed circles indicate acrylate conversion; open triangles indicate epoxide conversion.

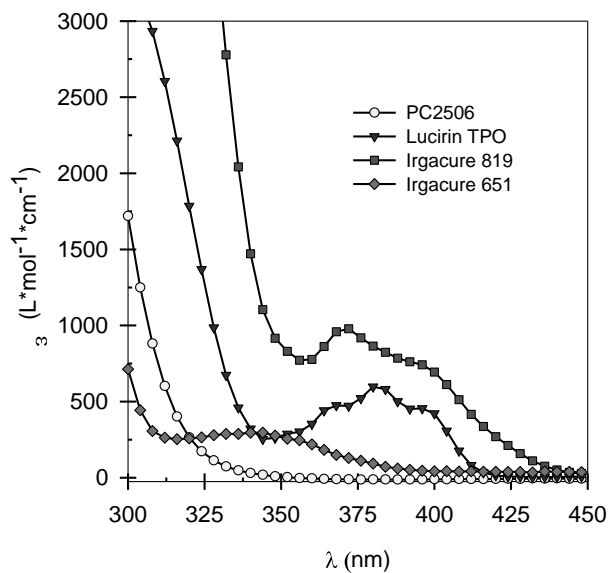


Figure 8.6: Molar absorptivities as a function of wavelength for the initiators used: PC-2506 (*open circles*), Lucirin TPO (*filled triangles*), Irgacure 819 (*filled squares*), Irgacure 651 (*filled diamonds*).

Notes

- (1) Fouassier, J. *Photoinitiation, Photopolymerization, and Photocuring*; Hanser/Gardner Publications, Inc.: Cincinnati, OH, 1995; , pp 375.
- (2) Koleske, J. V. *Radiation Curing of Coatings*; ASTM International: West Conshohocken, PA, 2002; Vol. 1, pp 244.
- (3) Andrzejewska, E. "Photopolymerization kinetics of multifunctional monomers." *Progress in Polymer Science* **2001**, 26, 605-665.
- (4) Gou, L.; Opheim, B.; Scranton, A. B. "The effect of oxygen in free radical photopolymerization." *Recent Research Developments in Polymer Science* **2004**, 8, 125.
- (5) O'Brien, A. K.; Bowman, C. N. "Modeling the effect of oxygen on photopolymerization kinetics." *Macromolecular Theory and Simulations* **2006**, 15, 176-182.
- (6) Gou, L.; Opheim, B.; Scranton, A. B. *In Methods to overcome oxygen inhibition in free radical photopolymerizations*. Chemistry of Synthetic High Polymers; 2006; , pp 301-310.
- (7) Decker, C. "Photoinitiated cationic polymerization of epoxides" *Polymer International* **2001**, 50, 986-997.
- (8) Bi, Y.; Neckers, D. C. "A Visible Light Initiating System for Free Radical Promoted Cationic Polymerization." *Macromolecules* **1994**, 27, 3683-3693.
- (9) Yagci, Y.; Schnabel, W.; Ledwith, A. "Synthesis and reactions of polymers with photoactive terminal groups - 3. The use of radical promoted cationic polymerization for the synthesis of poly(n-butyl vinyl ether) with N-acyl dibenz(b,f)azepine terminal units." *European Polymer Journal* **1987**, 23, 737-740.
- (10) Cowell, G. W.; Kocharyan, K.; Ledwith, A.; Woods, J. H. "Initiation of cationic polymerization by electron transfer: polymerization of N-vinyl carbazole by hexachloroantimonate (SbCl<sub>6</sub><sup>-</sup>) ion." *European Polymer Journal* **1970**, 6, 561-567.
- (11) Dursun, C.; Degirmenci, M.; Yagci, Y.; Jockusch, S.; Turro, N. J. "Free radical promoted cationic polymerization by using bisacylphosphine oxide photoinitiators: substituent effect on the reactivity of phosphinoyl radicals." *Polymer* **2003**, 44, 7389-7396.

- (12) Bulut, U.; Crivello, J. V. "Investigation of the Reactivity of Epoxide Monomers in Photoinitiated Cationic Polymerization." *Macromolecules* **2005**, *38*, 3584-3595.
- (13) Durmaz, Y. Y.; Moszner, N.; Yagci, Y. "Visible Light Initiated Free Radical Promoted Cationic Polymerization Using Acylgermane Based Photoinitiator in the Presence of Onium Salts." *Macromolecules (Washington, DC, United States)* **2008**, *41*, 6714-6718.
- (14) Lalevee, J.; Tehfe, M.; Morlet Savary, F.; Graff, B.; Allonas, X.; Fouassier, J. "Oxygen mediated and wavelength tunable cationic photopolymerization reactions under air and low intensity: A new concept" *Progress in organic coatings* **2011**, *70*, 23.
- (15) Lalevée, J.; Fouassier, J. P. "Recent advances in sunlight induced polymerization: role of new photoinitiating systems based on the silyl radical chemistry" *Polymer Chemistry* **2011**.
- (16) Tehfe, M.; Lalevee, J.; Gimes, D.; Fouassier, J. "Green Chemistry: Sunlight-Induced Cationic Polymerization of Renewable Epoxy Monomers Under Air" *Macromolecules* **2010**, *43*, 1364.
- (17) Tehfe, M.; Lalevee, J.; Allonas, X.; Fouassier, J. "Long Wavelength Cationic Photopolymerization in Aerated Media: A Remarkable Titanocene/Tris(trimethylsilyl)silane/Onium Salt Photoinitiating System." *Macromolecules* **2009**, *42*, 8669.
- (18) Crivello, J. V.; Ortiz, R. A. "Benzyl alcohols as accelerators in the photoinitiated cationic polymerization of epoxide monomers." *Journal of Polymer Science, Part A: Polymer Chemistry* **2002**, *40*, 2298-2309.
- (19) Crivello, J. V.; Rajaraman, S.; Mowers, W. A.; Liu, S. "Free radical accelerated cationic polymerizations." *Macromolecular Symposia* **2000**, *157*, 109-119.
- (20) Rajaraman, S. K.; Mowers, W. A.; Crivello, J. V. "Interaction of Epoxy and Vinyl Ethers During Photoinitiated Cationic Polymerization" *Journal of Polymer Science Part A: Polymer Chemistry* **1999**, *37*, 4007-4018.
- (21) Ortiz, R. A.; Lopez, D. P.; Cisneros, M. d. L. G.; Valverde, J. C. R.; Crivello, J. V. "A kinetic study of the acceleration effect of substituted benzyl alcohols on the cationic photopolymerization rate of epoxidized natural oils." *Polymer* **2005**, *46*, 1535-1541.
- (22) Dillman, B.; Jessop, J. L. P. "Chain transfer agents in cationic photopolymerization of a bis-cycloaliphatic epoxide monomer: Kinetic and physical property

effects" *Journal of Polymer Science Part A: Polymer Chemistry* **2013**, *51*, 2058-2067.

- (23) Cai, Y.; Jessop, J. L. P. "Decreased oxygen inhibition in photopolymerized acrylate/epoxide hybrid polymer coatings as demonstrated by Raman spectroscopy." *Polymer* **2006**, *47*, 6560-6566.
- (24) Cai, Y.; Jessop, J. L. P. "Effect of water concentration on photopolymerized acrylate/epoxide hybrid polymer coatings as demonstrated by Raman spectroscopy" *Polymer* **2009**, *50*, 5409-5413.

CHAPTER 9  
SOLVENTLESS SYNTHESIS AND FREE-RADICAL  
PHOTOPOLYMERIZATION OF A CASTOR OIL-BASED ACRYLATE  
OLIGOMER

9.1 Introduction

The fabrication of protective organic coatings can be done in many ways. Historically, organic solvents used either as a polymerization medium or simply as a resin carrier were evaporated, leaving a thin polymeric film as a protective coating over the substrate.<sup>1</sup> The solvent evaporation technique is clearly environmentally deleterious and is a health hazard to coating applicators and other individuals near the application area. The development of waterborne and so-called 100% solids systems has provided significant decreases in volatile organic compound (VOC) emissions in coatings production processes.<sup>2-4</sup>

Photo-induced polymerization of 100% solids resins is particularly efficient in that considerably lower energy input is required to produce polymeric films in comparison to thermal curing schemes. In order to increase the environmental benefits of photopolymerization, renewable materials can replace petroleum-derived monomers as feedstock.<sup>5-7</sup> Triglycerides, derived from seed oils, are especially attractive starting materials for photopolymerization for two reasons: intrinsically high molecular weight and high functionality.

Castor oil triglycerides offer a promising route to synthesize reactive oligomers for photopolymerization<sup>8-10</sup> and exhibit numerous advantages. For example, the high molecular weight would mitigate polymerization-induced shrinkage<sup>11,12</sup>, which causes internal stresses and surface deformations in the polymer film.<sup>13-15</sup> In addition to lower shrinkage, the high molecular weight would render the resin non-volatile, which simplifies the processing of the resin and reinforces the low to no VOC quality often

associated with photopolymerizable resins. The fatty acid composition in castor oil triglycerides differs from most other triglycerides, which are typically high in saturated fatty acids, as well as mono and di-unsaturated fatty acids. About 90% of the acid residues in castor oil triglycerides are ricinoleic acid. Ricinoleic acid is singly unsaturated and bears one hydroxyl group, see Figure 9.1.<sup>16</sup> The hydroxyl group allows for direct modification of the triglycerides, resulting in a multifunctional, renewable oligomer accomplished in a single modification reaction step.

Hydroxyl groups can couple readily with esters, epoxides, and isocyanates. The coupling with isocyanates is the most rapid and thermodynamically favourable of these reactions and has no secondary reaction products, as shown in Figure 9.2.<sup>17,18</sup> The reaction can take place without solvent or catalyst, but a simple tertiary amine catalyst accelerates the reaction and reduces the reaction temperature. A solventless modification can then be carried out if both reactants are compatible and in the liquid state when combined. In this work, a unique hybrid monomer that has both acrylate and isocyanate functional groups (AOI) is used to functionalize the castor oil.

The functionalization of castor oil using AOI is an efficient technique that can be used to prepare oligomers for polymerization in a facile way and facilitates the transition from pure petroleum-based feeds to a combination of petroleum and renewable ones. The synthesis of acrylated castor oil (ACO), the photopolymerization behaviour, and the material properties of the resulting polymer in both neat and co- polymerizations are detailed in this work.

## 9.2 Experimental

### 9.2.1 Materials

Castor oil, CVS brand (USP grade), was purchased at a local pharmacy. 2-Acryloyloxyethyl isocyanate (AOI) was donated by Showa Denko. AOI is a highly hazardous isocyanate monomer, and a thorough understanding of its toxicity and



reactivity must be obtained before handling it. The acrylate monomers used as reactive diluents were chosen to span a range of functionalities, hydrophobicity, and rigidity via secondary functional groups. These ranges of different diluent properties were explored to demonstrate the compatibility of acrylated castor oil (ACO) with various commercial acrylate monomers. Hydroxy ethyl acrylate (HEA) and hydroxy butyl acrylate (HBA) monomers were donated by BASF. Hexyl acrylate (HA) and ethylene glycol methyl ether acrylate (EGMEA) monomers were purchased from Aldrich. Isobornyl acrylate (IBA) was donated by Cytec. Tripropylene glycol diacrylate (TrPGDA) and trimethylol propane triacrylate (TrMPTrA) monomers were donated by Sartomer. Hexanediol diacrylate (HDDA) was purchased from Alfa Aesar. N,N-diisopropylethylamine (Hünigs base) was purchased from Aldrich. Hydroquinone, which was used as a stabilizer, was purchased from Alfa Aesar. The radical photoinitiator Darocur 1173 (2-hydroxy-2-methyl-1-phenyl-1-propanone) was donated by BASF. All materials were used as received.

### 9.2.2 Synthesis of ACO

The preparation of ACO was carried out by reacting AOI with the hydroxyl groups on castor oil in the presence of a tertiary amine catalyst, Hünigs base. Since tertiary amines are commonly used in photopolymerization and are known not to interfere with the polymerization, Hünigs base was chosen over Sn catalysts, which are more typically used in isocyanate-hydroxyl reactions. Castor oil (36.3 g, 0.10 mol OH), AOI (14.8 g, 0.10 mol), Hünigs base (1.8 g, 0.014 mol), and acrylate-stabilizing hydroquinone (0.05 g, 0.49 mmol) were added to a three-necked, round-bottom flask equipped with a reflux condenser. The reaction vessel was submerged in an oil bath, which was at a constant temperature of 83°C, stirring at 150 rpm with a magnetic stir bar. The isocyanate-hydroxyl coupling reaction was monitored by FT-IR spectroscopy. Samples were taken from the reaction mixture, in triplicate, every 30 minutes and diluted by an equivalent mass of THF. The diluted samples were then placed on a ZnSe ATR crystal

and FT-IR spectra collected with a Thermo Nicolet 670 Nexus spectrometer equipped with liquid nitrogen cooled MCT detector, producing spectra with  $4\text{ cm}^{-1}$  resolution. The isocyanate conversion was determined by monitoring the isocyanate peak centered at  $2275\text{ cm}^{-1}$  using the univariate method described in Eq. 1 below:

$$X = A_o - A_t/A_o \quad 9.1$$

where  $X$  is the functional group conversion,  $A_o$  is the initial functional group absorbance, and  $A_t$  is the functional group absorbance at time  $t$ . The reaction was quenched (after 3-4 hours) once the isocyanate conversion reached ~95% conversion. The reaction mixture was cooled, and a viscous, colorless oil was obtained. The ACO was stored in a freezer when not in use.

A Bruker AVANCE 300 MHz spectrometer was used to collect  $^1\text{H}$  NMR spectra of samples diluted in  $\text{CDCl}_3$  containing 0.03% (v/v) TMS as an internal standard.

### 9.2.3 Formulations

Photopolymerization kinetic experiments, as well as physical/mechanical property experiments, were carried out using formulations of neat ACO and ACO mixed with various reactive diluents. Reactive diluents are low viscosity, low molecular weight monomers that, when mixed with high molecular weight or high viscosity oligomers, allow for freely flowing resins to be prepared from otherwise unmanageable oligomers. Rather than cutting the oligomer with a solvent, using reactive diluents allows formulators to retain the 100% solids status of the parent resin. The mixtures consisted of a mass ratio of ACO to reactive diluent equal to 60:40. The photoinitiator concentration for all formulations was 1 wt% percent of the resin (ACO mass + reactive diluent mass).

### 9.2.4 Photopolymerization kinetics

The UV-induced acrylate conversion was monitored by real-time FT-IR (RT-IR) spectroscopy. Formulations were sandwiched between two salt plates fitted with  $15\text{ }\mu\text{m}$

spacers and placed on an in-house fabricated horizontal sampling accessory, which enabled real-time monitoring of the photopolymerization. The photopolymerization was initiated by illuminating the NaCl sandwich with a 100 W high-pressure mercury lamp (Acticure® Ultraviolet/Visible spot cure system, EXFO Photonic Solutions, Inc.) with an effective irradiance in the UV (250-450 nm) of 50 mW/cm<sup>2</sup> incident on the sample surface. Baseline spectra were obtained over a period of 20 seconds before illuminating with the UV lamp. Using the univariate method discussed previously, the acrylate functional group conversion was calculated as a function of illumination time. The peak height of the band centered at 810 cm<sup>-1</sup>, which corresponds to the vinyl C-H out-of-plane bending, was used in the kinetic analysis. A minimum of three replicates was used in the analysis of each formulation, and the experimental repeatability was within 5% (final conversion values).

### 9.2.5 Dynamic mechanical analysis

Homopolymer and copolymer specimens for dynamic mechanical analysis (DMA) were prepared by filling glass molds prepared from silanized (Rain-x treated) glass slides, which were separated by a double thickness of 150 μm glass cover slips, with resins. Each resin-filled glass mold was passed twice through a belt-driven Fusion curing system (model LC-6B), which has an irradiator (model 1300MB) with an aluminium reflector and a high intensity H-bulb. The belt speed was 9 ft/min (0.05 m/s), delivering a UV dose of ~3.5 J/cm<sup>2</sup> per run. The resulting polymers were stored in the dark at room temperature for 24 hours, then cut to approximate dimensions of 15 x 5 x 0.3 mm. A TA Instruments Q800 dynamic mechanical analyzer was used to characterize the thermo-mechanical properties of the polymer specimens. Samples were placed in a vertical film tension clamp and ramped from -50 to 100°C at a heating rate of 3°C/min and 1 Hz sinusoidal strain of 0.05%. The glass transition temperature (T<sub>g</sub>) was taken as the temperature corresponding to the tan δ maximum.

## 9.3 Results and Discussion

### 9.3.1 Synthesis of ACO

Solventless reactions are more economical and do not require solvent recycling or separation upon completion of the coupling reactions. Many functionalizations of seed oils have been carried out<sup>19-23</sup>; however, very few have been done under solventless conditions.<sup>24</sup> Recently, the solventless functionalization of linseed oil was reported: the double bonds of the fatty acid residues were reacted with maleic anhydride, followed by coupling of the anhydride moieties with 2-hydroxyethyl methacrylate (HEMA) and subsequent UV-induced polymerization.<sup>25</sup> However, this functionalization of linseed oil requires very high reaction temperatures (270-300°C).

The tertiary amine catalyzed hydroxyl-isocyanate coupling reaction between castor oil and AOI (see Figure 9.3) requires relatively mild conditions (60-85°C) to achieve nearly 100% isocyanate conversion (see Figure 9.4 and Figure 9.5).

The acrylate functional group is capable of undergoing Michael addition reactions under basic conditions and therefore potentially sensitive to the functionalization procedure. Functional groups such as amines, thiols, and potentially alcohols can react with acrylate moieties via Michael addition. FT-IR and <sup>1</sup>H NMR spectroscopies showed that the acrylate functional group was preserved (see Figure 9.4 and Figure 9.6). The tertiary amine was not removed from the product because it only constitutes ~3 wt% of the resin and could be incorporated into the polymeric matrix by behaving as a chain transfer agent similar to triethylamine. If visible light curing is desired, the tertiary amine catalyst used for the hydroxyl-isocyanate reaction may also be used as a co-initiator in conjunction with camphorquinone or another Type II photoinitiator<sup>3</sup>. In cases where the amine must be removed prior to polymerization, more volatile or water-soluble amines may be used for a more straightforward removal.

### 9.3.2 Photo-induced polymerization and co-polymerizations

Kinetic experiments were carried out using RT-IR spectroscopy to monitor the photopolymerization of ACO and its co-polymerization with different acrylate monomers (see Figure 9.7). Typical characteristics of acrylate photopolymerizations were observed.<sup>26,27</sup> The induction period was very short, which is attributed to the laminate configuration of the samples. In a laminate system, the only path for oxygen to diffuse into the polymerizing system is by lateral flux. Since the oxygen flow into the system during photopolymerization was likely very low because little surface area of the resin was exposed to air, the inhibition was predominantly due to dissolved oxygen and other stabilizers. The initial monomer conversion was minimal as the dissolved oxygen and other stabilizers were rapidly consumed, and this induction period was followed by autoaccelerated polymerization. Conversion continued until the increase in viscosity and ultimately solidification of the polymer severely limited monomer and free-radical diffusion for a particular system.

Neat ACO achieved very high acrylate conversions (>95%). The addition of monoacrylate monomers to ACO resulted in slightly higher rates, exhibited by the slope of the conversion profiles, and even higher ultimate conversions (see Figure 9.7A). The higher rates are due to the higher acrylate functional group density of the oligomer-monomer blends, which is directly proportional to the rate of photopolymerization.<sup>27,28</sup>

When multifunctional acrylates were added to ACO, higher rates of polymerization were also observed (see Figure 9.7B). In contrast to the monoacrylate mixtures, the addition of multifunctional acrylates resulted in lower ultimate conversions. The decreased conversion values relative to neat ACO were slight with the diacrylates (TrPGDA at ~93% and HDDA at ~90%) and most prominent with the triacrylate (TrMPTrA at ~73%). The decreased conversions correspond to the functionality and functional group density of the co-monomer. With higher functionality, gelation and

vitrification occur at earlier stages, which limit the attainable conversion at the curing temperature (room temperature in these studies).

### 9.3.3 Polymer properties

The physical properties of photo-cross-linked films prepared from ACO and its co-polymerization with different acrylate monomers were characterized by DMA. The diluents studied range in properties from the highly hydrophobic HA to the water-soluble HEA and range in functionality from mono-acrylates to tri-acrylates. The  $\tan \delta$  as a function of temperature for neat ACO and formulations containing mixtures of ACO and mono-functional or multi-functional acrylates are shown in Figures 9.8A and 9.8B, respectively. No phase separation was observed in any copolymer films: the samples were completely transparent, and the  $\tan \delta$  profiles were characterized by a single, symmetric peak. The  $T_g$  of neat ACO was 3°C, and the introduction of the monoacrylates HA, EGMEA, and HBA reduced the  $T_g$  by 5-10%. Since the homopolymers of HA, EGMEA, and HBA are flexible materials with sub-ambient  $T_g$  values, it is expected that the introduction of these monomers would reduce the  $T_g$  of the copolymer. The monoacrylates HEA and IBA increased the  $T_g$  by 5-10%, which is also expected since the homopolymers of these materials have  $T_g$  values equal to or above room temperature. The higher  $T_g$  for HEA is due to strong hydrogen-bonding interactions and di-acrylate impurities, while IBA has a very high  $T_g$  considering it is a mono-acrylate. The bulky norbornane substituents with low conformational mobility are responsible for the disproportionately high  $T_g$  of IBA. Although HBA also has hydrogen-bonding capabilities, the effect is less in this monomer mixture relative to HEA due to the two extra methylene groups. A summary of the physical properties of the homopolymers and copolymers is provided in Table 1.

The Fox equation describes the relationship between the glass transition temperature of two homopolymers and that of the copolymer formed from

copolymerizing the parent monomers.<sup>29</sup> In its simplest form, the weighted average of the homopolymer  $T_g$ 's predicts the  $T_g$  of the copolymer, see Eq. 2:

$$\frac{w_i}{T_{g_i}} + \frac{w_j}{T_{g_j}} = \frac{1}{T_{g_c}} \quad 9.2$$

where  $w_i$  is the  $i$ th component's weight fraction,  $T_{g_i}$  is the  $i$ th component's glass transition temperature, and  $T_{g_c}$  is the copolymer's glass transition temperature. As a first approximation, the copolymer  $T_g$ 's were calculated based on the neat diluent and ACO  $T_g$  data and compared to the measured copolymer  $T_g$ 's. The agreement was very good despite the broad range of properties discussed earlier, see Figure 9.9. Hexyl acrylate was not included in the analysis because, in its cured state, it was tacky and not amenable to  $T_g$  determination via DMA. The Fox equation, in its simplest form (as used here), predicts  $T_g$ 's well for linear copolymers; however, a more detailed analysis is required in systems with crosslinking such as these.<sup>30-32</sup> Typically, higher crosslink density materials would introduce a positive bias relative to the predicted values arrived at via the simple Fox equation, as is exhibited in Figure 9.9. Although these results appear to provide a rough estimate useful for formulators, further analysis is required to develop a fundamentally based relationship for these crosslinked systems, which is beyond the intent of this initial work.

The storage modulus of the polymer films based on neat ACO, as well as formulations with monofunctional and multifunctional acrylates, are shown in Figures 9.8C and 9.8D, respectively and summarized in Table 1. According to rubber elasticity theory, the storage modulus in the rubbery plateau, above the  $T_g$ , is linearly proportional to the cross-link density ( $\nu_e$ ), as described by Eq. 7.3.<sup>33,34</sup>

$$E' = \nu_e 3RT \quad 9.3$$

where  $E'$  is the storage modulus of the polymer in the rubbery plateau,  $R$  is the gas constant ( $8.314 \text{ J} \cdot \text{K}^{-1} \cdot \text{mol}^{-1}$ ), and  $T$  is the absolute temperature (K).

The addition of monofunctional acrylate monomers decreases the cross-link density because a greater fraction of linear polymer will be produced. Conversely, multifunctional acrylate monomers will increase the cross-link density. The apparent changes in cross-link density, observed via the rubbery plateau modulus, due to the functionality of the reactive diluent are clearly shown in Table 1. Formulations of ACO with monofunctional acrylates resulted in crosslink density values less than that for neat ACO. The multifunctional acrylates show a distinct order in increasing the cross-link density of the resin: TrMPTrA > HDDA > TrPGDA. These results can be explained by a combination of acrylate functionality and molecular length. The highest cross-link density is associated with the triacrylate TrMPTrA, which has a functionality of six. The diacrylate TrPGDA is of similar molecular weight as TrMPTrA, but has a functionality of four. HDDA is also a diacrylate, but the connection between the two esters is two bonds shorter.

#### 9.4 Conclusions

A renewable acrylate oligomer was synthesized by a simple coupling of hydroxyl and isocyanate functional groups from castor oil and the hybrid monomer AOI, respectively. The functionalization was carried out under solventless conditions and resulted in very high yields of viscous oligomer. This synthesis provides a robust material suitable for highly efficient photopolymerization processes.

The photopolymerization of ACO was rapid as a neat resin and accelerated when combined with commercially available acrylate monomers. ACO is compatible with all the acrylates in this study, which spanned a range of functionalities and hydrophobicity. The addition of acrylate co-monomers reduced the apparent viscosity and increased the rate of acrylate conversion relative to the parent resin. The thermal transitions of the neat ACO and the co-monomer formulations were monomodal, suggesting good co-polymerization behaviour and no phase separation. The  $T_g$  values in



this study range from  $-15^{\circ}\text{C}$  to  $45^{\circ}\text{C}$  by blending ACO with HA and TrMPTrA, respectively, and can be coarsely estimated *a priori* using the Fox correlation. Thus, ACO is a useful oligomer based on renewable feedstock and suitable for replacement of 100% petroleum-based oligomers in UV-curable formulations requiring high cure speeds and  $T_g$  values near room temperature. Although ACO is a step in the right direction, continued efforts are required to “green” the entire synthetic and polymerization processes.

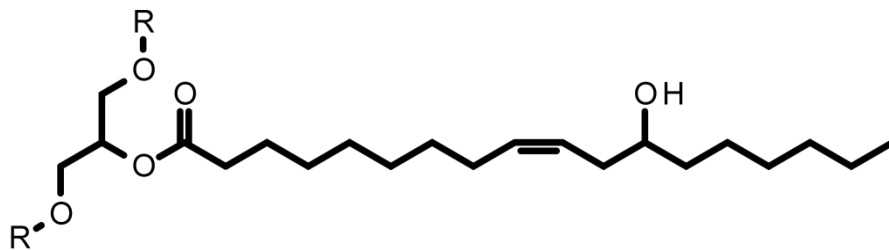


Figure 9.1: Chemical structure of ricinoleic acid in triglyceride form.

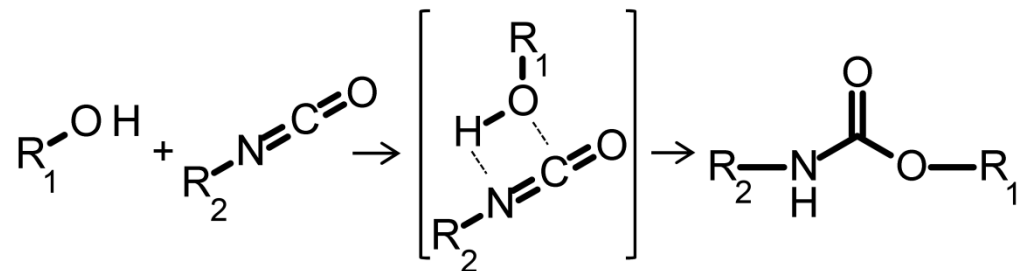


Figure 9.2: Isocyanate and alcohol functional groups readily couple with the hydrogen-bonded complex as the intermediate. isocyanate-coupling reaction.

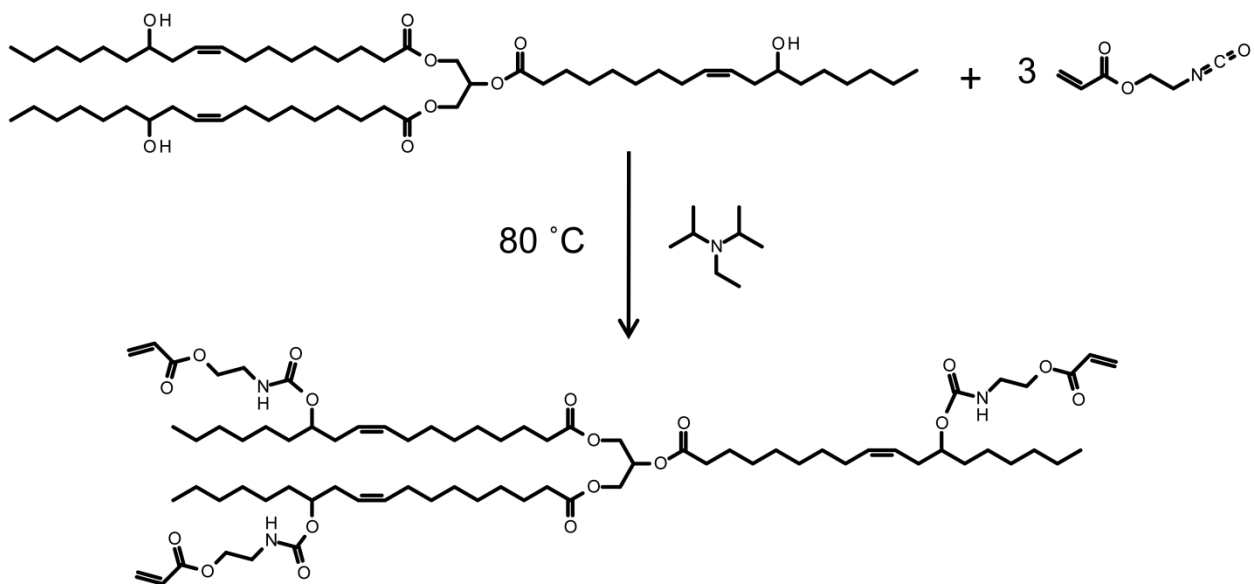


Figure 9.3: Castor oil reacts with AOI monomer in the presence of a tertiary amine catalyst to form acrylated castor oil (ACO), represented by an ideal triglyceride composed of three ricinoleic acid residues.

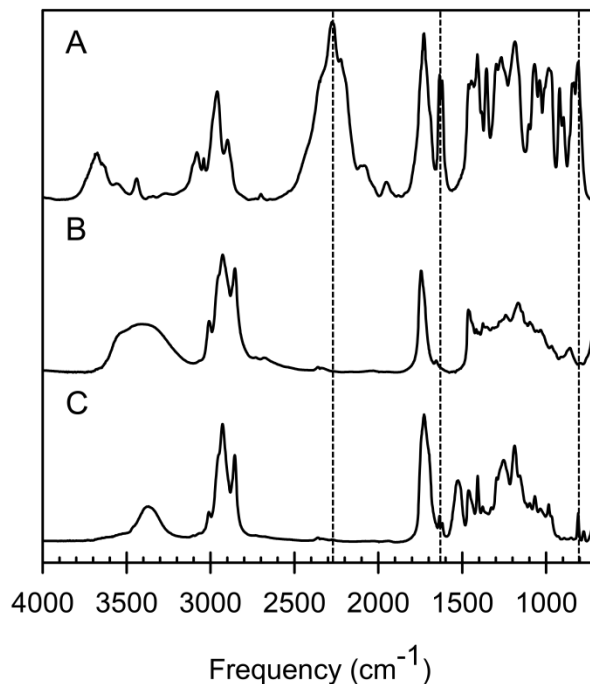


Figure 9.4: FT-IR spectra of neat AOI monomer (A), neat castor oil (B), and the product of AOI-castor oil coupling (C). Spectrum A shows the strong absorbance of the NCO band centered around 2270  $\text{cm}^{-1}$ , as well as the carbonyl peak centered around 1710  $\text{cm}^{-1}$  and the acrylate peaks at 1640  $\text{cm}^{-1}$  and 810  $\text{cm}^{-1}$ . Spectrum B shows the broad OH band centered around 3300  $\text{cm}^{-1}$  and the carbonyl centered at 1710  $\text{cm}^{-1}$ . Spectrum C indicates quantitative consumption of the NCO functional group as there is no peak at 2270  $\text{cm}^{-1}$ . In addition to the NCO consumption, the acrylate functional group is retained according to the absorbances at 1640-1 and 810  $\text{cm}^{-1}$ . Dashed lines highlight the peaks at 2270, 1640, and 810  $\text{cm}^{-1}$ .

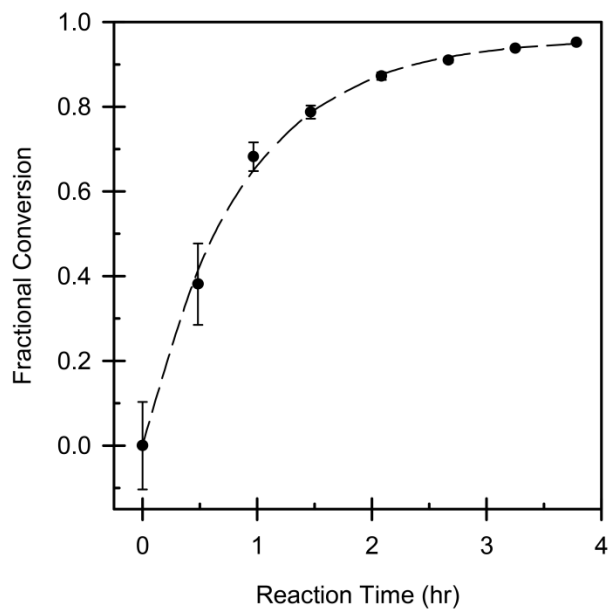


Figure 9.5: The isocyanate conversion by coupling with castor oil monitored by FT-IR spectroscopy. The isocyanate band centered at 2270  $\text{cm}^{-1}$  was used for analysis.

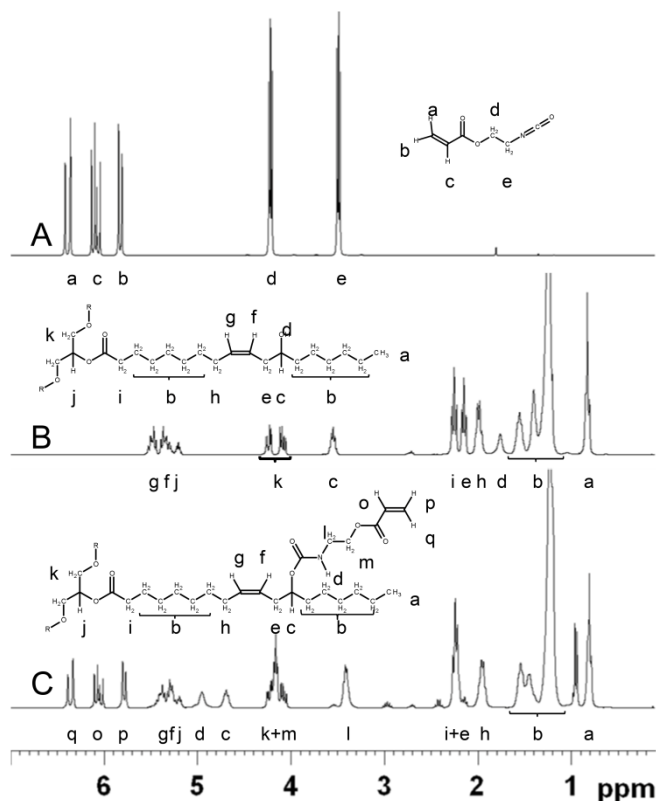


Figure 9.6: <sup>1</sup>H NMR spectra of neat AOI monomer (A), neat castor oil (B), and the product of AOI-castor oil coupling (C). Spectrum A shows peaks characteristic of the olefinic protons of the acrylate double bond and the methylene protons on carbons adjacent to the ester and isocyanate functional groups. Spectrum B is more complex due to the variety of protons present. The bands diagnostic of the reaction are the hydroxyl proton (2.74 ppm) and the proton of the carbon alpha to the hydroxyl group (3.56 ppm). Spectrum C shows the consumption of the O-H band and the appearance of the N-H band (4.96 ppm), as well as the shift of the alpha-hydroxy proton (3.56 ppm) to an alpha-carbamate proton (4.69 ppm).

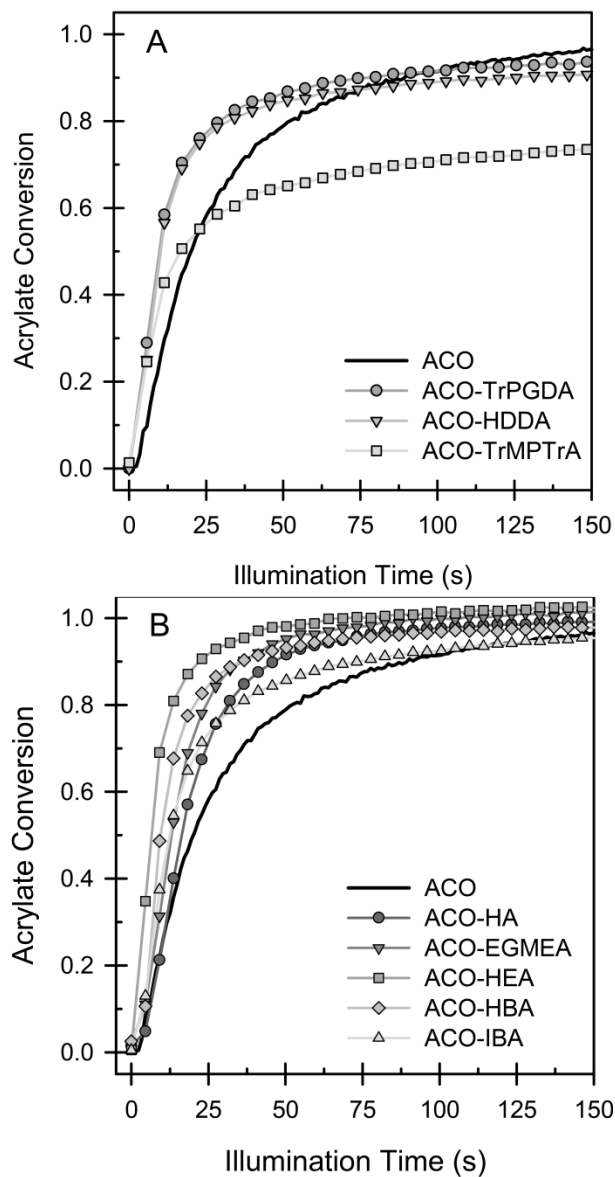


Figure 9.7: Acrylate conversions obtained by RT-IR spectroscopy: Neat ACO and copolymerizations with mono-acrylate monomers (A) and multi-acrylate monomers (B). Room-temperature photopolymerizations with 1wt% free-radical photoinitiator and 50 mW/cm<sup>2</sup> effective irradiance.



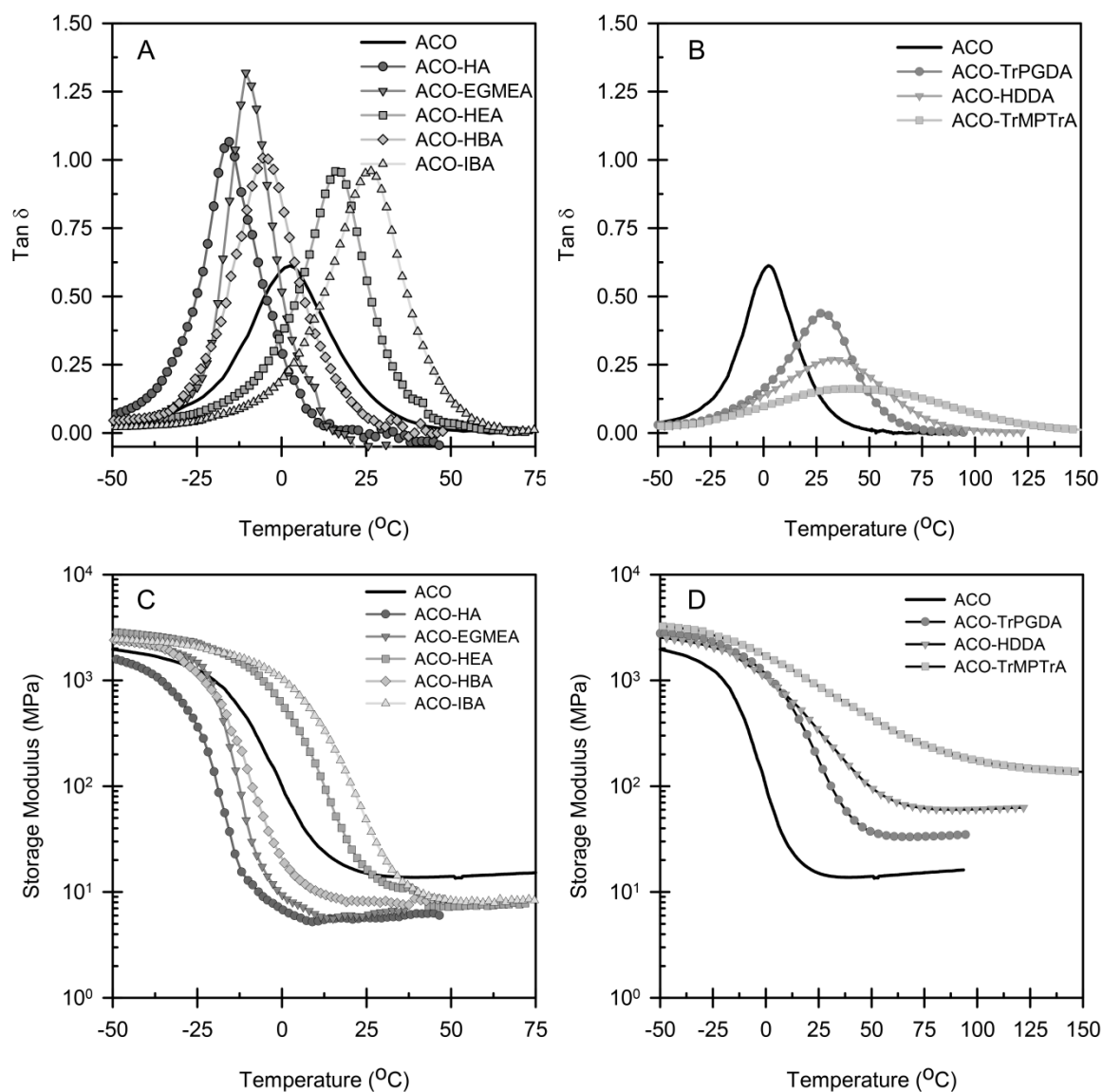


Figure 9.8: Dynamic mechanical analysis of photopolymerized films with a nominal thickness of 300  $\mu\text{m}$ :  $\tan \delta$  profiles of polymerized ACO and copolymers of mono-acrylate monomers (A) and multi-acrylate monomers (B), as well as storage modulus as a function of temperature for polymerized ACO and copolymers of mono-acrylate monomers (C) and multi-acrylate monomers (D).

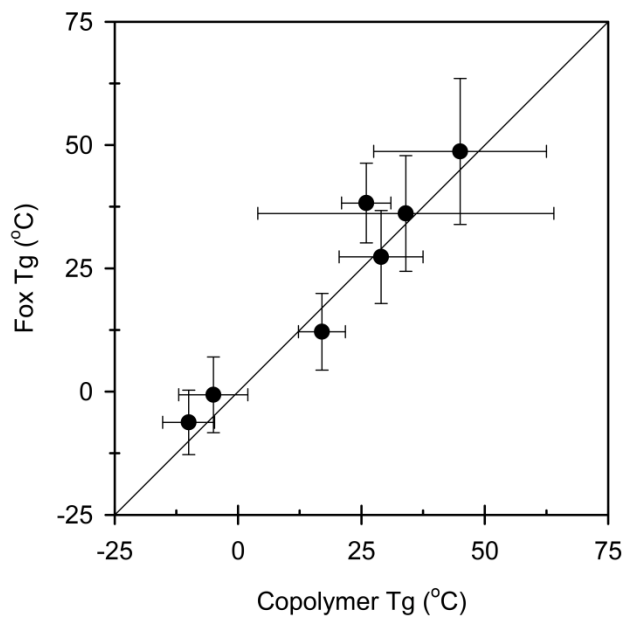
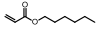
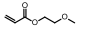
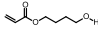
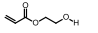

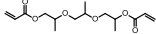
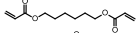
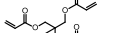


Figure 9.9: A comparison of the Fox correlation-derived Tg and the measured copolymer Tg taken as the temperature corresponding to the  $\tan \delta$  maximum. The line represents perfect correlation between measured and predicted Tg's.

Table 9.1: Monomer structures and physical properties of polymers formed from neat resins and blended formulations.

Structure	Acronym	Neat Polymer $T_g$ (°C) <sup>a</sup>	Copolymer $T_g$ (°C) <sup>a</sup>	Functionality	Rubbery Modulus (MPa) <sup>b</sup>	X-link Density (mol/m <sup>3</sup> x 10 <sup>-3</sup> ) <sup>c</sup>
---	ACO	3	---	2-6	13.79	1.76
	HA	---- <sup>d</sup>	-15	2	5.55	0.8
	EGMEA	-19	-10	2	6.28	0.8
	HBA	-6	-5	2	7.36	0.9
	HEA	27	17	2	8.17	1.1
	IBA	112	26	2	8.49	1.0
	TrPGDA	73	29	4	33.44 <sup>e</sup>	3.8
	HDDA	104	34	4	60.16 <sup>e</sup>	6.8
	TrMPTrA	155	45	6	297.6 <sup>f</sup>	28.8

<sup>a</sup> Glass transition taken from the  $\tan \delta$  maximum.

<sup>b</sup> Rubbery modulus value taken from the storage modulus plots at a Temp. =  $T_g + 40$  °C unless noted otherwise.

<sup>c</sup> Crosslink density calculated from the rubbery modulus using equation 3.

<sup>d</sup> Neat HA polymer was not analyzed via DMA due to the tacky properties of the resulting film.

<sup>e</sup> Rubbery modulus taken at Temp =  $T_g + 50$  °C.

<sup>f</sup> Rubbery modulus taken at Temp =  $T_g + 100$  °C.

Notes

- (1) Solomon, D. H. *The chemistry of organic film formers*; Wiley. New York. NYUSA: 1967 .
- (2) Koleske, J. V. *Radiation Curing of Coatings*; ASTM International: West Conshohocken, PA, 2002; Vol. 1, pp 244.
- (3) Fouassier, J. *Photoinitiation, Photopolymerization, and Photocuring*; Hanser/Gardner Publications, Inc.: Cincinnati, OH, 1995; , pp 375.
- (4) Chattopadhyay, D. K. "Structural engineering of polyurethane coatings for high performance applications" *Progress in polymer science* **2007**, *32*, 352-418.
- (5) Meier, M. A. R.; Metzger, J. O.; Schubert, U. S. "Plant oil renewable resources as green alternatives in polymer science" *Chemical Society Reviews* **2007**, *36*, 1788-1802.
- (6) Sharma, V.; Kundu, P. P. "Addition polymers from natural oils-A review." *Progress in Polymer Science* **2006**, *31*, 983-1008.
- (7) Lu, Y.; Larock, R. "Novel Polymeric Materials from Vegetable Oils and Vinyl Monomers: Preparation, Properties, and Applications" *ChemSusChem* **2009**, *2*, 136.
- (8) Palanisamy, A. "Photo-DSC and dynamic mechanical studies on UV curable compositions containing diacrylate of ricinoleic acid amide derived from castor oil" *Progress in organic coatings* **2007**, *60*, 161-169.
- (9) Rao, B. S.; Palanisamy, A. "Synthesis, photo curing and viscoelastic properties of triacrylate compositions based on ricinoleic acid amide derived from castor oil" *Progress in organic coatings* **2008**, *63*, 416-423.
- (10) Rao, B. S.; Palanisamy, A. "Photocuring and thermomechanical properties of multifunctional amide acrylate compositions derived from castor oil" *Progress in organic coatings* **2010**, *67*, 6-11.
- (11) Patel, M. P.; Braden, M.; Davy, K. W. M. "Polymerization shrinkage of methacrylate esters" *Biomaterials* **1987**, *8*, 53-56.
- (12) Anseth, K. S.; Bowman, C. N.; Peppas, N. A. "Polymerization kinetics and volume relaxation behavior of photopolymerized multifunctional monomers producing highly crosslinked networks" *Journal of Polymer Science Part A: Polymer Chemistry* **1994**, *32*, 139-147.

- (13) Davidson, C. L.; Feilzer, A. J. "Polymerization shrinkage and polymerization shrinkage stress in polymer-based restoratives" *Journal of dentistry* **1997**, *25*, 435-440.
- (14) Payne, J.; Francis, L.; McCormick, A. "The effects of processing variables on stress development in ultraviolet-cured coatings" *Journal of Applied Polymer Science* **1997**, *66*, 1267.
- (15) Vaessen, D.; Ngantung, F.; Palacio, M.; Francis, L.; McCormick, A. "Effect of lamp cycling on conversion and stress development in ultraviolet-cured acrylate coatings" *Journal of Applied Polymer Science* **2002**, *84*, 2784.
- (16) Lie Ken Jie, M. S. F.; Cheng, A. K. L. "Confirmation of the carbon chemical shifts of ethylenic carbon atoms in methyl ricinoleate and methyl ricinelaidate" **1993**, *3*, 65-69.
- (17) Krol, P. "Synthesis methods, chemical structures and phase structures of linear polyurethanes. Properties and applications of linear polyurethanes in polyurethane elastomers, copolymers and ionomers" *Progress in materials science* **2007**, *52*, 915-1015.
- (18) Chang, M.; Chen, S. "Kinetics and Mechanism of Urethane Reactions - Phenyl Isocyanate Alcohol Systems" *Journal of polymer science. Part A, Polymer chemistry* **1987**, *25*, 2543.
- (19) Swern, D.; Billen, G.; Findley, T.; Scanlan, J. "Hydroxylation of Monounsaturated Fatty Materials with Hydrogen Peroxide" *Journal of the American Chemical Society* **1945**, *67*, 1786-1789.
- (20) Crivello, J. V.; Narayan, R. "Epoxidized Triglycerides as Renewable Monomers in Photoinitiated Cationic Polymerization" *Chemistry of Materials* **1992**, *4*, 692-699.
- (21) Park, S.; Jin, F.; Lee, J.; Shin, J. "Cationic polymerization and physicochemical properties of a biobased epoxy resin initiated by thermally latent catalysts" *European polymer journal* **2005**, *41*, 231.
- (22) Khot, S. N.; Lascala, J. J.; Can, E.; Morye, S. S.; Williams, G. I.; Palmese, G. R.; Kusefoglu, S. H.; Wool, R. P. "Development and application of triglyceride-based polymers and composites" *Journal of Applied Polymer Science* **2001**, *82*, 703-723.
- (23) La Scala, J.; Wool, R. "The effect of fatty acid composition on the acrylation kinetics of epoxidized triacylglycerols" *Journal of the American Oil Chemists' Society* **2002**, *79*, 59-63.

- (24) Venturello, C.; Dalosio, R. "Quaternary Ammonium Tetrakis(diperoxotungsto)phosphates(3<sup>-</sup>) as a New Class of Catalysts for Efficient Alkene Epoxidation with Hydrogen-Peroxide" *Journal of organic chemistry* **1988**, *53*, 1553.
- (25) Zovi, O.; Lecamp, L.; Loutelier Bourhis, C.; Lange, C.; Bunel, C. "A solventless synthesis process of new UV-curable materials based on linseed oil" *Green Chemistry* **2011**, *13*, 1014-1022.
- (26) Decker, C. "Photoinitiated Crosslinking Polymerization." *Progress in Polymer Science* **1996**, *21*, 593-650.
- (27) Andrzejewska, E. "Photopolymerization kinetics of multifunctional monomers." *Progress in Polymer Science* **2001**, *26*, 605-665.
- (28) Bowman, C. N.; Kloxin, C. "Toward an Enhanced Understanding and Implementation of Photopolymerization Reactions" *AIChE Journal* **2008**, *54*, 2775-2795.
- (29) Hiemenz, P. C.; Lodge, T. P. *Polymer Chemistry Second Edition*; CRC Press: Boca Raton, FL, 2007; .
- (30) Fox, T. G.; Loshaek, S. "Influence of Molecular Weight and Degree of Crosslinking on the Specific Volume and Glass Transition Temperature of Polymers" *Journal of Polymer Science* **1955**, *15*, 371-390.
- (31) Bicerano, J.; Sammler, R. L.; Carriere, C. J.; Seitz, J. T. "Correlation between Glass Transition Temperature and Chain Structure of Randomly Crosslinked High Polymers" *Journal of Polymer Science Part B: Polymer Physics* **1996**, *34*, 2247-2259.
- (32) Kannurpatti, A. R.; Anseth, J. W.; Bowman, C. N. "A study of the evolution of mechanical properties and structural heterogeneity of polymer networks formed by photopolymerizations of multifunctional (meth)acrylates" *Polymer* **1998**, *39*, 2507-2513.
- (33) Menard, K. *Dynamic Mechanical Analysis: A Practical Introduction*; CRC Press: Boca Raton, FL, 2008; , pp 218.
- (34) Murayama, T. *Dynamic Mechanical Analysis of Polymeric Material*; Elsevier Scientific Publishing Company: New York, 1978; Vol. 1, pp 231.

## CHAPTER 10

### CONCLUSIONS AND RECOMMENDATIONS

#### 10.1 Conclusions

Photopolymerization, using light rather than heat to induce and sustain polymer-forming reactions, has been studied with respect to epoxide and acrylate monomers in both neat cationic or free-radical systems and in hybrid cationic-free radical systems. Overall, cationically polymerizable epoxide monomers were studied and well characterized via kinetic and physical property modulation afforded via CTA formulation. Other factors in photopolymerization, such as curing conditions, photoinitiation systems, monomer selection for neat epoxide, epoxide-acrylate, and neat acrylate systems, were also investigated.

In Chapter 3, RT-NIR spectroscopy was used to determine the moisture content of monomers accurately, as well as the rate of water consumption during the polymerization. Together, the RT-MIR and RT-NIR experiments show a distinct kinetic dependence of epoxide reaction on the amount of water present. These results indicate that the AM mechanism dominates in the presence of water. The amount of alkyl hydroxyls produced has a direct relationship to the amount of water present in the system. Additionally, the “long-term” study shows that the hydroxyl content is constant once the water in the system is consumed. This persistent hydroxyl concentration further confirms the AM mechanism as shown in Figure 1.10. For every water molecule reacting with an activated monomer, one or two alkyl hydroxyl groups are produced, depending on whether the oxygen of the activated monomer is bound to a carbon or hydrogen, respectively. For every alkyl hydroxyl reacting with an activated monomer bound to hydrogen, there is no net change in the amount of hydroxyls present.

Chapter 4 moves beyond water. Various alcohols were selected and studied as CTAs in the cationic crosslinking epoxide polymerization of EEC. Increasing the

concentration of the CTA in a given formulation generally produces greater conversions and polymerization rates. Multifunctional CTAs were found to retain the high properties ( $T_g$ , crosslink density, and gel fraction) of the parent resin more fully than the monofunctional CTAs. The size of monofunctional CTAs had minimal effects on conversion and polymerization rates, but reduced the  $T_g$ . Diols also produced lower  $T_g$  materials with increasing CTA size. However, as the size of the diol increased, the increase in the rate of polymerization was less due to dilution effects. High epoxide conversion was obtained without respect to the size of the CTA. Two groups of CTAs with lower nucleophilicities resulted in lower reactivity with the epoxide: (1) alcohols with high steric shielding near the active hydroxyl group and (2) alcohols with acidic hydroxyl groups arising from low electron density around the active hydroxyl groups via resonant and/or inductive effects. In general, CTAs can be used to tune the properties of epoxy resins over a very broad range of  $T_g$ 's and crosslink densities through selection of CTA alkyl chain length.

In Chapter 5, epoxide resins were cured in humid and dry atmospheres, and humidity had no effect on the bulk polymer properties of the cross-linked materials. AFM was used to determine the relative hardness of the polymer surface when cured under dry and humid atmospheres. The apparent surface modulus and therefore hardness were negatively impacted when cured in a humid atmosphere. The decrease in properties due to humidity is explained by the AM mechanism. Water vapor at the air-resin interface acts as a CTA and reduces the cross-link density in the surface layer of the cured material relative to materials prepared under dry conditions.

In Chapter 6, changes in polymer physical properties were attained through final curing conditions. All polymer specimens were photocured, followed by dark storage at room temperature. One group was thermally annealed prior to mechanical analysis. For high  $T_g$  epoxide polymers, an annealing step is clearly required for stable physical properties. This research used very long times to thermally anneal, or cure, the specimens



post-illumination; it is likely that shorter annealing times may result in similar properties. Further work in process optimization is required to quantify the minimum annealing time for materials with stable physical properties and good, non-brittle mechanical properties.

The AM mechanism was studied via thermally initiated cationic polymerization of cycloaliphatic epoxides in Chapter 7. Specialty prepolymers were prepared via RAFT polymerization consisting of one polymer composed of butyl acrylate monomer and another composed of a 1:10 mixture of hydroxyl acrylate:butyl acrylate. Cyclohexene oxide was polymerized in the presence of both polymer, and GPC traces were collected. The experiments showed an increase in molecular weight of the prepolymer containing hydroxyl butyl acrylate; whereas, the prepolymer prepared from neat butyl acrylate showed no change in molecular weight. In each case, the molecular weight of poly(cyclohexene oxide) was unchanged. Thus, the AM mechanism is effective in inducing chain propagation, and the AM and ACE mechanisms propagate in parallel. In addition, the physical properties of polymers prepared from bis-cycloaliphatic epoxide resins containing the polyacrylate polymers prepared via RAFT polymerization or containing polyTHF 250 were studied. The high molecular weight polyacrylates did not change the physical properties ( $T_g$  or cross-link density) of the epoxide resin in a significant way. The polyTHF 250 behaved as other lower molecular weight CTAs, with a decrease in  $T_g$  and cross-link density proportional to the amount of CTA in the formulation.

In Chapter 8, the competitive and complementary effects of dual initiators were investigated in hybrid and neat epoxide resins. The addition of phosphine oxide radical initiators decreased the epoxide conversion in neat epoxide and hybrid acrylate-epoxide systems. Decreases in conversion were explained by deep-UV photon competition between the cationic and the phosphine oxide radical initiators. The negligible increase in epoxide conversion for the diepoxide with acetophenone radical initiator and the reduced epoxide conversion for the diepoxide with the phosphine oxide radical initiators showed

that the radical promoted cationic polymerization (RPCP) mechanism was not significant in the neat diepoxide systems. In the neat monoepoxide, the relative rates of polymerization showed the same order for the different photoinitiation systems (cationic photoinitiator > acetophenone radical initiator > phosphine oxide radical initiators). In summary, the polymerization of cycloaliphatic epoxides (the diepoxide in particular) in neat and hybrid formulations is not enhanced by the RPCP mechanism and underscores the importance of carefully choosing the photoinitiator system to avoid deleterious effects on the conversion of either monomer system. Future work will focus on optimizing cationic and acetophenone radical initiator systems for hybrid acrylate-epoxide resins.

Finally, a renewable acrylate oligomer based on castor oil was studied in Chapter 9. The synthesis was carried out under solventless conditions and resulted in very high yields of viscous oligomer. This synthesis provides a robust material suitable for highly efficient photopolymerization processes. The photopolymerization of acrylated castor oil (ACO) was rapid as a neat resin and accelerated when combined with commercially available acrylate monomers. ACO is compatible with all the acrylates in the study, which spanned a range of functionalities and hydrophobicity. The addition of acrylate co-monomers reduced the apparent viscosity and increased the rate of acrylate conversion relative to the parent resin. The thermal transitions of the neat ACO and the co-monomer formulations were monomodal, suggesting good co-polymerization behavior and no phase separation. The  $T_g$  values in this study range from  $-15^{\circ}\text{C}$  to  $45^{\circ}\text{C}$  in the co-monomer formulations and can be coarsely estimated *a priori* using the Fox correlation. Thus, ACO is a useful oligomer based on renewable feedstock and suitable for replacement of 100% petroleum-based oligomers in UV-curable formulations requiring high cure speeds and  $T_g$  values near room temperature. Although ACO is a step in the right direction, continued efforts are required to “green” the entire synthetic and polymerization processes.

## 10.2 Recommendations

Epoxide systems remain a rich group of monomers to study fundamentally. It is clear that the two propagation mechanisms occur in concert since the reactive species required for both mechanisms are present in formulations with CTAs included. The observed rate of epoxide conversion may be expressed generally as the sum of the rate of epoxide conversion via ACE propagation and via AM propagation shown in Equations 10.1 and 10.2.

$$Rate_{overall} = Rate_{ACE} + Rate_{AM} \quad 10.1$$

$$Rate_{overall} = k_{ACE}[M^+][M] + k_{AM}[M^+][OH] \quad 10.2$$

The AM mechanism may be further characterized by studying mono-epoxide monomers that form linear polymers (limiting the mobility/diffusion effects on kinetic profiles). However, the monomer must be non-volatile. Cyclohexene oxide, vinyl cyclohexene monoxide, and limonene monoxide are all volatile and therefore poor model compounds for photopolymerization studies. A non-volatile cycloaliphatic epoxide may be synthesized in two steps. The compound 3-cyclohexene-1-carboxylic acid may be esterified via methanol treatment. Following esterification, the double bond can be oxidized to an epoxide.<sup>1</sup> The newly synthesized epoxide monomer would have a boiling point approaching or surpassing 200 °C (estimated by comparison to the boiling point of methyl benzoate 200 °C).<sup>2</sup>

A study of the AM/ACE mechanisms requires a CTA. Because the propagation of epoxide monomers (not only chain transfer events) is the interest, the CTA should have a similar structure and substitution as the alcohols formed by opening the epoxide rings (a secondary alcohol attached to the cyclohexene ring). Choice of similar structure is required to minimize differences between the reactivity and nucleophilicity of the CTA in the formulation and the hydroxyls produced via ring-opening events. An ideal CTA in

this case would be the diol formed from the hydrolysis of cyclohexene oxide (1,2-cyclohexanediol). 1,2-Cyclohexanediol may be synthesized by simply reacting with an excess of hot water.<sup>3</sup> The synthesized monomer and CTA, as well as the photoinitiator, must be stored in solvent (e.g.,  $\text{CHCl}_3$ ) over molecular sieves or anhydrous sodium sulfate in order to remove all water from the reaction vessel.

Kinetic experiments may then be carried out with formulations that vary the CTA concentration while keeping the monomer and photoinitiator concentration constant. According to Equation 10.2, the overall rate would primarily represent ACE kinetics in formulations that have low hydroxyl concentrations. Alternatively, the overall rate would primarily represent AM kinetics in formulations with high hydroxyl concentrations. The conversion vs. illumination time profiles may be collected via RT-Raman spectroscopy by observing the decrease in the epoxide peak height ( $790\text{ cm}^{-1}$ ) while under UV illumination. Comparing the rates of epoxide conversion, observed at a specific UV exposure, as a function of hydroxyl concentration should result in a plot which intercepts the y-axis at a rate approximately equal to the pure ACE propagation rate. The rate should increase with increasing hydroxyl concentration and asymptotically approach a ceiling epoxide conversion rate. The ceiling epoxide conversion rate is approximately equal to the pure AM propagation rate. A strict ACE propagation rate is impossible to achieve because each secondary oxonium ion that is opened results in a hydroxyl group that has potential to react via the AM mechanism. Strict AM propagation is likewise impossible to achieve because, in every epoxide formulation, neutral monomers will be present that can propagate via the ACE mechanism. Although the limits between ACE and AM propagation are not readily measurable, the relationship between the two mechanisms can be quantified via the experiments described above.

In Chapter 7, special acrylate polymers were prepared via RAFT polymerization<sup>4</sup> with the purpose of further elucidating the AM mechanism. When incorporated into a crosslinking resin, the RAFT polymers did not exhibit any special physical properties to

the cross-linked material. However, rather than randomly distributing the hydroxy acrylates along the polymer back bone, block copolymers could be formed via sequential RAFT polymerization.<sup>5</sup> A block copolymer synthesized from butyl acrylate and hydroxy butyl acrylate may be very useful in preparing tough epoxy-based materials. The block copolymer would phase segregate (nanoscale self-assembly) due to the disparity between the chemical potential of butyl acrylate and hydroxy butyl acrylate side groups.<sup>6,7</sup> Once included into an epoxy resin, the block copolymers would presumably retain some degree of self-assembly.<sup>8,9</sup> There would potentially be three domains: neat epoxy, hydroxy butyl acrylate/epoxy, butyl acrylate. The neat epoxy and hydroxy butyl acrylate domains would be relatively hard and likely glassy domains, while the butyl acrylate domains would be rubbery. The rubbery domains included in a glassy matrix may prove to be useful in designing polymers with good impact/energy absorbing properties. In addition to enhancing the physical properties, the type of block copolymer described above would achieve higher epoxide conversions (than an analogous block copolymer with an epoxy-containing acrylate monomer, in place of hydroxy butyl acrylate) via the AM mechanism, enhancing the rate of polymerization, and altering the physical properties. Without block copolymers, the effects of hydroxyl acrylates will simply be averaged throughout the entire volume of the material and will have less of an impact compared to block copolymer materials in which the hydroxy acrylates are concentrated and localized via nanoscale self-assembly.

Another characteristic of cationically cured epoxides is the long-lived active centers produced during photoinitiation. The study of "dark cure," the curing that continues to occur after the illuminating light source has been shuttered off, has been investigated by few researchers.<sup>10-13</sup> The prolonged curing period offered via dark cure may allow otherwise sluggish epoxide monomers to be used in applications that do not require "instantaneous" curing. Epoxide systems may also undergo some "shadow cure," in which the active centers migrate from the illuminated area to a non-illuminated area

and therefore propagate polymerization to areas that cannot be easily cured via photopolymerization alone. Characterization of the kinetics of dark and shadow cure for a variety of epoxide systems builds a very useful framework to be used in new photopolymerization applications.

Multiple variables may contribute to a resin's capacity to undergo dark and/or shadow cure including curing temperature,  $T_g$ , photoinitiator (counter anion specifically), monomer type, and propagation mechanisms. In Chapter 4, the  $T_g$  of epoxide systems was modulated via CTA formulation. In dark/shadow cure studies, these formulations would change the degree of AM mechanism promotion while also changing the  $T_g$ . In order to deconvolute these confounding variables, the  $T_g$  of epoxide resins must be modulated without adding CTAs. Diepoxide materials may be synthesized such that the linker between the epoxide moieties (composed of a polyTHF diol) varies from a short linker (e.g., 1,4-butanediol or polyTHF 250) to very long linkers (e.g., polyTHF 650 or polyTHF100). By varying the linker size/length, the crosslink density of the cured material would be varied along with the  $T_g$  without affecting the primary propagation mechanism. Alternatively, the  $T_g$  could be modulated by adding CTAs, as in Chapter 4, to the diepoxide monomer, therefore changing the  $T_g$  and the propagation mechanism. By comparing the dark and shadow cure of the two types of systems (see Figure 10.1), the importance of synthesizing new diepoxide monomers for the purpose of  $T_g$  modulation and dark/shadow cure optimization may be elucidated.

Further investigation of cationic epoxide polymerization kinetics, hybrid acrylate-epoxide systems (including GPN forming systems), and dark/shadow cure of epoxide resins will serve to clearly characterize this unique class of photopolymerizable materials and open up new applications for photopolymerization in general.

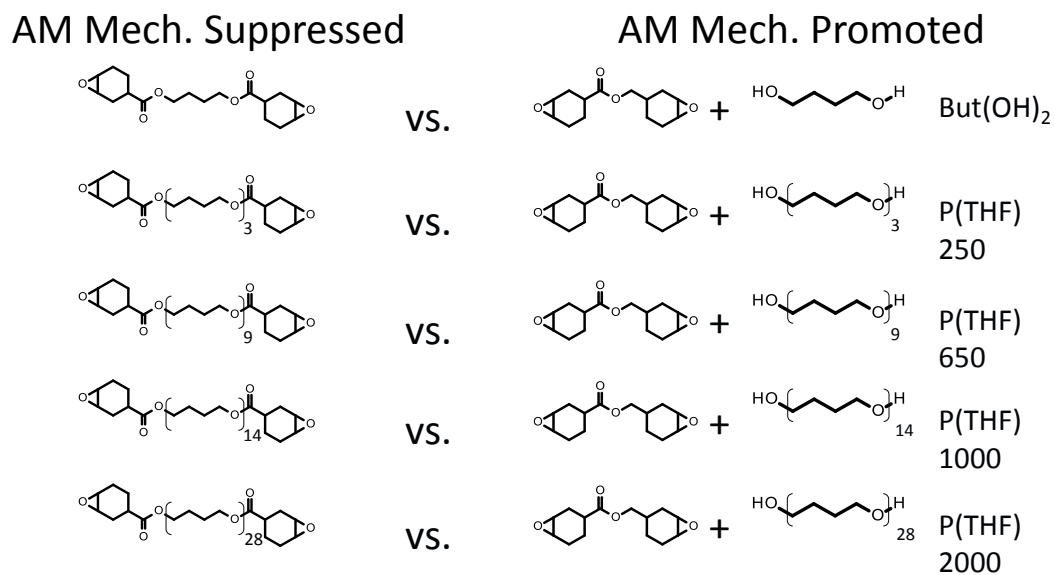


Figure 10.1: An experimental matrix designed to compare dark cure and shadow cure in epoxide systems that vary in  $T_g$  without promoted the AM mechanism (*left column*) to epoxide systems that vary in  $T_g$  but do have CTAs which strongly promote the AM mechanism (*right column*).

### Notes

- (1) Crivello, J. V.; Varlemann, U. "Mechanistic study of the reactivity of 3,4-epoxycyclohexylmethyl 3',4'-epoxycyclohexanecarboxylate in photoinitiated cationic polymerizations." *Journal of Polymer Science Part A: Polymer Chemistry* **1995**, *33*, 2473-2486.
- (2) Kondo, M.; Oyama Okubo, N.; Ando, T.; Marchesi, E.; Nakayama, M. "Floral scent diversity is differently expressed in emitted and endogenous components in *Petunia axillaris* lines." *Annals of botany* **2006**, *98*, 1253-9.
- (3) Wang, Z.; Cui, Y.; Xu, Z.; Qu, J. "Hot Water-Promoted Ring-Opening of Epoxides and Aziridines by Water and Other Nucleophiles." *Journal of Organic Chemistry* **2008**, *73*, 2270-2274.
- (4) Chiefari, J.; Chong, Y. K.; Ercole, F.; Krstina, J.; Jeffery, J.; Le, T. P. T.; Mayadunne, R. T. A.; Meijs, G. F.; Moad, C. L.; Moad, G.; Rizzardo, E.; Thang, S. H. "Living Free-Radical Polymerization by Reversible Addition-Fragmentation Chain Transfer: The RAFT Process." *Macromolecules* **1998**, *31*, 5559-5562.
- (5) Fiten, M.; Paulus, R.; Schubert, U. "Systematic parallel investigation of RAFT polymerizations for eight different (meth)acrylates: A basis for the designed synthesis of block and random copolymers" *Journal of polymer science. Part A, Polymer chemistry* **2005**, *43*, 3831-3839.
- (6) Leibler, L. "Nanostructured plastics: Joys of self-assembling." *Progress in Polymer Science* **2005**, *30*, 898-914.
- (7) Lynd, N. A.; Meuler, A. J.; Hillmyer, M. A. "Polydispersity and block copolymer self-assembly." *Progress in Polymer Science* **2008**, *33*, 875-893.
- (8) Ritzenthaler, S.; Court, F.; David, L.; Girard-Reydet, E.; Leibler, L.; Pascault, J. P. "ABC Triblock Copolymers/Epoxy-Diamine Blends. 1. Keys To Achieve Nanostructured Thermosets." *Macromolecules* **2002**, *35*, 6245-6254.
- (9) Ritzenthaler, S.; Court, F.; Girard-Reydet, E.; Leibler, L.; Pascault, J. P. "ABC triblock copolymers/epoxy-diamine blends. 2. Parameters controlling the morphologies and properties." *Macromolecules* **2003**, *36*, 118-126.
- (10) Oxman, J. D.; Jacobs, D. W.; Trom, M. C.; Sipani, V.; Ficek, B.; Scranton, A. B. "Evaluation of initiator systems for controlled and sequentially curable free-radical/cationic hybrid photopolymerizations." *Journal of Polymer Science Part A: Polymer Chemistry* **2005**, *43*, 1747-1756.
- (11) Sipani, V.; Scranton, A. B. "Dark-cure studies of cationic photopolymerizations of epoxides: Characterization of the active center lifetime and kinetic rate



constants" *Journal of Polymer Science Part A: Polymer Chemistry* **2003**, *41*, 2064-2072.

- (12) Sipani, V.; Kirsch, A.; Scranton, A. B. "Dark cure studies of cationic photopolymerizations of epoxides: Characterization of kinetic rate constants at high conversions." *Journal of Polymer Science Part A: Polymer Chemistry* **2004**, *42*, 4409-4416.
- (13) Ficek, B.; Thiesen, A.; Scranton, A. B. "Cationic photopolymerizations of thick polymer systems: Active center lifetime and mobility" *European Polymer Journal* **2008**, *44*, 98-105.

## REFERENCES

- Acosta Ortiz, R.; Sangermano, M.; Bongiovanni, R.; Garcia Valdez, A. E.; Duarte, L. B.; Saucedo, I. P.; Priola, A. "Synthesis of hybrid methacrylate-silicone-cyclohexanepoxide monomers and the study of their UV induced polymerization." *Progress in Organic Coatings* **2006**, *57*, 159-164.
- Anderson, D.; Davidson, R.; Elvery, J. "Thioxanthenes: Their fate when used as photoinitiators" *Polymer* **1996**, *37*, 2477.
- Andrzejewska, E. "Photopolymerization kinetics of multifunctional monomers." *Progress in Polymer Science* **2001**, *26*, 605-665.
- Anseth, K. S.; Bowman, C. N.; Peppas, N. A. "Polymerization kinetics and volume relaxation behavior of photopolymerized multifunctional monomers producing highly crosslinked networks" *Journal of Polymer Science Part A: Polymer Chemistry* **1994**, *32*, 139-147.
- Anslyn, E. V.; Dougherty, D. A. *Modern Physical Organic Chemistry*; University Science Books: Sausalito, California, 2006; , pp 1099.
- Ballinger, P. "Acid Ionization Constants of Alcohols. II. Acidities of Some Substituted Methanols and Related Compounds1, 2" *Journal of the American Chemical Society* **1960**, *82*, 795.
- Ballinger, P.; Long, F. "Acid ionization Constants of Alcohols. I. Trifluoroethanol in the Solvents H<sub>2</sub>O and D<sub>2</sub>O" *Journal of the American Chemical Society* **1959**, *81*, 1050-1053.
- Bi, Y.; Neckers, D. C. "A Visible Light Initiating System for Free Radical Promoted Cationic Polymerization." *Macromolecules* **1994**, *27*, 3683-3693.
- Bicerano, J.; Sammler, R. L.; Carriere, C. J.; Seitz, J. T. "Correlation between Glass Transition Temperature and Chain Structure of Randomly Crosslinked High Polymers" *Journal of Polymer Science Part B: Polymer Physics* **1996**, *34*, 2247-2259.
- Biedron, T.; Brzezinska, K.; Kubisa, P.; Penczek, S. "Macromonomers by Activated Polymerization of Oxiranes - Synthesis and Polymerization" *Polymer International* **1995**, *36*, 73-80.
- Boots, H.; Kloosterboer, J.; Vandehei, G.; Pandey, R. "Inhomogeneity During The Bulk-Polymerization of Divinyl Compounds - Differential Scanning Calorimetry Experiments and Percolation Theory" *British polymer journal* **1985**, *17*, 219.

- Bowman, C. N.; Kloxin, C. "Toward an Enhanced Understanding and Implementation of Photopolymerization Reactions" *AIChE Journal* **2008**, *54*, 2775-2795.
- Briscoe, B. J.; Fiori, L.; Pelillo, E. "Nano-indentation of polymeric surfaces" *Journal of Physics D: Applied Physics* **1998**, *31*, 2395-2405.
- Brzezinska, K.; Szymanski, R.; Kubisa, P.; Penczek, S. "Activated monomer mechanism in cationic polymerization. I: Ethylene oxide, formulation of mechanism" *Die Makromolekulare Chemie Rapid Communications* **1986**, *7*, 1-4.
- Bulut, U.; Crivello, J. V. "Investigation of the Reactivity of Epoxide Monomers in Photoinitiated Cationic Polymerization." *Macromolecules* **2005**, *38*, 3584-3595.
- Cai, Y.; Jessop, J. L. P. "Effect of water concentration on photopolymerized acrylate/epoxide hybrid polymer coatings as demonstrated by Raman spectroscopy" *Polymer* **2009**, *50*, 5409-5413.
- Cai, Y.; Jessop, J. L. P. "Decreased oxygen inhibition in photopolymerized acrylate/epoxide hybrid polymer coatings as demonstrated by Raman spectroscopy." *Polymer* **2006**, *47*, 6560-6566.
- Carioscia, J. A.; Stansbury, J. W.; Bowman, C. N. "Evaluation and control of thiol-ene/thiol-epoxy hybrid networks" *Polymer* **2007**, *48*, 1526-1532.
- Carioscia, J. A.; Schneidewind, L.; O'Brien, C.; Ely, R.; Feeser, C.; Cramer, N.; Bowman, C. N. "Thiol-norbornene materials: approaches to develop high Tg thiol-ene polymers." *Journal of Polymer Science Part A: Polymer Chemistry* **2007**, *45*, 5686-5696.
- Chalmers, J. *Handbook of Vibrational Spectroscopy*; J. Wiley: New York, 2002; Vol. 1, pp 3862.
- Chang, M.; Chen, S. "Kinetics and Mechanism of Urethane Reactions - Phenyl Isocyanate Alcohol Systems" *Journal of polymer science. Part A, Polymer chemistry* **1987**, *25*, 2543.
- Chattopadhyay, D. K. "Structural engineering of polyurethane coatings for high performance applications" *Progress in polymer science* **2007**, *32*, 352-418.
- Chiefari, J.; Chong, Y. K.; Ercole, F.; Krstina, J.; Jeffery, J.; Le, T. P. T.; Mayadunne, R. T. A.; Meijs, G. F.; Moad, C. L.; Moad, G.; Rizzardo, E.; Thang, S. H. "Living Free-Radical Polymerization by Reversible Addition-Fragmentation Chain Transfer: The RAFT Process." *Macromolecules* **1998**, *31*, 5559-5562.

- Cook, W.; Chen, F.; Ooi, S.; Moorhoff, C.; Knott, R. "Effect of curing order on the curing kinetics and morphology of bisGMA/DGEBA interpenetrating polymer networks" *Polymer International* **2006**, *55*, 1027-1039.
- Cowell, G. W.; Kocharyan, K.; Ledwith, A.; Woods, J. H. "Initiation of cationic polymerization by electron transfer: polymerization of N-vinyl carbazole by hexachloroantimonate (SbCl<sub>6</sub><sup>-</sup>) ion." *European Polymer Journal* **1970**, *6*, 561-567.
- Cramer, N. B.; Bowman, C. N. "Kinetics of thiol-ene and thiol-acrylate photopolymerizations with real-time Fourier transform infrared" *Journal of Polymer Science Part A: Polymer Chemistry* **2001**, *39*, 3311-3319.
- Cramer, N. B.; Davies, T.; O'Brien, A. K.; Bowman, C. N. "Mechanism and Modeling of a Thiol-Ene Photopolymerization." *Macromolecules* **2003**, *36*, 4631-4636.
- Cramer, N. B.; Reddy, S. K.; O'Brien, A. K.; Bowman, C. N. "Thiol-Ene Photopolymerization Mechanism and Rate Limiting Step Changes for Various Vinyl Functional Group Chemistries." *Macromolecules* **2003**, *36*, 7964-7969.
- Crandall, E. W. "Spectroscopic analysis using the near-infrared region of the electromagnetic spectrum" *Journal of Chemical Education* **1987**, *64*, 466-467.
- Crivello, J. V. "A new visible light sensitive photoinitiator system for the cationic polymerization of epoxides." *Journal of Polymer Science Part A: Polymer Chemistry* **2009**, *47*, 866-875.
- Crivello, J. V. "Radical-Promoted Visible Light Photoinitiated Cationic Polymerization of Epoxides." *Journal of Macromolecular Science Part A: Pure and Applied Chemistry* **2009**, *46*, 474-483.
- Crivello, J. V. "Benzophenothiazine and benzophenoxazine photosensitizers for triarylsulfonium salt cationic photoinitiators" *Journal of Polymer Science Part A: Polymer Chemistry* **2008**, *46*, 3820-3829.
- Crivello, J. V. "The discovery and development of onium salt cationic photoinitiators." *Journal of Polymer Science Part A: Polymer Chemistry* **1999**, *37*, 4241-4254.
- Crivello, J. V.; Conlon, D. A.; Olson, D. R.; Webb, K. K. "The Effects of Polyols as Chain Transfer Agents and Flexibilizers in Photoinitiated Cationic Polymerization" *Journal of Radiation Curing* **1986**, 3-9.
- Crivello, J. V.; Falk, B.; Zonca, M. R., Jr "Study of cationic ring-opening photopolymerizations using optical pyrometry." *Journal of Applied Polymer Science* **2004**, *92*, 3303-3319.

- Crivello, J. V.; JO, K. "Propenyl Ethers I The Synthesis of Propenyl Ether Monomers" *Journal of Polymer Science Part A: Polymer Chemistry* **1993**, *31*, 1473-1482.
- Crivello, J. V.; JO, K. "Propenyl Ethers II Study of the Photoinitiated Cationic Polymerization of Propenyl Ether Monomers" *Journal of Polymer Science Part A: Polymer Chemistry* **1993**, *31*, 1483-1491.
- Crivello, J. V.; Lam, J. H. W. "Diaryliodonium Salts. A New Class of Photoinitiators for Cationic Polymerization." *Macromolecules* **1977**, *10*, 1307-1315.
- Crivello, J. V.; Liu, S. "Photoinitiated cationic polymerization of epoxy alcohol monomers" *Journal of polymer science. Part A, Polymer chemistry* **2000**, *38*, 389-401.
- Crivello, J. V.; Narayan, R. "Epoxidized Triglycerides as Renewable Monomers in Photoinitiated Cationic Polymerization" *Chemistry of Materials* **1992**, *4*, 692-699.
- Crivello, J. V.; Ortiz, R. A. "Benzyl alcohols as accelerators in the photoinitiated cationic polymerization of epoxide monomers." *Journal of Polymer Science, Part A: Polymer Chemistry* **2002**, *40*, 2298-2309.
- Crivello, J. V.; Rajaraman, S.; Mowers, W. A.; Liu, S. "Free radical accelerated cationic polymerizations." *Macromolecular Symposia* **2000**, *157*, 109-119.
- Crivello, J. V.; Varlemann, U. "Mechanistic study of the reactivity of 3,4-epoxycyclohexylmethyl 3',4'-epoxycyclohexanecarboxylate in photoinitiated cationic polymerizations." *Journal of Polymer Science Part A: Polymer Chemistry* **1995**, *33*, 2473-2486.
- Davidson, C. L.; Feilzer, A. J. "Polymerization shrinkage and polymerization shrinkage stress in polymer-based restoratives" *Journal of dentistry* **1997**, *25*, 435-440.
- Dean, K.; Cook, W. "Effect of curing sequence on the photopolymerization and thermal curing kinetics of dimethacrylate/epoxy interpenetrating polymer networks" *Macromolecules* **2002**, *35*, 7942-7954.
- Dean, K.; Cook, W.; Zipper, M.; Burchill, P. "Curing behaviour of IPNs formed from model VERs and epoxy systems I amine cured epoxy" *Polymer* **2001**, *42*, 1345-1359.
- Decker, C. "Photoinitiated cationic polymerization of epoxides" *Polymer International* **2001**, *50*, 986-997.
- Decker, C. "Photoinitiated Crosslinking Polymerization." *Progress in Polymer Science* **1996**, *21*, 593-650.

- Decker, C.; Jenkins, A. "Kinetic Approach of Oxygen Inhibition in Ultraviolet-Induced and Laser-Induced Polymerizations" *Macromolecules* **1985**, *18*, 1241-1244.
- Decker, C.; Moussa, K. "Kinetic-Study of the Cationic Photopolymerization of Epoxy Monomers" *Journal of Polymer Science Part A: Polymer Chemistry* **1990**, *28*, 3429-3443.
- Decker, C.; Moussa, K. "Photopolymerization of multifunctional monomers in condensed phase." *Journal of Applied Polymer Science* **1987**, *34*, 1603-1618.
- Decker, C.; Nguyen Thi Viet, T.; Decker, D.; Weber-Koehl, E. "UV-radiation curing of acrylate/epoxide systems." *Polymer* **2001**, *42*, 5531-5541.
- Dietliker, K.; Jung, T.; Studer, K.; Benkhoff, J. "Photolatent Tertiary Amines A New Technology Platform for Radiation Curing" *CHIMIA International Journal for Chemistry* **2007**, *61*, 655-660.
- Dietliker, K.; Huesler, R.; Birbaum, J. -.; Ilg, S.; Villeneuve, S.; Studer, K.; Jung, T.; Benkhoff, J.; Kura, H.; Matsumoto, A.; Oka, H. "Advancements in photoinitiators-Opening up new applications for radiation curing." *Progress in Organic Coatings* **2007**, *58*, 146-157.
- Dillman, B.; Jessop, J. L. P. "Chain transfer agents in cationic photopolymerization of a bis-cycloaliphatic epoxide monomer: Kinetic and physical property effects" *Journal of Polymer Science Part A: Polymer Chemistry* **2013**, *51*, 2058-2067.
- Durmaz, Y. Y.; Moszner, N.; Yagci, Y. "Visible Light Initiated Free Radical Promoted Cationic Polymerization Using Acylgermane Based Photoinitiator in the Presence of Onium Salts." *Macromolecules (Washington, DC, United States)* **2008**, *41*, 6714-6718.
- Dursun, C.; Degirmenci, M.; Yagci, Y.; Jockusch, S.; Turro, N. J. "Free radical promoted cationic polymerization by using bisacylphosphine oxide photoinitiators: substituent effect on the reactivity of phosphinoyl radicals." *Polymer* **2003**, *44*, 7389-7396.
- Esposito Corcione, C.; Malucelli, G.; Frigione, M.; Maffezzoli, A. "UV-curable epoxy systems containing hyperbranched polymers: Kinetics investigation by photo-DSC and real-time FT-IR experiments." *Polymer Testing* **2009**, *28*, 157-164.
- Ficek, B.; Thiesen, A.; Scranton, A. B. "Cationic photopolymerizations of thick polymer systems: Active center lifetime and mobility" *European Polymer Journal* **2008**, *44*, 98-105.

- Finter, J.; Riediker, M.; Rohde, O.; Rotzinger, B. "Photosensitive systems for microlithography based on organometallic photoinitiators" *Die Makromolekulare Chemie. Macromolecular symposia* **1989**, *24*, 177.
- Fiten, M.; Paulus, R.; Schubert, U. "Systematic parallel investigation of RAFT polymerizations for eight different (meth)acrylates: A basis for the designed synthesis of block and random copolymers" *Journal of polymer science. Part A, Polymer chemistry* **2005**, *43*, 3831-3839.
- Fouassier, J. *Photoinitiation, Photopolymerization, and Photocuring*; Hanser/Gardner Publications, Inc.: Cincinnati, OH, 1995; , pp 375.
- Fox, T. G.; Loshaek, S. "Influence of Molecular Weight and Degree of Crosslinking on the Specific Volume and Glass Transition Temperature of Polymers" *Journal of Polymer Science* **1955**, *15*, 371-390.
- Ghosh, N. N.; Palmese, G. R. "Electron-beam curing of epoxy resins: Effect of alcohols on cationic polymerization." *Bulletin of Materials Science* **2005**, *28*, 603-607.
- Gou, L.; Opheim, B.; Scranton, A. B. *In Methods to overcome oxygen inhibition in free radical photopolymerizations*. Chemistry of Synthetic High Polymers; 2006; , pp 301-310.
- Gou, L.; Opheim, B.; Scranton, A. B. "The effect of oxygen in free radical photopolymerization." *Recent Research Developments in Polymer Science* **2004**, *8*, 125-141.
- Groenenboom, C. J.; Hageman, H. J.; Overeem, T.; Weber, A. J. M. "Photoinitiators and photoinitiation. 3. Comparison of the photodecompositions of alpha - methoxy- and alpha ,alpha -dimethoxydeoxybenzoin in 1,1-diphenylethylene as model substrate." *Makromolekulare Chemie* **1982**, *183*, 281-292.
- Hartwig, A. "Influence of moisture present during polymerisation on the properties of a photocured epoxy resin" *International Journal of Adhesion and Adhesives* **2002**, *22*, 409-414.
- Hartwig, A.; Schneider, B.; Lühring, A. "Influence of moisture on the photochemically induced polymerisation of epoxy groups in different chemical environment" *Polymer* **2002**, *43*, 4243-4250.
- Hartwig, A.; Harder, A.; Lühring, A.; Schröder, H. "(9-Oxo-9H-fluoren-2-yl)-phenyl-iodonium hexafluoroantimonate(V) – a photoinitiator for the cationic polymerisation of epoxides" *European Polymer Journal* **2001**, *37*, 1449-1455.

- Hartwig, A.; Koschek, K.; Luhring, A.; Schorsch, O. "Cationic polymerization of a cycloaliphatic diepoxide with latent initiators in the presence of structurally different diols" *Polymer* **2003**, *44*, 2853.
- Hartwig, A.; Sebald, M. "Preparation and properties of elastomers based on a cycloaliphatic diepoxide and poly(tetrahydrofuran)" *European polymer journal* **2003**, *39*, 1975.
- He, Y.; Xiao, M.; Wu, F.; Nie, J. "Photopolymerization kinetics of cycloaliphatic epoxide-acrylate hybrid monomer." *Polymer International* **2007**, *56*, 1292-1297.
- Hiemenz, P. C.; Lodge, T. P. *Polymer Chemistry Second Edition*; CRC Press: Boca Raton, FL, 2007; .
- Hoyle, C. E.; Lee, T. Y.; Roper, T. "Thiol-enes: Chemistry of the past with promise for the future." *Journal of Polymer Science Part A: Polymer Chemistry* **2004**, *42*, 5301-5338.
- Jakubiak, J.; Allonas, X.; Fouassier, J.; Sionkowska, A.; Andrzejewska, E.; Linden, L. "Camphorquinone-amines photoinitiating systems for the initiation of free radical polymerization" *Polymer* **2003**, *44*, 5219.
- Jancovicova, V.; Brezova, V.; Ciganek, M.; Cibulkova, Z. "Photolysis of diaryliodonium salts (UV/Vis, EPR and GC/MS investigations)." *Journal of Photochemistry and Photobiology, A: Chemistry* **2000**, *136*, 195-202.
- Jang, M.; Crivello, J. V. "Synthesis and cationic photopolymerization of epoxy-functional siloxane monomers and oligomers" *Journal of Polymer Science Part A: Polymer Chemistry* **2003**, *41*, 3056-3073.
- Jansen, B.; Rastogi, S.; Meijer, H.; Lemstra, P. "Rubber-modified glassy amorphous polymers prepared via chemically induced phase separation. 4. Comparison of properties of semi- and full-IPNs, and copolymers of acrylate-aliphatic epoxy systems" *Macromolecules* **1999**, *32*, 6290-6297.
- Jansen, J. F. G. A.; Dias, A. A.; Dorschu, M.; Coussens, B. "Fast Monomers: Factors Affecting the Inherent Reactivity of Acrylate Monomers in Photoinitiated Acrylate Polymerization." *Macromolecules* **2003**, *36*, 3861-3873.
- Kannurpatti, A. R.; Anseth, J. W.; Bowman, C. N. "A study of the evolution of mechanical properties and structural heterogeneity of polymer networks formed by photopolymerizations of multifunctional (meth)acrylates" *Polymer* **1998**, *39*, 2507-2513.



- Khot, S. N.; Lascala, J. J.; Can, E.; Morye, S. S.; Williams, G. I.; Palmese, G. R.; Kusefoglu, S. H.; Wool, R. P. "Development and application of triglyceride-based polymers and composites" *Journal of Applied Polymer Science* **2001**, *82*, 703-723.
- Kloosterboer, J. "Network Formation by Chain Crosslinking Photopolymerization and its Applications in Electronics" *Advances in polymer science* **1988**, *84*, 1.
- Kloosterboer, J.; Vandehei, G.; Boots, H. "Inhomogeneity During the Photopolymerization of Diacrylates - DSC Experiments and Percolation Theory" *Polymer communications* **1984**, *25*, 354.
- Kolczak, U.; Rist, G.; Dietliker, K.; Wirz, J. "Reaction Mechanism of Monoacyl- and Bisacylphosphine Oxide Photoinitiators Studied by  $^{31}\text{P}$ -,  $^{13}\text{C}$ -, and  $^1\text{H}$ -CIDNP and ESR." *Journal of the American Chemical Society* **1996**, *118*, 6477-6489.
- Koleske, J. V. *Radiation Curing of Coatings*; ASTM International: West Conshohocken, PA, 2002; Vol. 1, pp 244.
- Kondo, M.; Oyama Okubo, N.; Ando, T.; Marchesi, E.; Nakayama, M. "Floral scent diversity is differently expressed in emitted and endogenous components in *Petunia axillaris* lines." *Annals of botany* **2006**, *98*, 1253-9.
- Krol, P. "Synthesis methods, chemical structures and phase structures of linear polyurethanes. Properties and applications of linear polyurethanes in polyurethane elastomers, copolymers and ionomers" *Progress in materials science* **2007**, *52*, 915-1015.
- Kubisa, P.; Penczek, S. "Cationic activated monomer polymerization of heterocyclic monomers." *Progress in Polymer Science* **2000**, *24*, 1409-1437.
- Kubisa, P.; Bednarek, M.; Biedron, T.; Biela, T.; Penczek, S. "Progress in activated monomer polymerization. Kinetics of AM polymerization." *Macromolecular Symposia* **2000**, *153*, 217-226.
- La Scala, J.; Wool, R. "The effect of fatty acid composition on the acrylation kinetics of epoxidized triacylglycerols" *Journal of the American Oil Chemists' Society* **2002**, *79*, 59-63.
- Lalevee, J.; Fouassier, J. P. "Recent advances in sunlight induced polymerization: role of new photoinitiating systems based on the silyl radical chemistry" *Polymer Chemistry* **2011**, *2*, 1107-1103.
- Lalevee, J.; Tehfe, M.; Morlet Savary, F.; Graff, B.; Allonas, X.; Fouassier, J. "Oxygen mediated and wavelength tunable cationic photopolymerization reactions

- under air and low intensity: A new concept" *Progress in organic coatings* **2011**, *70*, 23-31.
- Leibler, L. "Nanostructured plastics: Joys of self-assembling." *Progress in Polymer Science* **2005**, *30*, 898-914.
- Lewis, I. *Handbook of Raman Spectroscopy*; Marcel Dekker: New York, 2001; , pp 1054.
- Lie Ken Jie, M. S. F.; Cheng, A. K. L. "Confirmation of the carbon chemical shifts of ethylenic carbon atoms in methyl ricinoleate and methyl ricinelaide" **1993**, *3*, 65-69.
- Lin, Y.; Stansbury, J. W. "The impact of water on photopolymerization kinetics of methacrylate/vinyl ether hybrid systems" *Polymers for Advanced Technologies* **2005**, *16*, 195-199.
- Lin, Y.; Stansbury, J. W. "Near-infrared spectroscopy investigation of water effects on the cationic photopolymerization of vinyl ether systems" *Journal of Polymer Science Part A: Polymer Chemistry* **2004**, *42*, 1985-1998.
- Lu, Y.; Larock, R. "Novel Polymeric Materials from Vegetable Oils and Vinyl Monomers: Preparation, Properties, and Applications" *ChemSusChem* **2009**, *2*, 136.
- Lynd, N. A.; Meuler, A. J.; Hillmyer, M. A. "Polydispersity and block copolymer self-assembly." *Progress in Polymer Science* **2008**, *33*, 875-893.
- Magwood, L. Evaluation of the physical property evolution of the hybrid acrylate/epoxide photopolymerization system, University of Iowa, University of Iowa, 2009.
- Matsushima, H.; Shin, J.; Bowman, C. N.; Hoyle, C. E. "Thiol-Isocyanate-Acrylate Ternary Networks by Selective Thiol-Click Chemistry" *Journal of Polymer Science Part A: Polymer Chemistry* **2010**, *48*, 3255-3264.
- Meier, M. A. R.; Metzger, J. O.; Schubert, U. S. "Plant oil renewable resources as green alternatives in polymer science" *Chemical Society Reviews* **2007**, *36*, 1788-1802.
- Menard, K. *Dynamic Mechanical Analysis: A Practical Introduction*; CRC Press: Boca Raton, FL, 2008; , pp 218.
- Moussa, K.; Decker, C. "Light-Induced Polymerization of New Highly Reactive Acrylic-Monomers" *Journal of Polymer Science Part A: Polymer Chemistry* **1993**, *31*, 2197-2203.

- MS Salim *Overview of UV Curable Coatings*; DR Randell, Ed.; Radiation Curing of Polymers II; The Royal Society of Chemistry: Cambridge, 1991; .
- Murayama, T. *Dynamic Mechanical Analysis of Polymeric Material*; Elsevier Scientific Publishing Company: New York, 1978; Vol. 1, pp 231.
- Nelson, E.; Jacobs, J.; Scranton, A. B.; Anseth, K.; Bowman, C. N. "Photo-differential Scanning Calorimetry Studies of Cationic Polymerizations of Divinyl Ethers" *Polymer* **1995**, *36*, 4651-4656.
- Nelson, E.; Scranton, A. B. "In situ Raman spectroscopy for cure monitoring of cationic photopolymerizations of divinyl ethers" *Journal of Raman Spectroscopy* **1996**, *27*, 137-144.
- O'Brien, A. K.; Bowman, C. N. "Modeling the effect of oxygen on photopolymerization kinetics." *Macromolecular Theory and Simulations* **2006**, *15*, 176-182.
- Odian, G. *Principles of Polymerization (Fourth Edition)*; John Wiley and Sons: Hoboken, NJ, 2004; .
- Ortiz, R.; Lopez, D.; Cisneros, M.; Valverde, J.; Crivello, J. V. "A kinetic study of the acceleration effect of substituted benzyl alcohols on the cationic photopolymerization rate of epoxidized natural oils" *Polymer* **2005**, *46*, 1535-1541.
- Ortiz, R. A.; Lopez, D. P.; Cisneros, M. d. L. G.; Valverde, J. C. R.; Crivello, J. V. "A kinetic study of the acceleration effect of substituted benzyl alcohols on the cationic photopolymerization rate of epoxidized natural oils." *Polymer* **2005**, *46*, 1535-1541.
- Oxman, J. D.; Jacobs, D. W.; Trom, M. C.; Sipani, V.; Ficek, B.; Scranton, A. B. "Evaluation of initiator systems for controlled and sequentially curable free-radical/cationic hybrid photopolymerizations." *Journal of Polymer Science Part A: Polymer Chemistry* **2005**, *43*, 1747-1756.
- Palanisamy, A. "Photo-DSC and dynamic mechanical studies on UV curable compositions containing diacrylate of ricinoleic acid amide derived from castor oil" *Progress in organic coatings* **2007**, *60*, 161-169.
- Pappas, S. P., Ed.; *Radiation Curing Science and Technology*; Plenum Press: New York, 1992; .
- Pappas, S. P. *Radiation curing: science and technology*; Springer: 1992; .

- Park, S.; Jin, F.; Lee, J.; Shin, J. "Cationic polymerization and physicochemical properties of a biobased epoxy resin initiated by thermally latent catalysts" *European polymer journal* **2005**, *41*, 231.
- Patel, M. P.; Braden, M.; Davy, K. W. M. "Polymerization shrinkage of methacrylate esters" *Biomaterials* **1987**, *8*, 53-56.
- Payne, J.; Francis, L.; McCormick, A. "The effects of processing variables on stress development in ultraviolet-cured coatings" *Journal of Applied Polymer Science* **1997**, *66*, 1267.
- Peeters, S. *In Overview of dual-cure and hybrid-cure systems in radiation curing*. Section Title: Chemistry of Synthetic High Polymers; 1993; Vol. 3, pp 177-217.
- Rajaraman, S. K.; Mowers, W. A.; Crivello, J. V. "Interaction of Epoxy and Vinyl Ethers During Photoinitiated Cationic Polymerization" *Journal of Polymer Science Part A: Polymer Chemistry* **1999**, *37*, 4007-4018.
- Raman, C. "A change of wave-length in light scattering" *Nature* **1928**, *121*, 619.
- Raman, C.; Krishnan, K. "A new type of secondary radiation" *Nature* **1928**, *121*, 501.
- Rao, B. S.; Palanisamy, A. "Photocuring and thermomechanical properties of multifunctional amide acrylate compositions derived from castor oil" *Progress in organic coatings* **2010**, *67*, 6-11.
- Rao, B. S.; Palanisamy, A. "Synthesis, photo curing and viscoelastic properties of triacrylate compositions based on ricinoleic acid amide derived from castor oil" *Progress in organic coatings* **2008**, *63*, 416-423.
- Ritzenthaler, S.; Court, F.; David, L.; Girard-Reydet, E.; Leibler, L.; Pascault, J. P. "ABC Triblock Copolymers/Epoxy-Diamine Blends. 1. Keys To Achieve Nanostructured Thermosets." *Macromolecules* **2002**, *35*, 6245-6254.
- Ritzenthaler, S.; Court, F.; Girard-Reydet, E.; Leibler, L.; Pascault, J. P. "ABC triblock copolymers/epoxy-diamine blends. 2. Parameters controlling the morphologies and properties." *Macromolecules* **2003**, *36*, 118-126.
- Rutsch, W.; Dietliker, K.; Leppard, d.; Koehler, M.; Misev, L.; Kolczak, U.; Rist, G. "Recent developments in photoinitiators." *Progress in Organic Coatings* **1996**, *27*, 227-239.
- Sangermano, M.; Bongiovanni, R.; Malucelli, G.; Roppolo, I.; Priola, A. "Siloxane additive as modifier in cationic UV curable coatings" *Progress in organic coatings* **2006**, *57*, 44.

- Sangermano, M.; Bongiovanni, R.; Priola, A.; Pospiech, D. "Fluorinated alcohols as surface-active agents in cationic photopolymerization of epoxy monomers" *Journal of polymer science.Part A, Polymer chemistry* **2005**, *43*, 4144-4150.
- Sangermano, M.; Malucelli, G.; Bongiovanni, R.; Priola, A.; Harden, A. "Investigation on the effect of the presence of hyperbranched polymers on thermal and mechanical properties of an epoxy UV-cured system." *Polymer International* **2005**, *54*, 917-921.
- Sangermano, M.; Tasdelen, M.; Yagci, Y. "Photoinitiated curing of mono- and bifunctional Epoxides by combination of active chain end and activated monomer cationic polymerization methods" *Journal of polymer science.Part A, Polymer chemistry* **2007**, *45*, 4914-4920.
- Scherzer, T.; Decker, U. "The effect of temperature on the kinetics of diacrylate photopolymerizations studied by Real-time FTIR spectroscopy" *Polymer* **2000**, *41*, 7681.
- Senyurt, A. F.; Hoyle, C. E.; Wei, H.; Piland, S. G.; Gould, T. E. "Thermal and Mechanical Properties of Cross-Linked Photopolymers Based on Multifunctional Thiol-Urethane Ene Monomers." *Macromolecules* **2007**, *40*, 3174-3182.
- Senyurt, A. F.; Wei, H.; Hoyle, C. E.; Piland, S. G.; Gould, T. E. "Ternary Thiol-Ene/Acrylate Photopolymers: Effect of Acrylate Structure on Mechanical Properties." *Macromolecules* **2007**, *40*, 4901-4909.
- Sharma, V.; Kundu, P. P. "Addition polymers from natural oils-A review." *Progress in Polymer Science* **2006**, *31*, 983-1008.
- Shin, J.; Matsushima, H.; Comer, C. M.; Bowman, C. N.; Hoyle, C. E. "Thiol-Isocyanate-Ene Ternary Networks by Sequential and Simultaneous Thiol Click Reactions." *Chemistry of Materials* **2010**, *22*, 2616-2625.
- Sipani, V.; Scranton, A. B. "Dark-cure studies of cationic photopolymerizations of epoxides: Characterization of the active center lifetime and kinetic rate constants" *Journal of Polymer Science Part A: Polymer Chemistry* **2003**, *41*, 2064-2072.
- Sipani, V.; Kirsch, A.; Scranton, A. B. "Dark cure studies of cationic photopolymerizations of epoxides: Characterization of kinetic rate constants at high conversions." *Journal of Polymer Science Part A: Polymer Chemistry* **2004**, *42*, 4409-4416.
- Solomon, D. H. *The chemistry of organic film formers*; Wiley. New York. NYUSA: 1967; .

- Sophiea, D.; Klempner, D.; Sendijarevic, V.; Suthar, B.; Frisch, K. C. "Interpenetrating polymer networks as energy-absorbing materials." *Advances in Chemistry Series* **1994**, *239*, 39-75.
- Sperling, L. H. "Interpenetrating polymer networks: an overview." *Advances in Chemistry Series* **1994**, *239*, 3-38.
- Swern, D.; Billen, G.; Findley, T.; Scanlan, J. "Hydroxylation of Monounsaturated Fatty Materials with Hydrogen Peroxide" *Journal of the American Chemical Society* **1945**, *67*, 1786-1789.
- Tehfe, M.; Lalevee, J.; Allonas, X.; Fouassier, J. "Long Wavelength Cationic Photopolymerization in Aerated Media: A Remarkable Titanocene/Tris(trimethylsilyl)silane/Onium Salt Photoinitiating System." *Macromolecules* **2009**, *42*, 8669-8674.
- Tehfe, M.; Lalevee, J.; Gimes, D.; Fouassier, J. "Green Chemistry: Sunlight-Induced Cationic Polymerization of Renewable Epoxy Monomers Under Air" *Macromolecules* **2010**, *43*, 1364-1370.
- Timpe, H. J.; Ulrich, S.; Decker, C.; Fouassier, J. P. "Photoinitiated polymerization of acrylates and methacrylates with decahydroacridine-1,8-dione/onium salt initiator systems." *Macromolecules* **1993**, *26*, 4560-4566.
- Vaessen, D.; Ngantung, F.; Palacio, M.; Francis, L.; McCormick, A. "Effect of lamp cycling on conversion and stress development in ultraviolet-cured acrylate coatings" *Journal of Applied Polymer Science* **2002**, *84*, 2784.
- Venturello, C.; Dalosio, R. "Quaternary Ammonium Tetrakis(diperoxotungsto)phosphates(3<sup>-</sup>) as a New Class of Catalysts for Efficient Alkene Epoxidation with Hydrogen-Peroxide" *Journal of organic chemistry* **1988**, *53*, 1553.
- Wade, L. G. *Organic Chemistry*; Pearson Education Inc.: Upper Saddle River, NJ, 2006; , pp 1262.
- Wang, Z.; Cui, Y.; Xu, Z.; Qu, J. "Hot Water-Promoted Ring-Opening of Epoxides and Aziridines by Water and Other Nucleophiles." *Journal of Organic Chemistry* **2008**, *73*, 2270-2274.
- Xue, G. "Fourier transform Raman spectroscopy and its application for the analysis of polymeric materials." *Progress in Polymer Science* **1997**, *22*, 313-406.
- Xue, G. "Laser Raman spectroscopy of polymeric materials." *Progress in Polymer Science* **1994**, *19*, 317-388.

- Yagci, Y. "Photoinitiated cationic polymerization of unconventional monomers"  
*Macromolecular symposia* **2006**, *240*, 93-101.
- Yagci, Y.; Schnabel, W.; Ledwith, A. "Synthesis and reactions of polymers with photoactive terminal groups - 3. The use of radical promoted cationic polymerization for the synthesis of poly(n-butyl vinyl ether) with N-acyl dibenz(b,f)azepine terminal units." *European Polymer Journal* **1987**, *23*, 737-740.
- Ye, S.; Cramer, N.; Bowman, C. N. "Relationship between Glass Transition Temperature and Polymerization Temperature for Cross-Linked Photopolymers"  
*Macromolecules* **2011**, *44*, 490-494.
- Zovi, O.; Lecamp, L.; Loutelier Bourhis, C.; Lange, C.; Bunel, C. "A solventless synthesis process of new UV-curable materials based on linseed oil" *Green Chemistry* **2011**, *13*, 1014-1022.